OPEN ACCESS

University of BRISTOL

This electronic thesis or dissertation has been downloaded from Explore Bristol Research, http://research-information.bristol.ac.uk

Author:
Dobson, Tom M

Title:
Investigating the effects of low-dose UV-B and ambient temperature on dark-induced leaf senescence in Arabidopsis

General rights
Access to the thesis is subject to the Creative Commons Attribution - NonCommercial-No Derivatives 4.0 International Public License. A copy of this may be found at https://creativecommons.org/licenses/by-nc-nd/4.0/legalcode This license sets out your rights and the restrictions that apply to your access to the thesis so it is important you read this before proceeding.

Take down policy
Some pages of this thesis may have been removed for copyright restrictions prior to having it been deposited in Explore Bristol Research. However, if you have discovered material within the thesis that you consider to be unlawful e.g. breaches of copyright (either yours or that of a third party) or any other law, including but not limited to those relating to patent, trademark, confidentiality, data protection, obscenity, defamation, libel, then please contact collections-metadata@bristol.ac.uk and include the following information in your message:

• Your contact details
• Bibliographic details for the item, including a URL
• An outline nature of the complaint

Your claim will be investigated and, where appropriate, the item in question will be removed from public view as soon as possible.

Investigating the Effects of Low-Dose UV-B and Ambient Temperature on Dark-Induced Leaf Senescence in Arabidopsis

by

Thomas Magnus Dobson

Faculty of Life Sciences
University of Bristol

A thesis submitted to the University of Bristol in accordance with the requirements of the degree of Master of Research in the Faculty of Life Sciences.

January 2022

Word count: c. 15,300

Abstract

Senescence promotes the degradation of chlorophyll (Chl) pigments in aged and stressed leaves resulting in leaf yellowing. In crops, senescence can be triggered by light deprivation during postharvest transport and storage, known as dark-induced senescence (DIS). Yellowed produce is commercially undesirable and often discarded. Postharvest DIS therefore constitutes a prominent source of agricultural inefficiency. Although refrigeration is often used to suppress postharvest DIS, high energetic costs and chilling sensitivity in some species highlight the need for alternative solutions. PHYTOCHROME-INTERACTING FACTORS (PIFs) 4 and 5 (PIF4/5) positively regulate DIS by activating the expression of the master senescence promoting transcription factor *ORESARA1* (*ORE1*). Studies have shown that low-dose UV-B (UV-B^{LD}) treatments disrupt PIF4/5 activity. However, their capacity for DIS suppression remains poorly characterised. Here, we employ a non-invasive Chl assay and quantitative real-time PCR to quantify physiological and transcription-level effects of preharvest UV-B^{LD} on DIS in Arabidopsis leaves maintained at different ambient temperatures. We demonstrate that UV-B^{LD} treatments suppress DIS in leaves maintained at 20°C, an effect that is at least partly attributable to UV-B^{LD}–mediated repression of *ORE1* transcription. This was additive to refrigeration treatment at 12°C, supporting a potential application for UV-B^{LD} as a complementary DIS suppression measure. UV-B^{LD} treatments also suppressed DIS in leaves maintained at 28°C, supporting their use at elevated storage temperatures. Our findings indicate that UV-B^{LD} delays DIS in Arabidopsis by disrupting *ORE1* transcription, although considerable optimisation is required to develop an effective treatment for commercial applications.

Dedication and Acknowledgements

I am indebted to my supervisor, Prof. Keara Franklin. She was an ever-present source of kindness and motivation throughout this project. Thank you for your guidance, scientific and otherwise, and for granting me the freedom to explore interesting tangents whilst maintaining my direction. I am similarly indebted to Lucia Primavesi, whose encouragement and patience allowed me to build confidence in molecular techniques. I also want to express gratitude to Ashley Pridgeon and Aline Yochikawa for their invaluable assistance with complicated protocols. Many thanks to Jess Sweetman for laying the foundation for these experiments and for your kindness and support. Thank you to Mathilda Gustavsson, Chris Groves, Helen Martin, and Ashutosh Sharma for practical suggestions and advice. You're brilliant scientists without exception. My flatmates, Max and Wills, thanks for the countless hilarious memories. Millicent, your company whilst I sowed seed was always appreciated. And Sophie, thank you for pushing me to achieve my very best and for your unwavering support.

Author's Declaration

I declare that the work in this thesis was carried out in accordance with the requirements of the University's Regulations and Code of Practice for Research Degree Programmes and that it has not been submitted for any other academic award. Except where indicated by specific reference in the text, the work is the candidate's own work. Work done in collaboration with, or with the assistance of, others, is indicated as such. Any views expressed in the dissertation are those of the author.

SIGNED: ..... DATE: .....

Table of Contents

List of Figures **xi**

Nomenclature **xiii**

1 Introduction **1**

1.1. Senescence . . . 2
1.2. Leaf senescence . . . 3
1.2.1. Chloroplast and chlorophyll degradation . . . 4
1.2.2. Leaf yellowing and the senescence syndrome . . . 4
1.2.3. Late-stage leaf senescence . . . 5
1.2.4. Molecular regulation of leaf senescence . . . 6
1.2.4.1. Ethylene . . . 6
1.2.4.2. Abscisic acid . . . 7
1.3. Dark-induced leaf senescence . . . 7
1.3.1. Molecular regulation of DIS . . . 8
1.3.1.1. Phytochrome-interacting factors . . . 8
1.3.1.2. Experimental variation among DIS analyses . . . 9
1.4. Suppression of DIS . . . 9
1.4.1. Light signalling and light-mediated DIS suppression . . . 10
1.4.1.1. Red light . . . 10
1.4.1.1.1. Phytochrome B-mediated light signalling . . . 10
1.4.1.1.2. Red light-mediated DIS suppression . . . 11
1.4.1.2. UV-B radiation . . . 13
1.4.1.2.1. Mechanism of UVR8 photoperception . . . 13
1.4.1.2.2. UV-B–inducible UVR8–COP1 interaction . . . 14
1.4.1.2.3. UV-B–inducible changes to the stability of COP1-targeted transcription factors . . . 14
1.4.1.2.3.1. HY5 and HYH . . . 15
1.4.1.2.3.2. PIF4 and PIF5 . . . 15
1.4.1.2.4. Negative feedback regulation of UVR8 signalling . . . 15

1.4.1.2.5. UV-B–mediated DIS suppression 16
1.4.2. Temperature signalling and thermal DIS suppression 16
1.4.2.1. Phytochrome B 17
1.4.2.2. UVR8 17
1.5. Conclusions and perspectives 17

2 Materials and Methods **19**
2.1. Plant materials and growth conditions 19
2.2. Light treatments 20
2.3. Dark incubation conditions 20
2.4. Leaf chlorophyll quantification 20
2.4.1. Non-destructive chlorophyll measurement 20
2.4.2. Chlorophyll extraction and spectrophotometry 21
2.5. Quantitative reverse-transcription PCR 21
2.5.1. RNA extraction 21
2.5.2. RNA yield and integrity assessment 22
2.5.3. cDNA synthesis 22
2.5.4. Quantitative PCR 22
2.6. Photography 22
2.7. Statistical analysis and graphing 23
2.8. Method development 23
2.8.1. Estimation of initial leaf chlorophyll contents 23

3 Investigating the Efficacy of Low-Dose UV-B for the Suppression of Dark-Induced Leaf Senescence in Arabidopsis **25**
3.1. Results 27
3.1.1. The Dualex sensor accurately identifies leaf chlorophyll content at 7 DDI . . 27
3.1.2. Preharvest treatment with low-dose UV-B promotes marginal DIS suppression 27
3.1.3. Preharvest treatment with low-dose UV-B transiently suppresses *ORE1* transcript abundance 27
3.1.4. Postharvest retreatment with low-dose UV-B enhances DIS suppression . . . 29
3.1.5. Low-dose UV-B treatments administered preharvest and at 2 DDI promote significant DIS suppression 30
3.2. Discussion 31

4 Investigating the Effect of Ambient Temperature on Low-Dose UV-B–mediated Senescence Suppression in Arabidopsis **35**
4.1. Results 37
4.1.1. Preharvest treatment with low-dose UV-B additively enhances DIS suppression by LAT and suppresses DIS in leaves maintained at HAT 37

4.2. Discussion 37

5 Overall Discussion **43**

5.1. Conclusions and future directions 45

Bibliography **47**

Appendix **63**

List of Figures

Figure		Page
1.	The progression of visible yellowing in leaves of dark-incubated Arabidopsis.	5
2.	Hypothetical model of red light-, low-dose UV-B-, and low ambient temperature-mediated DIS suppression in Arabidopsis.	12
3.	Predetermined locations for Dualex measurement on the adaxial leaf surface.	21
4.	Dualex measurement and biochemical extraction identify similar levels of leaf chlorophyll degradation at 7 DDI.	28
5.	Preharvest low-dose UV-B slightly delays dark-induced chlorophyll degradation.	28
6.	Preharvest low-dose UV-B transiently suppresses *ORE1* transcript abundance.	29
7.	Double low-dose UV-B treatment is more effective than a single preharvest treatment for suppressing dark-induced leaf chlorophyll degradation.	30
8.	Postharvest treatment with WL and UV-B is more effective than WL for suppressing dark-induced chlorophyll degradation.	31
9.	Hypothetical model of the kinetics of PIF4/5 protein abundance under day/night and dark incubation conditions and following low-dose UV-B treatments.	33
10.	Preharvest treatment with low-dose UV-B enhances DIS suppression by low ambient temperature and suppresses DIS in leaves maintained at high ambient temperature.	39
S1.	Emission spectra of light sources.	64
S2.	Assessment of RNA integrity using 1% agarose electrophoresis.	65
S3.	Standard curve assessment of PCR primer efficiency.	65
S4.	Experimental replicates of Fig. 5.	66
S5.	Experimental replicate of Fig. 8.	67
S6.	Experimental replicates of Fig. 10b.	68

Nomenclature

+UV-B	White light with low-dose UV-B
λ_{max}	Wavelength maximally absorbed
∅	Diameter
A_{645} etc.	Absorbance of electromagnetic radiation of wavelength 645 nm
AAO3	ABSCISIC-ALDEHYDE OXIDASE 3
ABA	Abscisic acid
ABF	ABRE BINDING FACTOR
ABI5	ABA INSENSITIVE 5
ABRE	ABA-responsive element
ACT2	ACTIN 2
APB	Active phytochrome B binding
Arg	Arginine
Asp	Aspartic acid
AU	Arbitrary units
bHLH	Basic helix-loop-helix
BiFC	Bimolecular fluorescence complementation
BOP2	BLADE-ON-PETIOLE 2
bZIP	Basic leucine zipper
CCE	Chlorophyll catabolic enzyme
CCG	Chlorophyll catabolic gene

cDNA	Complementary deoxyribonucleic acid
ChIP	Chromatin immunoprecipitation
Chl	Chlorophyll
CHS	CHALCONE SYNTHASE
CK	Cytokinin
Co-IP	Co-immunoprecipitation
COP1	CONSTITUTIVELY PHOTOMORPHOGENIC 1
CRY1	CRYPTOCHROME 1
Ct	Cycle threshold
DDI	Days of dark incubation
DI	Dark incubation
DIN	DARK-INDUCIBLE
DIS	Dark-induced senescence
DLS	Developmental leaf senescence
DNA	Deoxyribonucleic acid
EC	Evening complex
EEL	ENHANCED EM LEVEL
EIN2/3	ETHYLENE INSENSITIVE 2/3
EL	Electrolyte leakage
ELF3/4	EARLY FLOWERING 3/4
ELISA	Enzyme-linked immunosorbent assay
EMSA	Electrophoretic mobility shift assay
FR	Far-red light
FW	Fresh weight
GA	Gibberellic acid

GA20ox2	GIBBERELLIN 20-OXIDASE 2
GA2ox1	GIBBERELLIN 2-OXIDASE 1
GFP	Green fluorescent protein
GHG	Greenhouse gas
GLK1/2	GOLDEN2-LIKE 1/2
HAT	High ambient temperature
HCAR	7-hydroxymethyl Chl *a* reductase
HFR1	LONG HYPOCOTYL IN FAR-RED 1
HPLC	High-performance liquid chromatography
HY5	ELONGATED HYPOCOTYL 5
HYH	HY5-HOMOLOG
JA	Jasmonic acid
LAT	Low ambient temperature
LED	Light-emitting diode
LUX	LUX ARRHYTHMO
MES	2-Morpholinoethanesulfonic acid
Mg^{2+}	Magnesium ion
mIR	Micro ribonucleic acid
mRNA	Messenger ribonucleic acid
N	Nitrogen
NAC	NAM, ATAF, and CUC
NAP	NAC-LIKE, ACTIVATED BY AP3/PI
NCC	Non-fluorescent chlorophyll catabolite
NOL	NYC1-like
NYC1	NON-YELLOW COLORING 1

NYE1/2	NON-YELLOWING 1/2
ORE1	ORESARA 1
OX	Overexpressing
P	Phosphorous
PAM	Pulse-amplitude-modulation
PAO	PHEOPHORBIDE α OXYGENASE
PAR	Photosynthetically active radiation
pFCC	Primary fluorescent chlorophyll catabolite
Pfr	Photoactivated phytochrome B
phyB	Phytochrome B
PIF	PHYTOCHROME INTERACTING FACTOR
PP2C	Type 2C PROTEIN PHOSPHATASE
PPH	Pheophytinase
Pr	Inactive phytochrome B
Pro	Proline
PYL9	PYRABACTIN RESISTANCE 1-LIKE 9
qPCR	Quantitative polymerase chain reaction
R	Red light
RAV1	RELATED TO ABA-INSENSITIVE 3/VP1
RCC	Red chlorophyll catabolite
RCCR	Red chlorophyll catabolite reductase
RING	Really interesting new gene
RNA	Ribonucleic acid
RNA-Seq	Ribonucleic acid sequencing
ROS	Reactive oxygen species

RUP1/2	REPRESSOR OF UV-B PHOTOMORPHOGENESIS 1/2
S	Sulphur
SA	Salicylic acid
SAG	Senescence-associated gene
SAXS	Small-angle X-ray scattering
SD	Standard deviation
SEM	Standard error of the mean
SEN4	SENESCENCE 4
SGR1/2	STAY-GREEN 1/2
SL	Strigolactone
SnRK2	SUCROSE NONFERMENTING 1-RELATED PROTEIN KINASE 2
SPA	Suppressor of phytochrome A
TAA1	TRYPTOPHAN AMINOTRANSFERASE OF ARABIDOPSIS 1
TAE	Tris-acetate
TR-SFX	Time-resolved serial femtosecond crystallography
Trp, W	Tryptophan
UV	Ultraviolet
UV-B^{LD}	Low-dose UV-B
UVR8	UV RESISTANCE LOCUS 8
UVR8^{C27}	UVR8 C-terminal 27 amino acid domain
Val	Valine
VP	Valine-proline
WL	White light
WRKY36	WRKY DNA-BINDING PROTEIN 36
YUC8	YUCCA8

Chapter 1

Introduction

Contents

1.1. Senescence . . . 2
1.2. Leaf senescence . . . 3
1.2.1. Chloroplast and chlorophyll degradation . . . 4
1.2.2. Leaf yellowing and the senescence syndrome . . . 4
1.2.3. Late-stage leaf senescence . . . 5
1.2.4. Molecular regulation of leaf senescence . . . 6
1.3. Dark-induced leaf senescence . . . 7
1.3.1. Molecular regulation of DIS . . . 8
1.4. Suppression of DIS . . . 9
1.4.1. Light signalling and light-mediated DIS suppression . . . 10
1.4.2. Temperature signalling and thermal DIS suppression . . . 16
1.5. Conclusions and perspectives . . . 17

The world population is expected to reach ~11 billion by the end of the century. It is predicted that this will drive a 60–80% increase in global demand for food (UN DESA, 2019; Depenbusch & Klasen, 2019). However, recent estimates indicate that the current growth rate of agricultural productivity is insufficient to meet future food requirements (Steensland & Thompson, 2020). Agricultural production is often driven by intensive applications of external inputs, such as water, synthetic fertilisers, and pesticides, and extensive agricultural expansion (Ramankutty *et al.*, 2008). Our reliance on these methods poses a serious environmental threat and is linked to declining biodiversity and increased rates of soil erosion and greenhouse gas (GHG) emission (Ramankutty *et al.*, 2018). These effects may exacerbate shortcomings in agricultural productivity by reducing pollinator abundance and soil quality whilst increasing the likelihood of extreme weather events (Ramankutty *et al.*, 2018). Additionally, more than one-third of all ice-free land is now used for agriculture, and

continued land conversion is unsustainable (FAOSTAT, 2019). To safeguard future food security, it is therefore essential to develop sustainable solutions to pre- and postharvest inefficiencies in the global food production system.

Approximately one-third of food crops grown globally, around 1.3 billion tonnes annually, never reach the consumer and are wasted in the supply chain–significantly constraining global agricultural efficiency (Gustavsson *et al.*, 2011). This figure can be partly attributed to the high cosmetic standards held by consumers and retailers for grown produce. Specifically, many retailers consider misshapen and miscoloured foods unsalable, resulting in their wastage. Dark-induced senescence (DIS) is a degenerative process that promotes the yellowing of leaves and is a leading cause of postharvest cosmetic depreciation in leafy vegetables. After harvest, crops are transported and stored in darkness as they progress through supply chains that are long and complex. This form of prolonged light deprivation triggers DIS-associated leaf yellowing, limiting the commercial storage life of crops and contributing to high levels of waste (Ahlawat & Liu, 2021). Advancing our understanding of the mechanisms governing DIS and developing strategies for DIS suppression are therefore of both agricultural and economic relevance.

This introduction will initially provide an overview of senescence, its occurrence in leaves, the emergent physiological processes of the senescent leaf and their adaptive evolutionary benefits. It will then outline the current understanding of the molecular mechanisms regulating leaf senescence and DIS in the *Arabidopsis thaliana* (Arabidopsis) model system. Finally, light- and temperature-based approaches to postharvest DIS suppression—strategies amenable to horticultural systems—will be critically evaluated. Whilst knowledge of DIS regulation and suppression in Arabidopsis may not directly translate into crops, insight in this model system will enhance the understanding of DIS in other plant species.

1.1. Senescence

The word ‘senescence’ derives from the Latin verb *“senēscere”*, meaning ‘to grow old’, or ‘to be in decline’. It describes a complex degenerative process that occurs universally in the aged cells of living organisms (Gan, 2018). In plants, senescence is characterised by physiological, transcriptomic, and biochemical changes. These include the ordered degradation of intracellular organelles and macromolecules, including proteins, nucleic acids, and chlorophyll (Chl) *a* and *b*, and the translocation of nutrients such as nitrogen (N), phosphorous (P), and sulphur (S) from senescent to developing tissues (Schippers *et al.*, 2015). Senescence can therefore be viewed as a recycling process used to maximise nutrient use efficiency.

Senescence occurs at all biological levels, and at the organism level precedes plant death. This process is typical of monocarpic plants, in which reproductive growth triggers senescence of the entire organism to support seed and fruit development (Gan, 2018). As such, individual survival is forgone to ensure optimal offspring production. Senescence also continuously occurs in a modular fashion throughout the plant lifecycle at the cellular, tissue, and organ levels to support the growth of

shoots, young leaves, flowers, and seeds (Guo *et al.*, 2021). Senescence is tightly genetically controlled. Transcriptomic and mutagenic studies have identified genes upregulated specifically during senescence, known as 'senescence-associated genes' (SAGs). To date, 5853 SAGs across 68 plant species have been manually curated and comprehensively databased (Li *et al.*, 2020b). These efforts have identified candidate SAGs for functional analysis, enabling significant advancement to our understanding of senescence.

1.2. Leaf senescence

At the organ level, senescence occurs conspicuously in leaves, a system of nutrient-rich photosynthetic structures responsible for chemical energy production. Leaf senescence is the final stage of leaf development and occurs ubiquitously in higher plants (Ali *et al.*, 2018). This process initiates and progresses autonomously in an age-dependent manner or in response to reproductive growth, termed 'developmental leaf senescence' (DLS; Rosenthal & Camm, 1996). Leaf senescence is also prematurely induced as an adaptive response to environmental stressors. These include nutrient deprivation, salt stress, drought, extremes of temperature, pathogen attack, wounding, and prolonged darkness (reviewed by Schippers *et al.*, 2015; Ali, Gao and Guo, 2018). Mass spectrometry and long-term pulse-chase isotope labelling have been used to quantify ^{15}N and ^{34}S flux in oilseed rape (*Brassica napus*) as a physiological marker of senescence-associated nutrient remobilisation. These experiments demonstrated that leaf senescence induced under N- and S-limiting conditions facilitates extensive N and S redistribution which sustains vegetative growth for up to six weeks (Abdallah *et al.*, 2010; Girondé *et al.*, 2015). Stress-induced leaf senescence therefore constitutes an evolutionary survival strategy that maximises individual and reproductive fitness under unfavourable growth conditions.

The advent of genome-scale analytical techniques such as microarray technology, combined with forward genetic screening, has rapidly enhanced our understanding of the mechanisms underlying leaf senescence. Several global transcriptome analyses have compared the molecular events of DLS and stress-induced leaf senescence in Arabidopsis, revealing similarities as well as differences in their gene expression profiles (Buchanan-Wollaston *et al.*, 2005; van der Graaff *et al.*, 2006; Guo & Gan, 2012; Allu *et al.*, 2014). A comparative time-course transcriptome study of leaves undergoing either DLS or one of 27 senescence-inducing stress treatments also demonstrated that each initially activates a distinct pattern of gene expression which converge as senescence progresses (Guo & Gan, 2012). This suggests that whilst DLS and stress-induced senescence are initiated by discrete signal transduction mechanisms, these trigger the expression of a shared complement of SAGs. So far, 3852 SAGs have been identified and extensively annotated in Arabidopsis, with putative roles in molecular degradation and transportation, transcriptional control, and stress tolerance (Li *et al.*, 2020b). Whilst the functions of many SAGs remain poorly understood, several, such as *SAG12*, *SAG13*, and *EIN3*, have become well characterised and are used as transcriptional markers of age-, dark- and ethylene-induced leaf senescence, respectively (Liu *et al.*, 2011; Zhao *et al.*, 2018).

1.2.1. Chloroplast and chlorophyll degradation

Chloroplasts, including Chl *a* and *b* pigments, constitute ~80% of total leaf N content and are the first in a sequence of intracellular components to be dismantled during leaf senescence (Dodge, 1970; Makino *et al.*, 2003). Forward genetic screens have identified stay-green mutants in which Chl degradation is impaired. Targeted studies in these plants have identified Chl catabolic genes (CCGs) and the stepwise biochemical programme of Chl degradation. For a comprehensive review of this process, readers are directed to Kuai *et al.* (2018).

Chl *a* and *b* pigments are degraded by Chl catabolic enzymes (CCEs). These include STAY-GREEN 1 (SGR1) and SGR2 (also named NON-YELLOWING 1 [NYE1] and NYE2), NON-YELLOW COLORING 1 (NYC1) and PHEOPHORBIDE α OXYGENASE (PAO), in the 'PAO/phyllobilin' pathway (Kuai *et al.*, 2018). The breakdown of Chl *b* first requires its conversion to Chl *a* due to the specificity of CCEs for Chl *a* and its metabolites (Shimoda *et al.*, 2016). Thus, before Chl *b* is degraded, it is reduced in a sequential two-step reaction catalysed by Chl *b* reductases: (1) NYC1 and its paralog NYC1-like (NOL) catalyse Chl *b* reduction, yielding 7-hydroxymethyl Chl *a*; (2) 7-hydroxymethyl Chl *a* is further reduced by 7-hydroxymethyl Chl *a* reductase (HCAR) completing Chl *b* to Chl *a* conversion (Kusaba *et al.*, 2007; Sato *et al.*, 2009; Horie *et al.*, 2009; Meguro *et al.*, 2011).

Chl *a* breakdown begins with the removal of a central magnesium ion (Mg^{2+}) and phytol in dechelation, and subsequent hydrolysis reactions. These are catalysed by SGR1 and SGR2, two Mg-dechelatases, and pheophytinase (PPH), respectively, yielding the intermediate compound pheophorbide α (Schelbert *et al.*, 2009; Shimoda *et al.*, 2016). Subsequent oxygenolytic opening of the pheophorbide α porphyrin ring is mediated by PAO, producing red Chl catabolite (RCC; Pružinská *et al.*, 2003). RCC reductase (RCCR) catalyses further RCC reduction, yielding primary fluorescent Chl catabolite (*p*FCC). Finally, *p*FCCs isomerise into colourless non-fluorescent Chl catabolites (NCCs) in a low pH-dependent reaction (Pružinská *et al.*, 2007; Oberhuber *et al.*, 2008). Interestingly, high-performance liquid chromatography (HPLC) and spectroscopic analysis of linoleic acid hyperperoxide formation has shown that NCCs function as antioxidants, indicating that NCCs may contribute to the conservation of cell integrity during Chl degradation (Müller *et al.*, 2007).

1.2.2. Leaf yellowing and the senescence syndrome

As leaf senescence progresses, leaf Chl content and photosynthetic capacity fall, electrolyte leakage (EL) increases, and a conspicuous transition from green to yellow occurs, known as 'leaf yellowing' (Fig. 1; Lutts *et al.*, 1996; Miersch *et al.*, 2000). These symptoms are collectively termed the 'senescence syndrome' and can be quantified to determine the rate at which leaf senescence progresses. Specifically, Chl pigment abundance can be estimated by spectrophotometry, photosynthetic efficiency by pulse-amplitude-modulation (PAM) fluorometry, and ion leakage rate by electroconductivity assessment (Sakuraba *et al.*, 2014a). These physiological assays are frequently combined with quantitative real-time polymerase chain reaction (qPCR) to determine the expression levels of senescence marker genes,

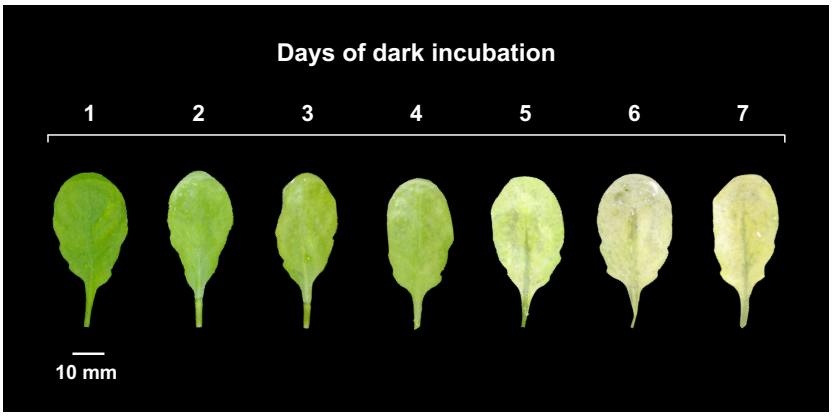

Figure 1. The progression of visible yellowing in fourth rosette leaves of four-week-old Arabidopsis during seven days of dark incubation at 20°C.

such as *ORESARA 1* (*ORE1*), *SGR1*, *SENESCENCE 4* (*SEN4*) and *SAG12* (Sakuraba *et al.*, 2014a; Kim *et al.*, 2020).

Leaf yellowing is the visible manifestation of leaf senescence, a phenotype resulting from the 'unmasking' of carotenoid pigments (Hörtensteiner & Lee, 2007). During DLS, yellowing typically initiates at the leaf tip and progresses towards the base, where cell integrity is preserved to enable efficient nutrient export (Buchanan-Wollaston *et al.*, 2005). By contrast, DIS promotes yellowing that is mostly uniform across the leaf surface. Several comparative transcriptomic studies have demonstrated similar patterns of gene expression during DLS and DIS; specifically, 291 genes are commonly upregulated whilst 191 genes are commonly downregulated (Buchanan-Wollaston *et al.*, 2005; van der Graaff *et al.*, 2006). The uniform progression of DIS and its inferred mechanistic similarity to DLS has made it a popular model for the study of senescence processes (Buchanan-Wollaston *et al.*, 2005).

1.2.3. Late-stage leaf senescence

In contrast to the early fates of chloroplasts and Chl pigments, mitochondria and cell nuclei are conserved until even the latest stages of leaf senescence (Keech *et al.*, 2007). This is supported by recent laser confocal and electron microscopic analyses in transgenic Arabidopsis expressing mitochondrially-targeted green fluorescence protein (β-ATPase-GFP). This approach demonstrated that whilst chloroplast integrity and functionality are readily compromised in the senescent leaf, mitochondrial ultrastructure is preserved even in the latest stages of leaf senescence (Chrobok *et al.*, 2016). Quantification of mitochondrial respiration and adenylate phosphorylation state analyses also demonstrated continuous mitochondrial respiration until late-stage leaf senescence. These results indicate that mitochondria are functionally conserved to sustain energy production throughout leaf senescence, a requirement for the export of cell hydrolysates (Chrobok *et al.*, 2016).

Once maximum nutrient remobilisation is achieved, fully senesced, dead leaves abscise and drop from the plant (Smart, 1994). This mode of self-pruning confers further fitness advantages. For example,

leaf abscission resulting from drought-induced senescence limits transpirational water loss, thus improving plant water-use efficiency (Zhao *et al.*, 2017). Moreover, the abscission of leaves hosting pests or pathogens spatially separates affected organs from healthy tissues, reducing the probability of reinfestation or reinfection (Williams & Whitham, 1986).

1.2.4. Molecular regulation of leaf senescence

Phytohormones are critical components of the molecular mechanism regulating leaf senescence, a network that has been reviewed extensively (Pyung *et al.*, 2007; Schippers *et al.*, 2015; Kim *et al.*, 2018a; Woo *et al.*, 2019; Guo *et al.*, 2021). Ethylene, abscisic acid (ABA), jasmonic acid (JA), salicylic acid (SA), and strigolactones (SLs) promote leaf senescence, whilst cytokinins (CKs), gibberellic acid (GA) and auxin suppress leaf senescence (Schippers *et al.*, 2015; Guo *et al.*, 2021). Leaf senescence is also controlled at the transcriptional level by hundreds of senescence-associated transcription factors. These include members of basic helix-loop-helix (bHLH), NAM, ATAF, and CUC (NAC), basic leucine zipper (bZIP), WRKY, AP2/EREPB, C2H2 zinc-finger and MYB families (Balazadeh *et al.*, 2008; Kim *et al.*, 2018a). Evidence also supports senescence regulation at the post-transcriptional, translational, and post-translational levels, highlighting the complexity of leaf senescence regulation (reviewed by Guo *et al.*, 2021). Given this intricacy, it is likely that a significant number of regulatory mechanisms and their associated components remain undiscovered. Ethylene- and ABA-mediated senescence regulation is well understood, and summaries of their respective signalling cascades are provided. See Woo *et al.* (2019) for an in-depth review.

1.2.4.1. Ethylene

Ethylene is a gaseous phytohormone and a key positive regulator of leaf senescence (Bleecker & Kende, 2000). Supporting this function for ethylene, physiological analyses have shown that exogenous ethylene applications accelerate leaf senescence, whilst ethylene inhibitors retard leaf senescence (Abeles *et al.*, 1988; Wang *et al.*, 2001). RNA sequencing (RNA-Seq) and microarray analyses have also demonstrated the upregulation of genes involved in ethylene biosynthesis and signalling during leaf senescence (van der Graaff *et al.*, 2006; Song *et al.*, 2014).

ETHYLENE INSENSITIVE 2 (EIN2) initiates ethylene signalling by triggering the expression of *EIN3*, a central transcription factor in the positive regulation of ethylene signalling. EIN3 directly activates the expression of the NAC transcription factors *ORE1* and *NAC-LIKE, ACTIVATED BY AP3/PI* (*NAP*), two master promoters of leaf senescence with both redundant and distinct functions in the upregulation of hundreds of SAGs (Kim *et al.*, 2014). EIN2 and EIN3 also repress the transcription of *microRNA* (*miR*)*-164*, a post-translational ORE1 repressor, resulting in enhanced ORE1 activity (Kim *et al.*, 2009; Li *et al.*, 2013).

Together, EIN3 and ORE1 form a coherent feed-forward loop to induce the co-expression of several CCGs (Sakuraba *et al.*, 2014a). These include *NYC1*, *SGR1*, and *PAO* (Kuai *et al.*, 2018). Integrative bimolecular fluorescence complementation (BiFC) and qPCR analyses have shown that ORE1 also forms

non–DNA-binding heterodimers with GOLDEN2-LIKE 1 (GLK1) and GLK2, two partially redundant transcription factors controlling Chl development and maintenance, thus disrupting GLK1 and GLK2 signalling (Rauf *et al.*, 2013). In addition, chromatin immunoprecipitation (ChIP) and qPCR data suggest that ORE1 directly activates the expression of *ACS2*, a gene responsible for ethylene biosynthesis, establishing a positive feedback loop to magnify downstream effects (Qiu *et al.*, 2015).

1.2.4.2. Abscisic acid

Exogenously applied ABA causes leaf senescence to accelerate in Arabidopsis, and 40% of ABA biosynthesis and signalling genes are upregulated during DLS (van der Graaff *et al.*, 2006; Lee *et al.*, 2011). These results are corroborated by competitive enzyme-linked immunosorbent assays (ELISAs), which demonstrated a ~20-fold enrichment in ABA concentration in Arabidopsis leaves undergoing DIS (Yang *et al.*, 2014).

ABA signalling is initiated by activation of the ABA receptor PYRABACTIN RESISTANCE 1-LIKE 9 (PYL9). In response to ABA, PYL9 inhibits the activity of clade A type 2C PROTEIN PHOSPHATASEs (PP2Cs), a group of post-translational repressors of subclass III SUCROSE NONFERMENTING 1-RELATED PROTEIN KINASE 2s (SnRK2s), thus restoring SnRK2 kinase activity (Zhao *et al.*, 2016). Phosphorylation targets of SnRK2s include the bZIP transcription factors ABA INSENSITIVE 5 (ABI5), ENHANCED EM LEVEL (EEL), ABA-responsive element (ABRE) BINDING FACTOR 2 (ABF2), ABF3, and ABF4, and RELATED TO ABA-INSENSITIVE 3/VP1 (RAV1; Zhao *et al.*, 2016). Phosphorylated ABF2 and RAV1 promote *NAP* and *ORE1* expression by interacting with their promoters at ABRE and RAV1-binding motifs (Zhao *et al.*, 2016). Once expressed, NAP activates the expression of *SAG113*, a gene controlling senescence-related stomatal movement, and *ABSCISIC-ALDEHYDE OXIDASE 3* (*AAO3*), a gene regulating ABA biosynthesis, establishing a positive feedback loop (Zhang *et al.*, 2012; Yang *et al.*, 2014).

Phosphorylated ABI5, EEL, ABF2, ABF3, and ABF4 activate the expression of CCEs such as *SGR1*, *NYC1*, and *PAO* by binding their promoters at ABRE motifs (Sakuraba *et al.*, 2014a; Gao *et al.*, 2016). Electrophoretic mobility shift assays (EMSAs) have also demonstrated ABF4 binding at the *SGR2* promoter, a close *SGR1* paralog (Gao *et al.*, 2016). SGR2 localises to the chloroplasts and partially compensates for SGR1 function in its absence, indicating that SGR2 functions as a CCE, although this is disputed (Sakuraba *et al.*, 2014b; Wu *et al.*, 2016). ABA also activates the expression *EIN2*, causing further expression of *ORE1* and *NAP* (see section 1.2.4.1; Wang *et al.*, 2007).

1.3. Dark-induced leaf senescence

Solar radiation is intercepted by dense canopies and competing vegetation, casting shade on lower leaf strata (Huber *et al.*, 2021). As sessile organisms, plants cannot physically escape shade. Instead, they have evolved a suite of dark-inducible phenotypic responses to outcompete neighbouring plants and forage for light, termed ‘shade avoidance’. These responses are species-specific and include leaf hyponasty, accelerated stem and petiole growth, and new leaf formation on upper shoots (Franklin, 2008; Casal,

2013). Shade avoidance is supported by DIS, which mediates extensive nutrient remobilisation in light deficient environments. Physiological analyses in Arabidopsis have shown that DIS initiates rapidly in dark-incubated leaves (Weaver & Amasino, 2001; Keech *et al.*, 2007). These results are corroborated by northern blot analyses demonstrating the upregulation of multiple SAGs of the *DARK-INDUCIBLE* (*DIN*) family within three hours of transfer to darkness (Fujiki *et al.*, 2001). These findings highlight the importance of light signalling in senescence regulation.

1.3.1. Molecular regulation of DIS

Significant progress has been made towards understanding the molecular regulation of DIS in Arabidopsis, particularly by PHYTOCHROME-INTERACTING FACTORs (PIFs).

1.3.1.1. Phytochrome-interacting factors

PIFs (1–8) are a sub-family of bHLH transcription factors that physically interact with the phytochrome B (phyB) photoreceptor and perform a multitude of roles in light-regulated plant development (reviewed by Pham *et al.*, 2018a). PIFs 4 and 5 (PIF4/5) are known to function as master regulators of DIS, with an additional potential role for PIF3 identified (Song *et al.*, 2014; Sakuraba *et al.*, 2014b). The transcript and protein abundance of PIF4/5 increase in dark-incubated Arabidopsis leaves, together with transcript levels of *PIF3* (Song *et al.*, 2014; Sakuraba *et al.*, 2014b). To determine the individual functions of PIFs in DIS, physiological and transcriptomic markers of DIS were analysed in PIF-deficient mutants. DIS was retarded in *pif4*, *pif5*, and *pif4pif5* mutants and accelerated in the corresponding PIF-overexpressing (-OX) lines (Song *et al.*, 2014; Sakuraba *et al.*, 2014b; Zhang *et al.*, 2015; Kim *et al.*, 2020; Ueda *et al.*, 2020). In contrast to the work of Song *et al.* (2014), which found that DIS was delayed in *pif3* mutants, Kim *et al.* (2020) observed that DIS progressed similarly in *pif4pif5* and *pif1pif3pif4pif5* (*pifQ*) mutants, indicating that PIF1 and PIF3 may not function in DIS regulation (Kim *et al.*, 2020). Together, these results suggest that PIFs have both redundant and distinct functions and that, amongst PIFs, PIF4/5 are the principal positive regulators of DIS. Further work in *pif2*, *pif6*, *pif7*, and *pif8* mutants will be necessary to establish their involvement in DIS regulation.

Immunoblot analyses have shown that PIF4 and PIF5 abundance is reduced in mutants deficient in the master photomorphogenic repressor and 'really interesting new gene' (RING)-finger E3 ubiquitin ligase, CONSTITUTIVELY PHOTOMORPHOGENIC 1 (COP1; Pham *et al.*, 2018b,c; Sharma *et al.*, 2019), whilst immunoprecipitation assays evidence direct COP1–PIF5 interaction (Sharma *et al.*, 2019). PIF4/5 degradation is impaired in the presence of a proteasome inhibitor (Xu *et al.*, 2017), suggesting that dark-induced PIF4/5 accumulation is attributable to COP1–PIF4/5 binding. This interaction may prevent the degradation of PIF4/5 by the 26S proteasome.

Comparative transcriptome and ChIP-qPCR analyses have uncovered several PIF4/5 target genes bound at G-box motifs (CACGTG; Song *et al.*, 2014; Sakuraba *et al.*, 2014a; Zhang *et al.*, 2015). These approaches have shown that PIF4/5 directly activate the expression of *ORE1* (Sakuraba *et al.*, 2014b; Zhang *et al.*, 2015). PIF4 and PIF5 also positively regulate ethylene and ABA signalling by triggering

the expression of *EIN3*, and *ABI5* and *EEL*, respectively (see section 1.2.4; Song *et al.*, 2014; Sakuraba *et al.*, 2014a). EIN3, ABI5, and EEL bind to the *ORE1* promoter at EIN3 and ABRE motifs, further enhancing *ORE1* transcription (Sakuraba *et al.*, 2014b). Thus, PIF4/5, EIN3, ABI5, and EEL form multiple coherent feed-forward loops to induce the expression of *ORE1*, which mediates global transcriptional reprogramming towards DIS (Sakuraba *et al.*, 2014a). ChIP-qPCR and EMSA analyses have shown that PIF4/5 also bind to the *SGR1* promoter, and PIF5 binds to the *NYC1* promoter, resulting in their activation (Song *et al.*, 2014; Zhang *et al.*, 2015). Similar research has demonstrated that EIN3, ABI5, EEL, and ORE1 directly trigger the expression of *SGR1*, *NYC1*, and *PAO* (Sakuraba *et al.*, 2014b; Qiu *et al.*, 2015). Thus, PIF4/5 and their target transcription factors form further coherent feed-forward loops to enhance CCG expression.

1.3.1.2. Experimental variation among DIS analyses

qPCR analysis by Ueda *et al.* (2020) found that *PIF4/5* transcription was unaffected by dark incubation (DI), a result that contradicts research by Song *et al.* (2014) and Sakuraba *et al.* (2014a). This discrepancy could be due to differences in the age of experimental leaves or photoperiodic differences. Specifically, Ueda *et al.* (2020) used the seventh and eighth rosette leaves of plants grown under short days, whilst Song *et al.* (2014) and Sakuraba *et al.* (2014a) used the third, fourth, and fifth rosette leaves of plants grown under long days.

Song *et al.* (2014) also reported that DIS was significantly delayed in *pif3* mutants, indicating that PIF3 may regulate DIS. This finding contradicts research by Sakuraba *et al.* (2014a) and Zhang *et al.* (2015). Similar leaf age differences may explain this contradiction. Specifically, Song *et al.* (2014) used the third and fourth rosette leaves of four-week-old plants, whilst Sakuraba *et al.* (2014a) and Zhang *et al.* (2015) used the fourth and fifth, and the entire rosette of three-week-old plants, respectively.

Leaf attachment and DI conditions also vary in the existing literature. For example, Song *et al.* (2014) excised leaves for individual DI in hermetically sealed Petri plates. By contrast, Zhang *et al.* (2015) dark-incubated entire plants whose leaves were subsequently detached for analysis. The former incubation condition risks the accumulation of gaseous ethylene, which may have accelerated DIS relative to other investigations (see section 1.2.4.1). Similar studies have performed DI on saturated filter paper, water, or MES buffer solution, whilst others have used covers to individually darken attached leaves (van der Graaff *et al.*, 2006; Keech *et al.*, 2007; Yang *et al.*, 2014; Sakuraba *et al.*, 2014b; Kim *et al.*, 2018b). These contradictions and methodological variations indicate that differences in experimental procedure might influence DIS. A standard protocol for DIS investigation will increase the comparability of future research.

1.4. Suppression of DIS

Genetic engineering provides a potential means to suppress leaf senescence. Specifically, knockout of signalling components such as *ORE1*, *ABI5*, *EEL*, *EIN3*, or *PIF4/5* has been shown to delay the onset of DIS (Woo *et al.*, 2002; Sakuraba *et al.*, 2014b; Ueda *et al.*, 2020). However, these modifications are associated

with agriculturally undesirable developmental effects (Oh *et al.*, 1997). Furthermore, restrictions surrounding the use of genetically modified crops limit the practicality of this approach. Here we integrate an understanding of Arabidopsis photo- and thermosensory mechanisms to review potential light- and temperature-mediated DIS suppression strategies. These derive from recent advances to our understanding of molecular-level DIS regulation by the red light (R) and ultraviolet (UV)-B photoreceptors, phytochrome B (phyB) and UV RESISTANCE LOCUS 8 (UVR8), respectively.

1.4.1. Light signalling and light-mediated DIS suppression

Photosynthetically active radiation (PAR; 400–700 nm) is absorbed by Chl pigments and drives carbon fixation by photosynthesis (McCree, 1971). Plants have also evolved a battery of non-photosynthetic photosensory proteins which enable the perception of a far broader spectral range (300–800 nm). Arabidopsis is known to perceive R and far-red light (FR) using phytochromes (Franklin, 2008), blue and UV-A light using cryptochromes (Lin, 2002), phototropins (Briggs & Christie, 2002) and ZEITLUPE/LOV KELCH PROTEIN 2/FLAVIN-BINDING KELCH REPEAT F BOX 1 (Demarsy & Fankhauser, 2009), and UV-B using UVR8 (Rizzini *et al.*, 2011). These complimentary photoreceptors enable plants to perceive light facets such as spectral composition, intensity, direction, and duration. Once photoactivated, photoreceptors trigger a wavelength-specific signalling cascade resulting in adaptive phenotypic responses. Light-induced responses are collectively termed 'photomorphogenesis' and include Chl biosynthesis, leaf and root growth, and suppression of stem elongation (Franklin & Quail, 2010).

The current understanding of R and UV-B signal transduction pathways and their putative mechanisms of DIS suppression is presented. Whilst evidence also supports cryptochrome-, phototropin- and photosynthesis-mediated mechanisms of DIS regulation, these topics are beyond the scope of this review, for which readers are directed to Sakuraba (2021).

1.4.1.1. Red light

R forms part of the visible daylight spectrum and, together with FR, provides a reliable signal of vegetation proximity and density (Franklin, 2008). When plants are grown openly, the R:FR ratio of incident sunlight is around 1.1–1.2. However, within dense vegetation, interception of R and reflection and transmission of FR by neighbouring plants reduces this ratio to as low as 0.23. Under severe shading or darkness, this value can become further reduced (Smith, 1982, 2000). Phytochromes promote photomorphogenic responses under high R:FR, whereas reduced phytochrome activity promotes shade avoidance under low R:FR (Franklin, 2008). Phytochrome-mediated R and FR (R/FR) signalling is therefore critical to optimising light acquisition and plant survival.

1.4.1.1.1. Phytochrome B-mediated light signalling In Arabidopsis, phytochromes comprise a family of photoreversible apoproteins (phyA–phyE). Phytochromes are covalently bound to a linear tetrapyrrole chromophore which enables R/FR absorption, known as phytochromobilin (Lagarias & Rapoport, 1980; Franklin & Quail, 2010). *In vivo*, phytochromes form homo- or heterodimers comprised

of a pair of ~1150 amino acid monomers of two photo-interconvertible forms: (1) an inactive, R absorbing ground state (Pr; λ_{max} 660 nm) in which phytochromes are synthesised and (2) a biologically active, FR absorbing state (Pfr; λ_{max} 730 nm; Franklin & Quail, 2010; Burgie & Vierstra, 2015). Thus, three phytochrome dimer species exist (1) Pr–Pr, (2) Pfr–Pr, and (3) Pfr–Pfr (Klose *et al.*, 2015).

Upon R exposure, phytochromes in the Pr base state are photoconverted to active Pfr in a reaction optimised under high R:FR and localise to the nucleus (Franklin & Quail, 2010). Nuclear Pfr interacts with transcription factors such as PIF4/5 to trigger their degradation, resulting in global transcriptional reprogramming towards photomorphogenesis. By contrast, low R:FR promotes the reversion of Pfr to the inactive Pr conformer, stabilising PIF4/5, activating PIF7, and triggering shade avoidance (Fernández-Milmanda & Ballaré, 2021). This photoreversibility produces a dynamic Pr:Pfr ratio known as a 'photoequilibrium' that optimises light responses under variable R:FR (Franklin & Quail, 2010).

1.4.1.1.2. Red light-mediated DIS suppression Symptoms of leaf senescence are suppressed by R in several plant species, including tomato (*Solanum lycopersicum*; Tucker, 1981), mustard (*Sinapis alba*; Biswal, Kasemir and Mohr, 1982), barley (*Hordeum vulgare*; Pfeiffer and Kleudgen, 1980) and Arabidopsis (Sakuraba *et al.*, 2014a). In the latter, R-mediated DIS suppression was abrogated in *phyB* null mutants. Furthermore, DIS was accelerated in *phyB* mutants, whereas DIS was suppressed in *PHYB-OX* lines. Simultaneously, rates of DIS were similar in *phyA*, *PHYA-OX*, and wild-type plants (Sakuraba *et al.*, 2014b). These results indicate that phyB is the principal phytochrome mediating R-inducible DIS suppression in Arabidopsis. However, rates of DIS in *phyC*, *phyD*, and *phyE* mutants must be determined to confirm this hypothesis.

Photoactivated phyB (phyB Pfr) is relocalised from the cytosol to the nucleus and binds to the active phyB-binding (APB) motif at the PIF4/5 N-terminus (Yamaguchi *et al.*, 1999; Lorrain *et al.*, 2008). This results in repression of dark-induced PIF4/5 accumulation under R, an effect that is abolished by subsequent FR treatment (Sakuraba *et al.*, 2014b). R-mediated PIF4/5 degradation is also abolished in the presence of proteasome inhibitors (Park *et al.*, 2004; Shen *et al.*, 2007, 2008; Lorrain *et al.*, 2008). ChIP assays have demonstrated that PIF4 enrichment at target gene promoters is lower under R than in the dark and enhanced in *phyB* mutants (Park *et al.*, 2012, 2018). Collectively, these data suggest that phyB Pfr inhibits PIF4/5 signalling by two modes of action: (1) phyB–PIF4/5 interaction initiates PIF4/5 degradation by the 26S proteasome (2) phyB–PIF4/5 complex formation sequesters PIF4/5 and inhibits their DNA binding (Fig. 2; Park *et al.*, 2018).

Transgenic lines over-expressing the phyB N-terminal 650 amino acids and in the *phyAphyB* mutant background (*PHYBN-OX*) are capable of PIF sequestration but incapable of PIF degradation (Park *et al.*, 2018). This indicates that the N-terminal of phyB is responsible for PIF4/5 sequestration whilst the C-terminal mediates PIF4/5 degradation. Further evidence suggests that phytochromes possess kinase function and catalyse PIF phosphorylation, although this role for phyB remains disputed. For a review of this discussion, see Favero (2020). Contrary to its effect on PIF4 protein abundance, FR-mediated phyB inactivation does not modulate dark-induced *PIF4* transcription, suggesting that phyB does not repress PIFs at the transcriptional level (Kim *et al.*, 2020).

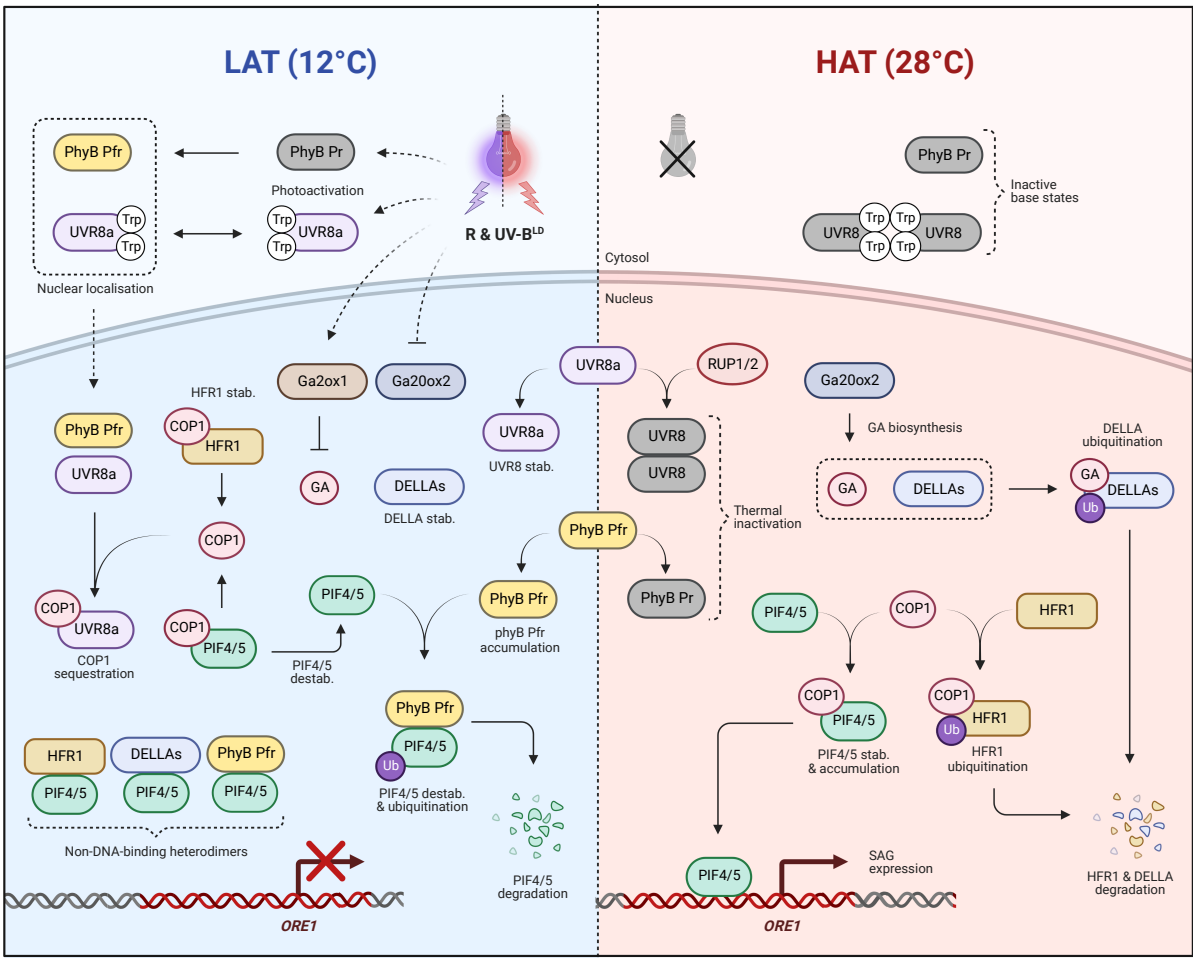

Figure 2. Hypothetical model of red light-, low-dose UV-B-, and low ambient temperature-mediated DIS suppression in Arabidopsis. When plants are supplemented with red light (R) and low-dose UV-B (UV-B^{LD}) and stored at low ambient temperature (LAT; left panel), cytosolic phyB and UVR8 are photoactivated and localise to the nucleus. Thermal inactivation of photoactivated phyB (phyB Pfr) and UVR8 (UVR8a) occurs slowly, causing phyB Pfr and UVR8a to accumulate. Nuclear UVR8a outcompetes HFR1 and PIF4/5 for COP1/SPA (COP1) binding, resulting in HFR1 stabilisation and accumulation and PIF4/5 destabilisation and degradation. Binding of phyB Pfr to PIF4/5 triggers the ubiquitination and degradation of PIF4/5. UV-B^{LD} activates the expression of *Ga2ox1* and represses the expression of *Ga20ox2*, resulting in reduced levels of GA and the stabilisation and accumulation of DELLA proteins (DELLAs). HFR1, DELLAs, and phyB Pfr each form non–DNA-binding heterodimers with PIF4/5, preventing the activation of PIF4/5 targets, including *ORE1*. When plants are not supplemented with R and UV-B^{LD} and stored at high ambient temperature (HAT; right panel), cytosolic phyB and UVR8 remain in their inactive base states. Residual phyB Pfr and UVR8a are inactivated by thermal reversion and RUP1/RUP2 (RUP1/2), respectively. Ga20ox2 activity promotes the biosynthesis of GA, which binds to DELLAs and triggers their ubiquitination and degradation. COP1 binds to HFR1 and PIF4/5, resulting in HFR1 ubiquitination and degradation, and PIF4/5 stabilisation and accumulation. PIF4/5–COP1 complexes activate the expression of *ORE1*, which triggers SAG expression. Created with BioRender.com.

1.4.1.2. UV-B radiation

Solar UV radiation comprises three wavebands: UV-A (315–400 nm); UV-B (280–315 nm); and UV-C (100–280 nm; Björn, 2015). UV-B and UV-C are high-energy and cytotoxic, causing damage to biomolecules, including DNA and photosynthetic components, and stimulating the generation of harmful reactive oxygen species (ROS; Hollósy, 2002). UV-C and high-frequency UV-B wavelengths (≤ 290 nm) are filtered by stratospheric ozone and do not reach the Earth's surface (Paul & Gwynn-Jones, 2003). Thus, solar UV-B is significantly attenuated in the biosphere (Aphalo, 2017). The identification of the first UV-B–specific photoreceptor, UVR8, has enabled a partial understanding of the mechanisms governing UV-B signalling (Rizzini *et al.*, 2011; Wu *et al.*, 2012; Christie *et al.*, 2012). Furthermore, protein crystallographic and small-angle X-ray scattering (SAXS) techniques have been used to solve the tertiary structure of Arabidopsis UVR8, a seven-bladed β-propeller protein comprised of 440 amino acids (Kliebenstein *et al.*, 2002; Wu *et al.*, 2012; Christie *et al.*, 2012; Lau *et al.*, 2019). UVR8 monomers form physiologically inactive homodimers, bound by a network of salt-bridge interactions between complementarily arranged, charged amino acid residues at the homodimer interface. These include arginines (Arg) and aspartic acids (Asp; Rizzini *et al.*, 2011; Christie *et al.*, 2012; Wu *et al.*, 2012; Heilmann *et al.*, 2016).

1.4.1.2.1. Mechanism of UVR8 photoperception UVR8 exploits the UV-B–absorbance of 18 tryptophan (Trp, W) residues. These funnel excitation energy to an additional cluster at the homodimer interface, specifically Trp-94, Trp-233, Trp-285, and Trp-337 (Rizzini *et al.*, 2011; Wu *et al.*, 2012; Christie *et al.*, 2012; O'Hara & Jenkins, 2012; Li *et al.*, 2020a). Trp-233, Trp-285, and Trp-337 are triadically organised and excitonically coupled to Trp-94 on the polar monomer (Christie *et al.*, 2012). Trp-94 forms the apex of a so-called 'Trp pyramid', the reaction centre of UV-B signalling (Christie *et al.*, 2012).

Conservative substitution of Trp for phenylalanine (F) or alanine (A) has been used to assign functions to individual residues of the Trp pyramid (Rizzini *et al.*, 2011; Wu *et al.*, 2012; Christie *et al.*, 2012; O'Hara & Jenkins, 2012). For example, the substitution of Trp-285 for F ($UVR8^{W285F}$) abrogates UV-B perception, indicating that Trp-285 serves this function (Rizzini *et al.*, 2011). Studies quantifying fluorescence emission spectra using fluorescence spectroscopy have demonstrated similar abrogation in $UVR8^{W233F}$ and $UVR8^{W285F}$ proteins (Wu *et al.*, 2012; Christie *et al.*, 2012). The UV-B photosensitivity of $UVR8^{W285A}$, $UVR8^{W233A}$, and $UVR8^{W337A}$ transgenic lines has also been measured using transcriptomic and physiological markers, showing this to be absent, highly reduced, and slightly reduced, respectively (O'Hara & Jenkins, 2012). Together, these results indicate that Trp-285 and Trp-233 are the chromophores of the UVR8 Trp pyramid, whereas Trp-237 appears less critical for UV-B perception.

Upon absorption of UV-B radiation, Trp-285 and Trp-233 residues are excited, causing inter-subunit interactions to be perturbed and the UVR8 homodimer to dissociate into two physiologically active monomers (Rizzini *et al.*, 2011; Wu *et al.*, 2012; Christie *et al.*, 2012). However, the precise photodynamic

mechanism of UV-B–mediated dimer dissociation is disputed. For example, it has been suggested that excitation of Trp-285 and Trp-233 may destabilise intramolecular cation–π interactions between Arg and Trp residues, triggering monomerisation due to a conformational change (Wu *et al.*, 2012). Alternative evidence suggests that excited Trp-285 and Trp-233 may mediate proton-coupled electron transfer, resulting in neutralisation of adjacent Arg and Asp residues and causing UVR8 monomerisation due to the disruption of cross-dimer salt-bridge interactions (Christie *et al.*, 2012; Mathes *et al.*, 2015). Dynamic crystallographic and spectroscopic data also suggest that UV-B may induce the reorientation of Trp-285 and Trp-233 residues, forcing the ejection of a proximal water molecule and destabilising inter-subunit interactions (Heilmann *et al.*, 2015; Zeng *et al.*, 2015). Emergent technologies such as time-resolved serial femtosecond crystallography (TR-SFX) could be used to test these hypotheses. This approach should enable the structural dynamics of UV-B–mediated UVR8 dimer dissociation to be resolved in real-time at a near-atomic resolution.

1.4.1.2.2. UV-B–inducible UVR8–COP1 interaction UV-B acclimation responses are highly impaired in *uvr8* and *cop1* mutants, highlighting the central roles of these components in UV-B signalling (Favory *et al.*, 2009). Studies employing yeast two-hybrid (Y2H) screens and co-immunoprecipitation (Co-IP) have also shown that COP1 forms a complex with SUPPRESSOR OF PHYA-105 (SPA) proteins 1–4 (Hoecker & Quail, 2001; Zhu *et al.*, 2008). In the dark, the COP1–SPA complex (COP1/SPA) modulates the stability of several transcription factors controlling photomorphogenesis (reviewed by Hoecker, 2017). For example, COP1/SPA destabilises the bZIP transcription factors ELONGATED HYPOCOTYL 5 (HY5) and HY5-HOMOLOG (HYH) and the bHLH transcription factor LONG HYPOCOTYL IN FAR-RED 1 (HFR1), triggering their 26S proteasome-mediated degradation (Osterlund *et al.*, 2000; Holm *et al.*, 2002; Xu *et al.*, 2017; Tavridou *et al.*, 2020b). By contrast, COP1/SPA mediates the stabilisation of PIF4/5, resulting in transcriptional reprogramming towards DIS (see section 1.3.1.1; Pham *et al.*, 2018b,c; Sharma *et al.*, 2019; Tavridou *et al.*, 2020a).

Photoactivated UVR8 initiates UV-B signalling by binding COP1/SPA, resulting in their rapid nuclear co-localisation by a poorly-understood COP1-dependent mechanism (Kaiserli & Jenkins, 2007; Favory *et al.*, 2009; Yin *et al.*, 2016; Sharma *et al.*, 2019). UVR8–COP1 binding results from the UV-B–dependent liberation of two distinct UVR8 domains. First, UVR8 monomerisation exposes a β-propeller core domain (amino acids 12–381), which binds to the WD40-repeat domain of COP1 (Favory *et al.*, 2009; Yin *et al.*, 2015). Second, a linear Val-Pro (VP) motif (Val-410 and Pro-411) of the UVR8 C-terminal 27 amino acid domain (UVR8^{C27}; amino acids 397–423) binds to the COP1 WD40-repeat domain under UV-B, stabilising the UVR8–COP1 complex (Cloix *et al.*, 2012; Wu *et al.*, 2013; Yin *et al.*, 2015; Lau *et al.*, 2019). Cooperative action at the UVR8 β-propeller core and C27 domains enable high-affinity UVR8–COP1 binding under UV-B (Lau *et al.*, 2019).

1.4.1.2.3. UV-B–inducible changes to the stability of COP1-targeted transcription factors UV-B–induced binding of UVR8 and COP1 sequesters COP1 from target substrates. These include HY5

and HYH (HY5/HYH), PIF4/5 and HFR1 proteins, resulting in changes to their stability (Holm *et al.*, 2002; Pham *et al.*, 2018c; Lau *et al.*, 2019; Tavridou *et al.*, 2020b).

1.4.1.2.3.1. HY5 and HYH HY5/HYH are central mediators of UV-B–inducible photomorphogenic responses. These proteins are stabilised under UV-B and accumulate as a result of UVR8-mediated COP1 sequestration (Brown & Jenkins, 2008). Photoactivated UVR8 also inhibits WRKY DNA-BINDING PROTEIN 36 (WRKY36), a transcriptional repressor of *HY5*, by direct binding. This interaction promotes *HY5* transcription under UV-B (Yang *et al.*, 2018). HY5/HYH form homo- and heterodimers that bind DNA and trigger UV-B–inducible gene expression, a function for which HY5 appears to be more critical (Holm *et al.*, 2002; Brown & Jenkins, 2008). A recent ChIP analysis and parallel DNA sequencing (ChIP-Seq) has identified 297 target genes for HY5, including *CHALCONE SYNTHASE* (*CHS*) and *MYB12*, two genes involved in the synthesis of UV-B–protectant metabolites, as well as *REPRESSOR OF UV-B PHOTOMORPHOGENESIS 1* (*RUP1*), *RUP2*, *HY5*, and *COP1*, the last of which forms a negative feedback loop to prevent HY5 hyperaccumulation (Binkert *et al.*, 2014; Bischof, 2020).

1.4.1.2.3.2. PIF4 and PIF5 Sequestration of COP1 by UVR8 also disrupts COP1-mediated PIF4/5 stabilisation, causing their 26S proteasome-mediated degradation under UV-B (Fig. 2; Xu *et al.*, 2017; Pham *et al.*, 2018c; Sharma *et al.*, 2019). UVR8–COP1 interaction also disrupts COP1-mediated HFR1 destabilisation, resulting in HFR1 accumulation (Tavridou *et al.*, 2020b). Co-IP analyses have shown that HFR1 and PIF4/5 form non–DNA-binding heterodimers, preventing the activation of PIF4/5 target genes under UV-B (Fig. 2; Hornitschek *et al.*, 2009).

Additionally, UV-B has been shown to stabilise DELLA proteins (DELLAs), a group of homologues under negative regulation by GA, resulting in their accumulation. Two mechanisms achieve this: (1) UV-B upregulates the expression of *GIBBERELLIN 2-OXIDASE 1* (*GA2ox1*), which encodes an enzyme responsible for GA inactivation, in an HY5- and UVR8-dependent manner and (2) UV-B represses the expression of the GA biosynthesis gene *GIBBERELLIN 20-OXIDASE 2* (*GA20ox2*) in a UVR8-dependent manner (Hayes *et al.*, 2014). DELLAs form non–DNA-binding heterodimers with PIF4/5, further disrupting PIF4/5 target gene expression and triggering PIF4/5 degradation by the 26S proteasome (Fig. 2; de Lucas *et al.*, 2008; Li *et al.*, 2016). The E3 ubiquitin ligase responsible for UV-B–induced PIF4/5 ubiquitination is unknown, and this process occurs independently from the known PIF4 E3 ubiquitin ligase, BLADE-ON-PETIOLE 2 (BOP2; Tavridou *et al.*, 2020a).

1.4.1.2.4. Negative feedback regulation of UVR8 signalling UVR8 monomers undergo complete redimerisation within two hours of UV-B exposure (Heijde & Ulm, 2013). This inactivation mechanism is mediated by two negative regulators of UVR8 signalling, RUP1/RUP2 (Heijde & Ulm, 2013; Binkert *et al.*, 2014). Accordingly, *rup1rup2* mutants exhibit hypersensitivity to UV-B, with elevated levels of UV-B–induced transcripts and protectant metabolites (Gruber *et al.*, 2010; Heijde & Ulm, 2013). Immunoblot analyses have shown that UVR8 redimerisation is highly impaired in *rup1rup2* mutants,

whilst quantitative Y2H assays demonstrated RUP1/RUP2 binding to $UVR8^{C27}$ (Cloix *et al.*, 2012; Heijde & Ulm, 2013; Yin *et al.*, 2015). Together, these results indicate that RUP1/RUP2 trigger the reversion of UVR8 to the homodimeric ground state by binding $UVR8^{C27}$. This is supported by proteomic data, which show that UVR8–COP1 binding is reduced in *RUP2-OX* plants and increased in *rup1rup2* mutants (Heijde & Ulm, 2013). UVR8 redimerisation is also unaffected by individual knockout of RUP1 or RUP2. These results indicate that RUP1/RUP2 proteins function redundantly to suppress UV-B signalling by disrupting UVR8–COP1 interaction (Fig. 2; Heijde & Ulm, 2013). This negative feedback regulation mechanism establishes a dynamic UVR8 dimer-to-monomer photoequilibrium that is adjusted depending on the intensity of incident UV-B (Findlay & Jenkins, 2016). However, the precise mechanism of RUP1/RUP2-mediated UVR8 redimerisation is unclear.

1.4.1.2.5. UV-B–mediated DIS suppression Studies have shown that 5–30 minutes of high-intensity UV-B supplementation can suppress DIS-associated Chl degradation in broccoli (*Brassica oleracea* var. *italica*), Tahiti lime (*Citrus latifolia* Tan.), and Arabidopsis (Aiamla-or *et al.*, 2010; Srilaong *et al.*, 2011; Sztatelman *et al.*, 2015). The underlying molecular mechanisms are unknown but are thought to involve the UV-B–induced production of antioxidant compounds. Given the central role performed by PIF4/5 in the promotion of DIS (Song *et al.*, 2014; Sakuraba *et al.*, 2014b), the inhibition and degradation of PIF4/5 by low-dose UV-B ($UV\text{-}B^{LD}$; 1.0–1.5 $\mu mol\, m^{-1}\, s^{-1}$; see section 1.4.1.2.3.2; Hayes *et al.*, 2014, 2017; Sharma *et al.*, 2019; Tavridou *et al.*, 2020a) suggests that $UV\text{-}B^{LD}$ application could be an effective solution to suppress DIS and enhance shelf life in leafy crops.

1.4.2. Temperature signalling and thermal DIS suppression

In nature, plants experience constant fluctuations in their thermal environment (Casal & Balasubramanian, 2019). To avoid heat-induced tissue damage, plants have evolved a suite of thermally regulated morphological adaptations, collectively termed 'thermomorphogenesis' (reviewed by Vu *et al.*, 2019). These responses are mediated by distinct thermosensory mechanisms, which enable the accurate perception of temperature changes within the physiological range, with a central role for PIF4 and PIF7 identified (Vu *et al.*, 2019).

Symptoms of DIS are suppressed in leafy crops stored at low ambient temperatures (LATs). This prolongs postharvest longevity by reducing ethylene production, moisture loss, and pathogen growth (reviewed by Jayas & Jeyamkondan, 2002). Accordingly, the transcript abundance of SAGs such as *ORE15*, *SAG12*, and *NAC29* was lower in leaves of cabbage and kale (*Brassica oleracea*) dark-incubated at 4°C than 25°C (Ahlawat & Liu, 2021). Studies also indicate that LATs can inhibit PIF4 activity by mechanisms involving phyB (Jung *et al.*, 2016; Kim *et al.*, 2020), supporting crosstalk between light and temperature signalling in DIS regulation.

1.4.2.1. Phytochrome B

In addition to its photosensory role, phyB is known to function in temperature perception and may contribute to DIS suppression at LATs. This is attributable to the low thermal stability of phyB Pfr relative to phyB Pr, resulting in enhanced phyB inactivation at elevated temperatures, termed 'thermal reversion' (reviewed by Klose *et al.*, 2020).

To investigate the thermal reversion of phyB *in vivo*, dual-wavelength ratio spectroscopy was conducted to quantify absorbance at 665 and 725 nm at different ambient temperatures as an indicator of phyB Pfr abundance. This study suggested that Pfr abundance and temperature were inversely proportional (Jung *et al.*, 2016). These results are corroborated by independent ChIP-Seq data, demonstrating lower phyB promoter enrichment at 27°C than 17°C (Legris *et al.*, 2016). In another recent study, FR treatments were applied to Arabidopsis leaves during DI. These experiments showed that phyB Pfr remains active for at least four days at 20°C but only two to three days at 28°C (Kim *et al.*, 2020). Finally, an FR treatment before DI accelerated DIS in *PHYB-OX* mutants at 28°C, indicating that although phyB Pfr is capable of DIS suppression at high ambient temperatures (HATs), thermal reversion reduces phyB Pfr abundance to beneath the necessary threshold for this effect (Kim *et al.*, 2020). phyB Pfr negatively regulates PIF4/5 signalling by disrupting PIF4/5–DNA interaction and inducing their 26S proteasome-mediated degradation (see section 1.4.1.1.2; Park *et al.*, 2018). Postharvest storage at LATs may therefore suppress DIS partly by limiting phyB thermal reversion (Fig. 2).

1.4.2.2. UVR8

UVR8 is speculated to contribute to thermosensitivity via the temperature-dependent activity of RUP1/RUP2 (see section 1.4.1.2.4). Immunoprecipitation and immunoblot analyses were used to monitor the kinetics of UVR8 redimerisation following UV-B treatment at different ambient temperatures. This approach demonstrated that UVR8 monomer abundance was suppressed at HATs in wild-type plants but not *rup1rup2* mutants (Findlay & Jenkins, 2016). This suggests that RUP1/RUP2-mediated UVR8 inactivation occurs more slowly at LATs. Photoactivated UVR8 inhibits PIF4/5 signalling via several independent mechanisms (see section 1.4.1.2.3.2). Postharvest storage of sunlight-grown plants at LATs may therefore also suppress DIS by limiting UVR8 redimerisation (Fig. 2).

1.5. Conclusions and perspectives

Research indicates that R, UV-B, and LAT treatments each suppress symptoms of DIS via overlapping signalling pathways involving phyB and UVR8. This crosstalk suggests that light and temperature treatments could have complementary effects. Specifically, PIF4/5 activity could be repressed by R or UV-B treatment and maintained by storage at LAT. Light-emitting diode (LED) technology provides an opportunity to implement supplementary lighting regimes in horticultural systems. Moreover, the growing affordability of modern LEDs and their low operating cost make this approach increasingly

cost-effective (Wargent, 2016). In these experiments, we investigate the effect of UV-B^{LD} treatments on DIS in leaves of Arabidopsis maintained at different ambient temperatures.

CHAPTER 2

Materials and Methods

Contents

2.1. Plant materials and growth conditions . . . 19
2.2. Light treatments . . . 20
2.3. Dark incubation conditions . . . 20
2.4. Leaf chlorophyll quantification . . . 20
2.4.1. Non-destructive chlorophyll measurement . . . 20
2.4.2. Chlorophyll extraction and spectrophotometry . . . 21
2.5. Quantitative reverse-transcription PCR . . . 21
2.5.1. RNA extraction . . . 21
2.5.2. RNA yield and integrity assessment . . . 22
2.5.3. cDNA synthesis . . . 22
2.5.4. Quantitative PCR . . . 22
2.6. Photography . . . 22
2.7. Statistical analysis and graphing . . . 23
2.8. Method development . . . 23
2.8.1. Estimation of initial leaf chlorophyll contents . . . 23

2.1. Plant materials and growth conditions

Seeds of *Arabidopsis thaliana* (L.) Heynh. ecotype Columbia (Col-0) were used in all experiments. Seeds were sown directly into cellular trays (24 cells, each 5 cm^3) containing a pre-saturated 3:1 (v/v) mixture of Levington F2 compost (Scotts Company, Ipswich, UK) and horticultural silver sand (Melcourt, Tetbury, UK). Cellular trays were placed in seed trays (38 × 24 × 5 cm) to permit watering by sub-irrigation. Following stratification for 2 d at 4°C in the dark, seeds were transferred to controlled-environment growth chambers (Microclima 1600E; Snijders Scientific BV, the Netherlands) with a long-day photoperiod (16 h light/8 h dark) at 20°C and 70% relative humidity. White light (WL)

and UV-B radiation were provided by cool-white (TL-D 36 W/840 [300–700 nm]) and UV-B narrowband fluorescent (TL 40 W/01 RS [305–315 nm; λ_{max} 311 nm]) light tubes, respectively (Philips, Eindhoven, the Netherlands). WL was provided at a PAR of 65 ± 5 µmol m^{-1} s^{-1} at plant height. Clear polycarbonate UV-filtering tube guards (6 mm thick) were used to exclude UV-B radiation during growth and WL treatments (for WL spectra, see Supplementary Fig. S1). Seed trays were arranged in a 2×2 configuration and reorganised every 2 d to minimise edge effects. Trays were fitted with transparent propagator lids, which were removed after 4 d. Seedlings were thinned to a single individual per cell at 10 d of age. Trays were irrigated with 500 ml deionised water 2–3 times weekly.

2.2. Light treatments

Four-week-old plants were irradiated at dawn for 4 h (10:00–14:00 h) with either WL (see section 2.1; WL treatment) or WL supplemented with UV-B^{LD} (+UV-B treatment). Supplemental UV-B was attenuated to ~1.0 µmol m^{-1} s^{-1} (~400 mW m^{-2}) using strips of UV-resistant tape applied to the emitting surface in a regular banded pattern (for +UV-B spectra see Supplementary Fig. S1). Subsequent light treatments were provided for 2 h at dawn (10:00–12:00 h) following removal of Petri plate lids. All light measurements were performed with a UV-visible spectroradiometer (FLAME-S-UV–VIS [200–850 nm]; Ocean Optics, FL, USA) equipped with a cosine corrected irradiance probe (CC-3-DA; Ocean Optics) and OceanView software, version 1.5 (Ocean Optics).

2.3. Dark incubation conditions

Unless otherwise stated, only fully expanded fourth and fifth rosette leaves were studied to minimise developmental effects. Leaves were detached by incising at the petiole base and submerged in freshly autoclaved Milli-Q water to remove residual soil matter. Leaves were suspended adaxial side up in separate 50 mm Petri plates containing 8 ml of 5 mM 2-Morpholinoethanesulfonic acid (MES) monohydrate (99+%; Acros Organics, Antwerp, Belgium) buffer solution (pH 5.8). Leaves were dark-incubated in controlled temperature cabinets (EB2E; Snijders Scientific BV) at either 12°C, 20°C, or 28°C for the indicated periods. Unless otherwise stated, each experiment was repeated at least once using independently grown plants.

2.4. Leaf chlorophyll quantification

2.4.1. Non-destructive chlorophyll measurement

Leaf Chl content was measured non-invasively using a Dualex portable Chl meter (Force-A, Orsay, France) as described by Goulas *et al.* (2004). Separate leaves were measured immediately after light treatment (see section 2.8.1) and following 1–7 d of DI (DDI). Leaves were extracted from buffer, dried on paper towels and, handled gently by the petiole, sampled at four predetermined locations on the

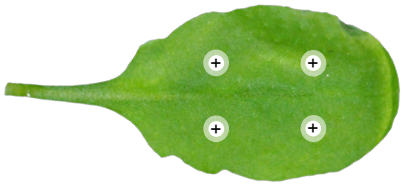

Figure 3. Predetermined locations for Dualex measurement on the adaxial leaf surface. Markers indicate measurement sites.

adaxial leaf surface (Fig. 3). Mean Chl content was calculated for each leaf to account for variation across the leaf surface.

2.4.2. Chlorophyll extraction and spectrophotometry

To assess the accuracy of the Dualex sensor in determining leaf Chl content this method was compared with Chl extraction and spectrophotometry (adapted from Witham *et al.*, 1971). Following Dualex measurement (see section 2.4.1), two leaf disks (∅ 1 cm), totalling 30 ± 5 mg fresh weight (FW), were excised from the centre of each leaf using a sterile Eppendorf tube lid. Each pair was weighed using an analytical balance (E10640; Ohaus, NJ, USA), snap-frozen in liquid N_2, and stored at −70°C. Frozen samples were homogenised with two sterilised steel beads (∅ 3 mm) in a bead mill (TissueLyser II; Qiagen, Tokyo, Japan) for 2 min at 30 Hz. Homogenates were immediately suspended in 2 ml of cooled 80% (v/v) acetone, thoroughly vortexed, and incubated for 1 h at 4°C. Samples were centrifuged at 16 000 ***g*** for 5 min at 4°C and supernatants were transferred into sterile Eppendorf tubes. Centrifugation and supernatant collection steps were repeated to ensure the absence of leaf solids. Extract absorbance (A) was measured at 645 and 663 nm using a spectrophotometer (WPA Biowave II; Biochrom, Cambridge, UK). Chl concentration was normalised to FW and extract volume (V) according to the following equation:

$$\text{Chl (mg g}^{-1}\text{ FW)} = \left(20.2\,(A_{645}) + 8.02\,(A_{663})\right) \times \frac{\text{V (ml)}}{\text{FW (mg)}}$$

2.5. Quantitative reverse-transcription PCR

2.5.1. RNA extraction

The relative transcript abundance of *ORE1* and *ACTIN 2* (*ACT2*) was compared in third, fourth, and fifth rosette leaves immediately after WL and +UV-B treatment, and following 3 or 7 DDI at 20°C (see section 2.3). At the indicated time points, leaves were divided into groups of equal weight (100 ± 10 mg FW), snap-frozen in liquid N_2, and stored at −70°C in sterile Eppendorf tubes. Tissues were homogenised as described in section 2.4.2. Total RNA was isolated from homogenates using a Spectrum Plant Total RNA Kit (Sigma-Aldrich, MO, USA) according to the manufacturer's instructions. Genomic DNA was removed from samples using an On-Column DNase I Digestion Set (Sigma-Aldrich).

2.5.2. RNA yield and integrity assessment

The concentration and quality of total RNAs were assessed using a NanoPhotometer (N60; Implen, Munich, Germany) and by gel electrophoresis, respectively. Samples were loaded alongside 1 kb Plus DNA Ladder (New England Biolabs, MA, USA) into wells of 1% (w/v) agarose Tris-acetate-EDTA (TAE) gel stained with Midori Green Advance DNA Stain (Nippon Genetics, Dueren, Germany) following the manufacturer's instructions. Gels were run in 1 × TAE buffer (pH 8.3) at 70 V for 1 h and visualised under UV light using a Fusion Pulse-6 gel documentation system (Vilber Lourmat, Marne-la-Vallée, France) and Evolution-Capt software for Windows, version 17 (Vilber Lourmat; see Supplementary Fig. S2).

2.5.3. cDNA synthesis

First-strand cDNA was synthesised from 2 µg total RNA using a High-Capacity cDNA Reverse Transcription Kit with RNase Inhibitor (Applied Biosystems, CA, USA) following the manufacturer's instructions.

2.5.4. Quantitative PCR

qPCR was conducted in 20 µl reactions using Brilliant III Ultra-Fast SYBR Green QPCR Master Mix (Agilent Technologies, CA, USA) according to the manufacturer's instructions. DNA amplification was performed using an Mx3005P system (Stratagene, CA, USA). Amplification curves and threshold cycle (Ct) values were obtained using MxPro qPCR software for Windows, version 4.1 (Stratagene). PCR primers were obtained from Eurofins Genomics and suspended in nuclease-free water. Primer efficiency was assessed before use by performing a standard curve analysis of serially diluted cDNA samples (see Supplementary Fig. S3). Relative *ORE1* transcript abundance was quantified using the ΔΔCt method and normalised to *ACT2*. All samples were run in triplicate. For a list of PCR primers used, refer to Table 1.

Table 1. PCR primers used with sequences provided.

Gene	Forward primer (5' → 3')	Reverse primer (5' → 3')
ORE1	GGTACAAAGGTTCCAATGTCAATGC	TGGTCGGAGAAGCAGGTCAC
ACT2	TCAGATGCCCAGAAGTGTTGTTCC	CCGTACAGATCCTTCCTGATATCC

2.6. Photography

Separate leaves were photographed following 1–7 DDI. Sample images were acquired using a Nikon D80 camera (Nikon, Tokyo, Japan) equipped with a 50 mm macro lens (F2.8 EX DG Macro; Sigma,

Tokyo, Japan) and fixed to a repro stand. A ruler was used for image calibration. Images were processed using Pixelmator Pro for macOS, version 2.1.4 (Pixelmator Team, London, UK).

2.7. Statistical analysis and graphing

Statistical tests were performed using SPSS Statistics for macOS, version 27.0.1 (IBM, IL, USA). All data were tested for normality and homogeneity of variances. Data meeting these assumptions were analysed using a one-way ANOVA and Tukey post-hoc test. A Welch ANOVA was performed when these assumptions were violated, followed by a Games-Howell post-hoc test. Extreme outliers were adjusted to within normal limits. Graphing was performed in GraphPad Prism for macOS, version 9.0.1 (GraphPad Software, CA, USA).

2.8. Method development

2.8.1. Estimation of initial leaf chlorophyll contents

In preliminary experiments, Dualex measurement was performed on fourth and fifth rosette leaves immediately after harvest to ensure that initial mean Chl content was approximately equal in each treatment group. However, this approach produced mechanical leaf damage, causing a rapid loss of structural integrity and accelerated Chl degradation during DI. To prevent this effect, initial values for fourth and fifth rosette leaves were estimated from third rosette leaves which were considered representative.

CHAPTER 3

Investigating the Efficacy of Low-Dose UV-B for the Suppression of Dark-Induced Leaf Senescence in Arabidopsis

Contents

3.1. Results . . . 27
3.1.1. The Dualex sensor accurately identifies leaf chlorophyll content at 7 DDI 27
3.1.2. Preharvest treatment with low-dose UV-B promotes marginal DIS suppression 27
3.1.3. Preharvest treatment with low-dose UV-B transiently suppresses *ORE1* transcript abundance . . . 27
3.1.4. Postharvest retreatment with low-dose UV-B enhances DIS suppression . 29
3.1.5. Low-dose UV-B treatments administered preharvest and at 2 DDI promote significant DIS suppression . . . 30
3.2. Discussion . . . 31

UV-B RADIATION CONSTITUTES an invisible fraction of sunlight whose intensity depends on environmental variables such as the solar angle, cloud cover, and shade (Paul & Gwynn-Jones, 2003). These wavelengths are deleterious to plants at high intensities, with effects including reduced photosynthetic efficiency, depressed growth, and cell death (Hollósy, 2002). To tolerate periods of high-intensity UV-B, plants have evolved a suite of adaptive UV-B acclimation responses, including the synthesis of UV-B–protectant epidermal compounds, DNA repair enzymes, and ROS scavenging antioxidants. UV-B also contributes to plant fitness at sub-lethal intensities by providing an unambiguous sunlight signal and promoting appropriate photomorphogenic development (Podolec *et al.*, 2021). UV-B–induced changes in gene expression occur at extremely low fluence rates ($\sim 0.1\,\mu mol\,m^{-1}\,s^{-1}$), highlighting the biological significance of $UV\text{-}B^{LD}$ (Brown & Jenkins, 2008).

Applications for UV-B include surface sterilisation, medical phototherapy, and as a potential postharvest technology for suppressing DIS-associated leaf yellowing in crops (Sharma, 2012; Balevi *et al.*, 2017; Sweetman, unpublished, MSc thesis, University of Bristol). DIS is an active degenerative

process that initiates in response to prolonged darkness, resulting in Chl degradation and consequent leaf yellowing (Gan, 2018). As yellowed crops are commercially undesirable, DIS-associated Chl degradation limits the storage life of leafy vegetables and contributes to high levels of food wastage. High-intensity UV-B treatments have been used to suppress dark-induced Chl degradation in broccoli florets and lime peel; an effect that occurs independently of both UVR8 and MAPK cascades in Arabidopsis leaves (Aiamla-or *et al.*, 2010; Srilaong *et al.*, 2011; Sztatelman *et al.*, 2015). However, this effect is accompanied by cell death, limiting the commercial value of high-intensity UV-B (Sztatelman *et al.*, 2015). By contrast, evidence suggests that UV-B^{LD} treatments are well tolerated and could potentially suppress dark-induced Chl degradation by inhibiting the DIS-promoting transcription factors, PIF4/5 (Sharma *et al.*, 2019).

PIF4/5 positively regulate DIS partly by inducing the expression of the master senescence regulator *ORE1*, which mediates global transcriptional reprogramming towards DIS (Sakuraba *et al.*, 2014a,c; Zhang *et al.*, 2015). PIF4/5 abundance is tightly governed by the combined effects of the circadian clock, an endogenous molecular oscillator with a ~24 h periodicity, and external light signals. Specifically, *PIF4/5* transcription is controlled by the evening complex (EC), comprising EARLY FLOWERING (ELF) 3, ELF4, and LUX ARRHYTHMO (LUX). The EC releases repression of *PIF4/5* transcription during the mid- to late-night, promoting PIF4/5 protein accumulation. Conversely, light-activated photoreceptors promote the phosphorylation and degradation of PIF4/5 at dawn (Nozue *et al.*, 2007; Nusinow *et al.*, 2011). The contribution of R to PIF4/5 degradation is well established. Specifically, R wavelengths induce phyB-mediated degradation of PIF4/5 via the 26S proteasome. This effect is known to suppress dark-induced Chl degradation in several species (Pfeiffer & Kleudgen, 1980; Tucker, 1981; Biswal *et al.*, 1982; Sakuraba *et al.*, 2014a).

More recently, UV-B^{LD} (1.0–1.5 $\mu mol\, m^{-1}\, s^{-1}$) treatments were shown to induce UVR8-dependent sequestration of COP1, resulting in PIF4/5 degradation and suppression of PIF4/5 enrichment at target promoter elements (see section 1.4.1.2.3.2; Hayes *et al.*, 2014, 2017; Sharma *et al.*, 2019; Tavridou *et al.*, 2020a). Several mechanisms of UV-B^{LD}–mediated PIF4/5 inhibition have been identified. First, photoactivated UVR8 is reported to outcompete PIF4/5 for COP1 binding, disrupting COP1-mediated PIF4/5 stabilisation and initiating the degradation of PIF4/5 by the 26S proteasome (Xu *et al.*, 2017; Pham *et al.*, 2018c; Sharma *et al.*, 2019). Second, UV-B^{LD}–induced UVR8–COP1 interaction disrupts COP1-mediated HFR1 inhibition, resulting in HFR1 protein accumulation. HFR1 sequesters PIF4/5, preventing their DNA binding (Tavridou *et al.*, 2020c). Third, UV-B^{LD} inhibits GA signalling, resulting in the UVR8-dependent accumulation of DELLAs, which sequester PIF4/5 and initiate their 26S proteasome-mediated degradation (de Lucas *et al.*, 2008; Hayes *et al.*, 2014b; Li *et al.*, 2016). Although the inhibitory effects of UV-B^{LD} on PIF4/5 signalling indicate that these treatments could suppress dark-induced Chl degradation, this capacity remains untested.

We hypothesised that (1) UV-B^{LD} treatment would suppress dark-induced Chl degradation in Arabidopsis leaves and (2) this effect would be mediated, in part, by disruption of PIF4/5-induced *ORE1* expression. To test these hypotheses, we combined Dualex-based leaf Chl assessment with qPCR analysis to determine the effect of UV-B^{LD} treatments on (1) rates of dark-induced Chl degradation

and (2) levels of *ORE1* expression in dark-incubated Arabidopsis leaves. Consistent with our hypotheses, we find that UV-B^{LD} suppresses dark-induced Chl degradation, and this is at least partially attributable to the transcriptional downregulation of *ORE1*.

3.1. Results

3.1.1. The Dualex sensor accurately identifies leaf chlorophyll content at 7 DDI

To test the accuracy of Dualex-based Chl quantification, the Dualex leaf clip sensor and biochemical extraction were used to assay mean Chl content during 7 DDI.* Visual comparison of the resulting Chl degradation curves revealed that Dualex-derived Chl values were higher than spectrophotometric values at 2, 3, 4, and 5 DDI (Fig. 4). However, these approaches yielded similar values at 6 and 7 DDI. This finding indicates that a Dualex-based approach is similar in precision to invasive spectrophotometry for determining mean leaf Chl content at 7 DDI.

3.1.2. Preharvest treatment with low-dose UV-B promotes marginal DIS suppression

Using the Dualex sensor, we next investigated whether preharvest UV-B^{LD} could suppress dark-induced Chl degradation. Four-week-old Arabidopsis plants were treated with either WL or WL supplemented with UV-B^{LD} for 4 h at dawn. After determining initial Chl content from third rosette leaves (see section 2.8.1), fully expanded fourth and fifth rosette leaves were detached and dark-incubated. Chl content was measured at 7 DDI. A one-way ANOVA was conducted to test for differences in mean Chl content between WL- and +UV-B–treated leaves following 7 DDI, revealing no statistically significant difference ($F_{1,12}$ = .011; p = .917; Fig. 5). Despite this, visual inspection of the boxplots revealed that the mean Chl content of +UV-B–treated leaves was consistently higher than WL-treated controls (Fig. 5, Supplementary Fig. S4). These results indicate that preharvest UV-B^{LD} causes DIS suppression; however, this effect is marginal.

3.1.3. Preharvest treatment with low-dose UV-B transiently suppresses *ORE1* transcript abundance

We hypothesised that the suppressive effect of UV-B^{LD} on dark-induced Chl degradation might result from transcriptional downregulation of the master senescence promoter, *ORE1*. To test this hypothesis, *ORE1* transcript abundance was quantified in WL- and +UV-B–treated leaves at 0, 3, and 7 DDI using qPCR. Three biological repeats were performed and averaged to obtain mean transcript abundance for each treatment at each timepoint. A Welch ANOVA revealed a statistically significant difference between treatment groups (Welch's $F_{5,5.1}$ = 4425.249, p < .001). Furthermore, Games-Howell post-hoc analysis revealed that *ORE1* transcript abundance significantly increased between 0 and 3 DDI for both leaves treated with WL (Fig. 6; 153.92, 95% CI [146.58, 161.26], p < .001) and +UV-B (132.73, 95%

*Experiment performed once only.

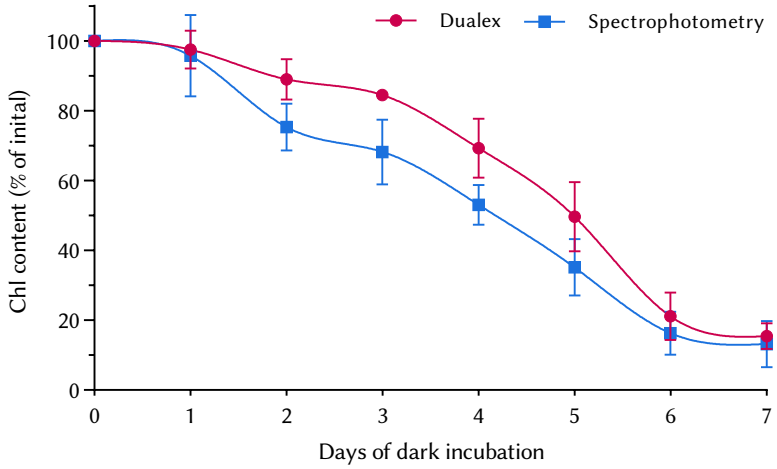

Figure 4. Dualex measurement and biochemical extraction identify similar levels of leaf chlorophyll degradation at 7 DDI. The fourth and fifth rosette leaves of four-week-old Arabidopsis plants were detached and dark-incubated for 0–7 d at 20°C. Mean Chl content was determined for each leaf at the indicated time points by performing Dualex measurement at four predetermined locations on the adaxial leaf surface (µg cm^{-2}) and Chl extraction and spectrophotometry (mg g^{-1} FW). Independent leaves were used at each time point. Results are shown as the percentage of initial Chl content (0 DDI). Vertical bars represent ± SD (n = 3).

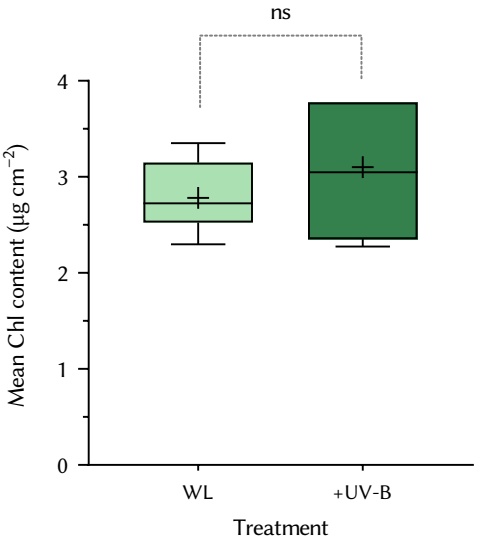

Figure 5. Preharvest low-dose UV-B treatment slightly delays dark-induced leaf chlorophyll degradation. Four-week-old Arabidopsis plants were treated with either WL or WL supplemented with low-dose UV-B (+UV-B; 1 µmol m^{-1} s^{-1}) for 4 h at dawn. Fourth and fifth rosette leaves were detached and dark-incubated for 7 d at 20°C. Mean Chl content (µg cm^{-2}) was determined by performing Dualex measurements at four predetermined locations on the adaxial leaf surface. Centre lines of box plots represent medians, + represent means, boxes delimit 25th and 75th percentiles, whiskers represent minimum and maximum values. ns indicates no statistically significant difference at $p \leq .05$ (n = 7).

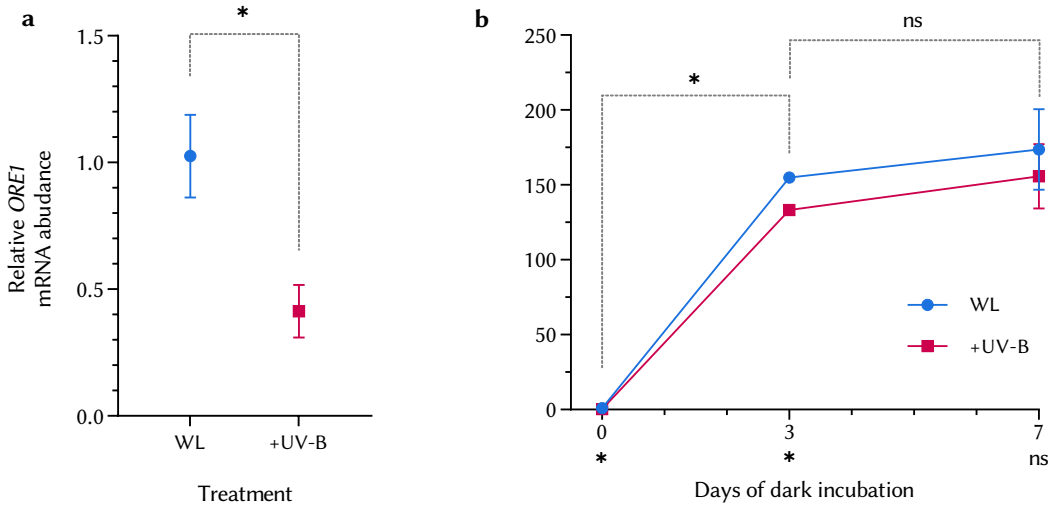

Figure 6. Preharvest low-dose UV-B treatment transiently suppresses *ORE1* transcript abundance. Four-week-old Arabidopsis plants were treated with either WL or WL supplemented with low-dose UV-B (+UV-B; 1 µmol m^{-1} s^{-1}) for 4 h at dawn. Fully expanded rosette leaves were detached and dark-incubated for 0, 3, or 7 d at 20°C. Relative *ORE1* transcript abundance was determined using reverse transcription and qPCR and normalised to *ACTIN2* (*ACT2*). **(a)** Relative *ORE1* transcript (mRNA) abundance at 0 DDI. **(b)** Relative *ORE1* transcript abundance at 0, 3, and 7 d. Data are presented as mean ± SEM. Asterisks indicate statistically significant effect of UV-B^{LD} or differences between time points at $p \leq .05$ (ns, non-significant; $n = 3$).

CI [119.22, 146.25], $p < .001$). By contrast, *ORE1* transcript abundance did not significantly change between 3 and 7 DDI for either leaves treated with WL ($p < .996$) or +UV-B ($p < .872$). These data indicate that *ORE1* transcription is upregulated between 0 and 3 DDI and plateaus between 3 and 7 DDI. Multiple one-way ANOVAs also revealed that *ORE1* transcript abundance was significantly lower in +UV-B- than WL-treated leaves at 0 DDI ($F_{1,4} = 9.958$, $p = .034$) and 3 DDI ($F_{1,4} = 9.958$, $p = .034$). However, no significant difference was observed at 7 DDI ($F_{1,4} = .267$, $p = .633$). These results indicate that DIS suppression by preharvest UV-B^{LD} results partly from transient repression of *ORE1* transcription at 0 and 3 DDI, an effect that is lost between 3 and 7 DDI.

3.1.4. Postharvest retreatment with low-dose UV-B enhances DIS suppression

Given that UV-B^{LD}–induced *ORE1* repression was lost between 3 and 7 DDI, we hypothesised that an additional, second UV-B^{LD} treatment at 1–5 DDI (+UV-B^{+1-5}) might prolong this effect, thereby amplifying DIS suppression. To test this, a second +UV-B treatment was administered to +UV-B–treated leaves on subsequent days. A one-way Welsch ANOVA was performed to test for differences in mean Chl content between WL-, +UV-B–, and +UV-B^{+1-5} double-treated leaves at 7 DDI, revealing a statistically significant difference between treatment groups (Welch's $F_{6,12.1} = 44.856$, $p < .001$). Games-Howell post-hoc analysis revealed that mean Chl content was significantly higher in +UV-B^{+2}–treated leaves (those receiving a second +UV-B treatment at 2 DDI) than those treated preharvest with WL (6.05, 95% CI [4.18, 7.92], $p < .001$) or +UV-B (6, 95% CI [4.14, 7.88], $p < .001$). Similarly, mean Chl

content was significantly higher in UV-B^{+4}–treated leaves (those receiving a second +UV-B treatment at 4 DDI) than those treated preharvest with WL (5.02, 95% CI [2.7, 7.33], p = .002) or +UV-B (4.97, 95% CI [2.65, 7.3], p = .002). As mean Chl content was highest in +UV-B^{+2}–treated leaves, this treatment was considered most effective (Fig. 7). Visual inspection of the boxplots also revealed that mean Chl content was higher in +UV-B^{+1}–, +UV-B^{+3}–, and +UV-B^{+5}–treated leaves than WL and +UV-B controls, although these differences were statistically insignificant. These results indicate that a second +UV-B treatment during DI significantly enhances the suppressive effect of preharvest +UV-B treatment on DIS and that this is most effective at 2 DDI.

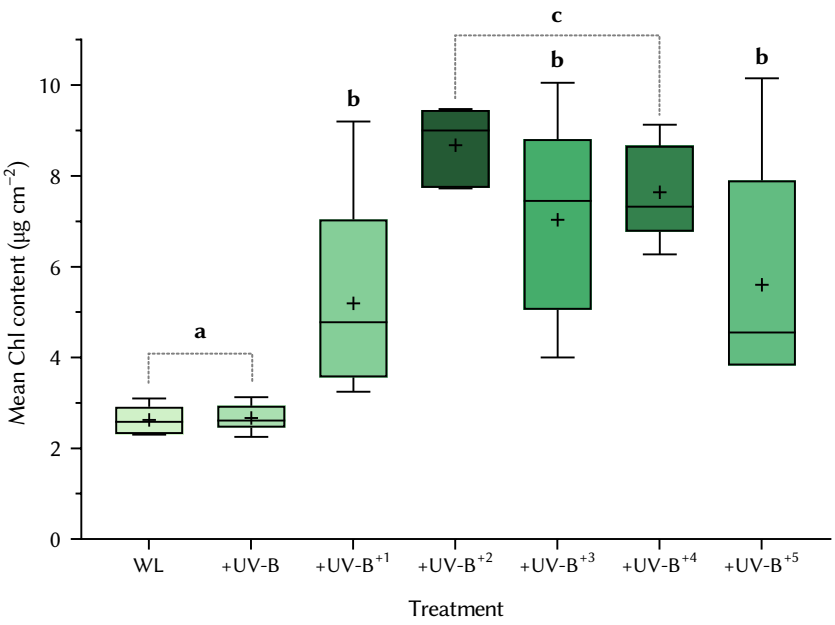

Figure 7. Double low-dose UV-B treatment is more effective than a single preharvest treatment for suppressing dark-induced leaf chlorophyll degradation. Four-week-old Arabidopsis plants were treated with either WL or WL supplemented with low-dose UV-B (1 µmol m^{-1} s^{-1}; +UV-B) for 4 h at dawn. Fourth and fifth rosette leaves were detached and dark-incubated for 7 d at 20°C. An additional 2 h +UV-B treatment was provided to some leaves at either 1, 2, 3, 4, or 5 DDI (+UV-B$^{+1–5}$). Mean Chl content (µg cm^{-2}) was determined by performing Dualex measurements at four predetermined locations on the adaxial leaf surface. Centre lines of box plots represent medians, + represent means, boxes delimit 25th and 75th percentiles, whiskers represent minimum and maximum values. Letters indicate statistically significant differences at $p \leq .05$ (n = 5–6).

3.1.5. Low-dose UV-B treatments administered preharvest and at 2 DDI promote significant DIS suppression

To investigate the relative contribution of WL to the suppressive effect of +UV-B^{+2} treatment, Chl content was compared in +UV-B^{+2}–treated leaves, WL-treated leaves retreated with WL at 2 DDI (WL^{+2}), and WL and +UV-B–treated controls at 7 DDI. A one-way Welch ANOVA revealed a statistically significant difference between treatment groups (Welch's $F_{3,12.84}$ = 27.126, p < .001). A Games-Howell

post-hoc test revealed that mean Chl content was significantly higher in +UV-B^{+2}–treated leaves than leaves treated preharvest with WL (Fig. 8; 4.51, 95% CI [2.65, 6.36], $p < .001$) or +UV-B (3.75, 95% CI [1.84, 5.67], $p < .001$). Similarly, mean Chl content was significantly higher in WL^{+2}-treated leaves than leaves treated preharvest with WL (2.2, 95% CI [1.28, 3.11], $p < .001$) or +UV-B (1.44, 95% CI [.29, 2.59], $p = .015$). Finally, mean Chl content was significantly higher in +UV-B^{+2}– than WL^{+2}-treated leaves (2.31, 95% CI [.47, 4.16], $p = .017$). These results indicate that +UV-B retreatment at 2 DDI enhances the efficacy of preharvest light treatments independently of UV-B^{LD}, although UV-B^{LD} significantly amplifies this effect.

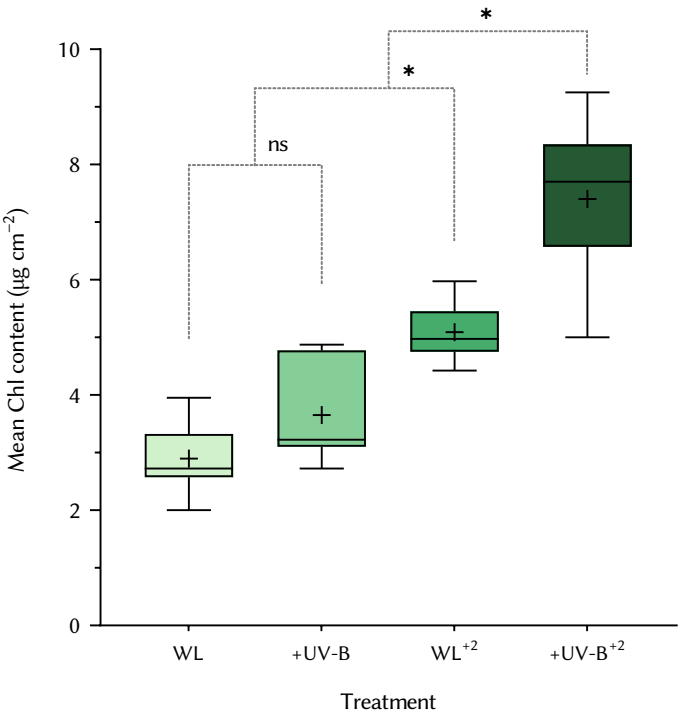

Figure 8. Postharvest treatment with WL and UV-B is more effective than WL for suppressing dark-induced chlorophyll degradation. Four-week-old Arabidopsis plants were treated with either WL or WL supplemented with low-dose UV-B (1 µmol m^{-1} s^{-1}; +UV-B) for 4 h at dawn. Fourth and fifth rosette leaves were detached and dark-incubated for 7 d at 20°C or retreated at 2 DDI for 2 h with WL or +UV-B (WL^{+2} or +UV-B+$^{+2}$). Mean Chl content (µg cm^{-2}) was determined by performing Dualex measurements at four predetermined locations on the adaxial leaf surface. Centre lines of box plots represent medians, + represent means, boxes delimit 25th and 75th percentiles, whiskers represent minimum and maximum values. Asterisks indicate statistically significant differences at $p \leq .05$ (ns, non-significant; $n = 7$).

3.2. Discussion

Whilst it has been shown that high-intensity UV-B treatments can suppress DIS-associated Chl degradation in several species, the efficacy of less damaging UV-B^{LD} treatments is unknown. PIF4/5

positively regulate DIS by inducing the expression of *ORE1* (Sakuraba *et al.*, 2014a). Given that UV-B^{LD} treatments promote the degradation of PIF4/5 (Hayes *et al.*, 2014b; Sharma *et al.*, 2019), we hypothesised that UV-B^{LD} might suppress dark-induced Chl degradation by disrupting PIF4/5-mediated *ORE1* transcription. Full molecular characterisation of the effects of UV-B^{LD} treatments on dark-induced Chl degradation will enable the development of light regimes to enhance postharvest longevity in leafy crops.

To examine the effect of UV-B^{LD} on DIS, we used the Dualex leaf clip sensor to determine the mean Chl content of leaves treated with either preharvest WL or +UV-B following 7 DDI. We found that the Chl content of leaves treated preharvest with +UV-B were higher than WL-treated controls. However, this difference was statistically insignificant. This result is corroborated by a preliminary study, which found that treatment preharvest with UV-B^{LD} promoted UVR8-dependent DIS suppression (Sweetman, unpublished, MSc thesis, University of Bristol). Whilst these data support an application for UV-B^{LD} as a technology for DIS suppression, this procedure requires optimisation to achieve greater effects. Subsequent experiments indicated that the effect of preharvest UV-B^{LD} might be more apparent at earlier time points (Fig. 10); however, due to time constraints, this was not investigated.

To test whether the suppressive effect of UV-B^{LD} results from repression of *ORE1* transcription, qPCR was used to compare levels of *ORE1* transcript in WL- and +UV-B–treated leaves at 0, 3, and 7 DDI. We found that *ORE1* transcript abundance increased between 0 and 3 DDI and plateaued between 3 and 7 DDI for both treatment groups. We also found that +UV-B–treated leaves contained lower levels of *ORE1* transcript than WL controls at 0 and 3 DDI, indicating that UV-B^{LD} represses *ORE1* transcription. As UV-B^{LD} promotes PIF4/5 degradation (Hayes *et al.*, 2014b, 2017a; Sharma *et al.*, 2019; Tavridou *et al.*, 2020a), this result supports a hypothetical DIS suppression mechanism in which UV-B^{LD} attenuates PIF4/5 protein abundance and consequently prevents the induction of the PIF4/5 target gene, *ORE1*. Future studies could test this by using immunoblotting and ChIP-qPCR to confirm reductions in PIF4/5 abundance and enrichment at the *ORE1* promoter under UV-B^{LD}.

In contrast to 0 and 3 DDI, *ORE1* transcript abundance was not significantly different in WL- and +UV-B–treated leaves at 7 DDI. This suggests that *ORE1* expression recovered between 3 and 7 DDI following initial downregulation by UV-B^{LD}. This effect might be attributable to circadian oscillations, which persist during DI and promote rhythmic expression of *PIF4/5* (Nozue *et al.*, 2007; Salomé *et al.*, 2008). We theorise that following UV-B^{LD}–induced PIF4/5 degradation, circadian *PIF4/5* transcription cycles drive the accumulation of *PIF4/5* transcripts, promoting the reaccumulation of PIF4/5 protein and the recovery of *ORE1* transcription in dark-incubated leaves. This theoretical mechanism is supported by studies in Arabidopsis, which show that *PIF4/5* transcript and protein abundance increase during DI (Sakuraba *et al.*, 2014a; Song *et al.*, 2014). Plateauing of *ORE1* expression between 3 and 7 DDI may also contribute to the recovery effect. Subsequent assays demonstrated that +UV-B^{+2} treatment suppressed dark-induced Chl degradation significantly more effectively than WL, +UV-B, and WL^{+2} controls. This observation might result from UV-B^{LD}–mediated repression of PIF4/5 reaccumulation. Based on our results, we propose a hypothetical model for the effects of UV-B^{LD} on the kinetics of PIF4/5 abundance (Fig. 9). Further qPCR analysis could be used to confirm whether +UV-B retreatment

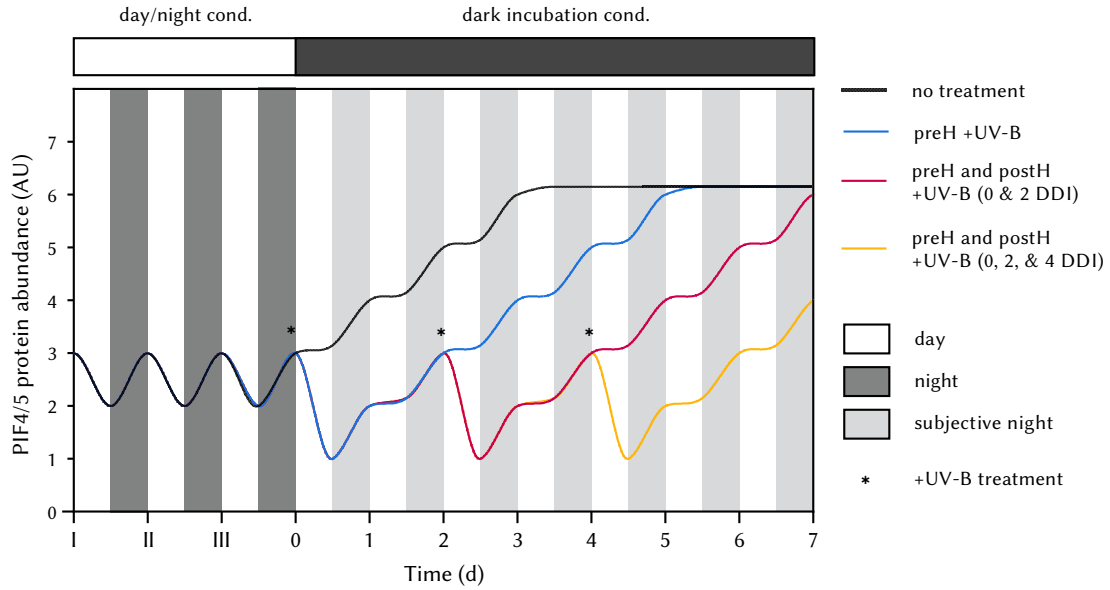

Figure 9. Hypothetical model of the kinetics of PIF4 and PIF5 (PIF4/5) protein abundance (arbitrary units, AU) under day/night and dark incubation conditions and following preharvest (PreH) and postharvest (PostH) +UV-B treatment. Under light/dark cycles, circadian rhythms drive night-time *PIF4/5* expression, causing PIF4/5 protein abundance to increase. Light signals suppress PIF4/5 abundance at dawn. Upon transfer to dark incubation conditions, circadian rhythms persist, promoting *PIF4/5* expression and PIF4/5 protein accumulation in the absence of light. PIF4/5 abundance plateaus between 3 and 7 DDI. Preharvest +UV-B treatment suppresses PIF4/5 abundance. Postharvest +UV-B treatments administered at 2 and 4 DDI repress PIF4/5 reaccumulation. Asterisks indicate +UV-B treatment.

prevents the recovery of *ORE1* transcription and support our model; however, due to time constraints, this was not performed. Our model predicts that DIS suppression is further enhanced by an additional, third UV-B^{LD} retreatment at 4 DDI. However, this was also not tested due to time constraints.

Finally, we found that WL^{+2} treatment suppressed Chl degradation independently of UV-B^{LD}, although this was significantly less effective than +UV-B^{+2} treatment. This observation is likely due to the established inhibitory effects of several components of WL on PIF4/5 signalling. Specifically, R is known to suppress Chl degradation by inducing phyB-mediated PIF4/5 sequestration and degradation (see section 1.4.1.1.2). Furthermore, blue-light wavelengths, perceived by CRYPTOCHROME 1 (CRY1), induce CRY1–PIF4 complex formation, preventing the expression of PIF4 target genes (Ma *et al.*, 2016). Notably, the suppressive effect of WL appears to be additive to that of UV-B^{LD}, indicating that for maximum efficacy these quanta should be provided in combination.

Our findings must be considered in light of several experimental limitations. First, although the use of four measurement sites for determining mean leaf Chl content likely accounted for most leaf surface variation, this approach does not entirely capture such variance. Consequently, tissues with outlying Chl values might have been inadvertently excluded from the mean, limiting the reliability of our Chl content estimates. Biochemical extraction of Chl from entire leaves for spectrophotometric analysis could be a more rigorous approach. Second, due to space and time constraints, the sample

size chosen for Chl degradation experiments was relatively small (n = 5–10). Given the high degree of variability in our data, we recommend that future work employ a greater sample size to confirm our findings.

In this study, we have demonstrated that UV-B^{LD} can be used to suppress dark-induced Chl degradation in Arabidopsis leaves, an effect that is due at least partly to transient repression of *ORE1* transcription. We have also confirmed that WL can suppress dark-induced Chl degradation independently of and additively to UV-B^{LD}. The advent of cost-effective LED lighting systems provides an opportunity to implement senescence-suppressing wavelengths in lighting regimes within controlled environment agriculture and shop storage to prevent postharvest leaf yellowing. However, further work is necessary to determine whether UV-B^{LD}–induced DIS suppression is effective in agriculturally relevant species. Studies have shown that rates of UVR8 inactivation positively correlate with ambient temperature, suggesting a secondary function for UVR8 in temperature perception (Findlay & Jenkins, 2016). Therefore, it would also be of interest to evaluate the efficacy of UV-B^{LD} treatments at different ambient temperatures.

CHAPTER 4

Investigating the Effect of Ambient Temperature on Low-Dose UV-B–mediated Senescence Suppression in Arabidopsis

Contents

4.1. Results 37
4.1.1. Preharvest treatment with low-dose UV-B additively enhances DIS suppression by LAT and suppresses DIS in leaves maintained at HAT 37
4.2. Discussion 37

Plants have evolved a suite of adaptive responses to elevated temperatures, known collectively as thermomorphogenesis. Hypocotyl elongation is amongst the earliest of these responses. This is believed to promote cooling by enhancing airflow and distancing sensitive photosynthetic tissues from heat-absorbing soil in addition to optimising light foraging during periods of enhanced respiration (Gray *et al.*, 1998; Romero-Montepaone *et al.*, 2021). Additional responses include petiole elongation and leaf hyponasty. These promote an open rosette structure that enables increased evapotranspirative cooling (Crawford *et al.*, 2012; Bridge *et al.*, 2013; Quint *et al.*, 2016). Elevated temperatures also accelerate leaf senescence (Ali *et al.*, 2018; Kim *et al.*, 2020).

Studies have shown that thermomorphogenesis is abolished in *pif4* null mutants and partially disrupted in *pif5* and *pif7* mutants (Koini *et al.*, 2009; Stavang *et al.*, 2009; Fiorucci *et al.*, 2020). These phenotypes support a central role for PIF4 and minor roles for PIF5 and PIF7 in these responses. *PIF4* transcript accumulates at HATs (Koini *et al.*, 2009). This effect is partly mediated by the EC, which binds to the *PIF4* promoter and prevents expression at LATs. ChIP-Seq and EMSA analyses have demonstrated that the affinity of this interaction is reduced at HATs, causing *PIF4* transcription to increase under these conditions (Ezer *et al.*, 2017; Silva *et al.*, 2020). Supplementary UV-B^{LD} has been shown to suppress *PIF4/5* transcript accumulation in a UVR8-dependent manner (Hayes *et al.*, 2014, 2017; Tavridou *et al.*, 2020b). This finding suggests that photoactivated UVR8 prevents *PIF4/5*

expression via an unknown mechanism. As inactivation of UVR8 by RUP1/RUP2 is enhanced at HATs (Kim *et al.*, 2020), this activity may limit UVR8-mediated repression of *PIF4/5* transcription, suggesting an additional HAT-dependent mechanism of *PIF4/5* transcriptional enhancement in sunlight.

At the protein level, PIF4/5 activity is regulated by phyB and UVR8 in their photoactivated forms. phyB Pfr physically interacts with PIF4/5, leading to their phosphorylation and degradation (Park *et al.*, 2012, 2018; Sakuraba *et al.*, 2014), whereas UVR8 promotes PIF4/5 degradation by disrupting their stabilisation by COP1 (Sharma *et al.*, 2019). In addition to RUP1/RUP2-mediated UVR8 inactivation, thermal inactivation of phyB is enhanced at HATs (Findlay & Jenkins, 2016; Kim *et al.*, 2020). This releases PIF4/5 inhibition, causing PIF4 to accumulate under these conditions (Kim *et al.*, 2020). However, immunoblot analyses are necessary to confirm whether PIF5 accumulation also occurs at HATs.

The phytohormone auxin is necessary and sufficient for PIF4-mediated thermoresponsive growth (Gray *et al.*, 1998; Stavang *et al.*, 2009; Franklin *et al.*, 2011; Sun *et al.*, 2012). Studies have shown that PIF4 activates the expression of the auxin biosynthetic genes *TRYPTOPHAN AMINOTRANSFERASE OF ARABIDOPSIS* (*TAA1*), *CYP79B2*, and *YUCCA8* (*YUC8*; Franklin *et al.*, 2011; Sun *et al.*, 2012; Di *et al.*, 2016). Consistent with reports of PIF4 accumulation at HATs, free auxin levels increased ~1.75-fold in wild-type seedlings grown at HAT, whereas this response was abolished in *pif4* mutants (Gray *et al.*, 1998; Franklin *et al.*, 2011). This supports a mechanism in which PIF4 accumulation triggers auxin biosynthesis, which initiates thermoresponsive growth at HATs. Evidence also supports key roles for brassinosteroids (BR) and GA in temperature-dependent responses (reviewed by Quint *et al.*, 2016).

In addition to driving stem elongation, PIF4/5 promote DIS by activating the expression of CCGs and the master senescence promoter, *ORE1* (Sakuraba *et al.*, 2014; Qiu *et al.*, 2015; Zhang *et al.*, 2015; Kim *et al.*, 2020). Research has shown that HATs cause DIS to accelerate in wild-type Arabidopsis leaves and that this response is significantly attenuated in *pif4pif5* double mutants (Kim *et al.*, 2020). These data support roles for PIF4 and/or PIF5 in high temperature-dependent DIS acceleration. Conversely, LATs retard DIS and are frequently maintained during storage to extend crop shelf life. However, several factors limit the value of this approach. Specifically, chilling-sensitive crops such as basil (*Ocimum basilicum*) develop leaf browning and necrosis when stored at LATs (Lange & Cameron, 1994). Furthermore, refrigeration is energy-intensive and therefore prohibitive from an economic and environmental perspective. Alternative strategies for DIS suppression must therefore be explored.

We previously reported that UV-B^{LD} treatments could be used to suppress DIS in Arabidopsis leaves stored at 20°C (see Chapter 3). This led us to question whether these treatments could enhance or constitute an alternative to LAT storage. In the absence of refrigeration, storage temperatures can vary based on climatic and seasonal factors. To determine suitable applications for UV-B^{LD}, it is therefore essential to study its efficacy in leaves maintained at different ambient temperatures. Using a combination of Dualex- and photography-based assays, we investigated the effect of a preharvest UV-B^{LD} treatment on leaves dark-incubated at 12°C, 20°C, or 28°C.

Preliminary data indicate that UV-B^{LD}–induced DIS suppression is UVR8-dependent (Sweetman, unpublished, MSc thesis, University of Bristol). By contrast, LATs can suppress DIS in a UVR8-independent manner (Jayas & Jeyamkondan, 2002; Devanesan *et al.*, 2011). Given these independent

modes of action, we first hypothesised that UV-B^{LD} would enhance DIS suppression by LAT. As UVR8 inactivation is accelerated at HATs, we also hypothesised that the efficacy of UV-B^{LD} would be reduced under these conditions (Findlay & Jenkins, 2016). Consistent with our first hypothesis, we found that a preharvest UV-B^{LD} treatment additively enhanced DIS suppression by LAT. We also found that UV-B^{LD} treatment caused DIS suppression in leaves maintained at HAT. Finally, we showed that preharvest UV-B^{LD} treatment was significantly less effective than LAT for DIS suppression. These results indicate that preharvest UV-B^{LD} treatments may be best utilised to enhance DIS suppression in crops stored at ≤ 20°C.

4.1. Results

4.1.1. Preharvest treatment with low-dose UV-B additively enhances DIS suppression by LAT and suppresses DIS in leaves maintained at HAT

To investigate the effect of preharvest UV-B^{LD} treatment on DIS in leaves maintained at different ambient temperatures, the mean Chl content of WL- and +UV-B–treated leaves was determined using the Dualex sensor following 7 DDI at 12°C, 20°C, or 28°C. Independent leaves of the above treatments were also photographed separately at 0–7 DDI (Fig. 10). Leaves maintained at 28°C were too highly degraded for Dualex-based measurement and were excluded from statistical analyses. A one-way ANOVA revealed a statistically significant difference in mean Chl content between treatment groups ($F_{3,24}$ = 458.824, p < .001). Subsequent Tukey post-hoc analysis revealed that mean Chl content was significantly higher in leaves incubated at 12°C than 20°C following treatment with either WL (7.28, 95% CI [6.51, 8.06], p < .001) or +UV-B (7.46, 95% CI [6.68, 8.24], p < .001; Fig. 10). Visual photographic comparison also indicated that, relative to leaves maintained at 20°C, Chl degradation progressed more slowly at 12°C and more quickly at 28°C. These results indicate that the rate of DIS progression positively correlates with ambient temperature in our experimental system.

Visual inspection of the boxplots revealed that mean Chl content was consistently higher in +UV-B- than WL-treated leaves at 12°C and 20°C (Fig. 10b, Supplementary Fig. S6). However, these differences were predominantly statistically insignificant. This indicates that preharvest UV-B^{LD} treatment slightly suppresses DIS in leaves maintained at 12°C and 20°C. Furthermore, visual photographic comparisons revealed that DIS progressed more slowly in +UV-B– than WL-treated leaves at 28°C. This suggests that UV-B^{LD} also slightly suppresses DIS in leaves maintained at 28°C. Finally, mean Chl content was significantly higher in WL-treated leaves incubated at 12°C than +UV-B–treated leaves incubated at 20°C (6.86, 95% CI [6.08, 7.64], p < .001). This result indicates that preharvest UV-B^{LD} treatment is less effective than LAT storage for DIS suppression.

4.2. Discussion

DIS is characterised by leaf yellowing resulting from Chl degradation. This causes leafy crops to cosmetically depreciate during postharvest transport and storage, resulting in high levels of postharvest

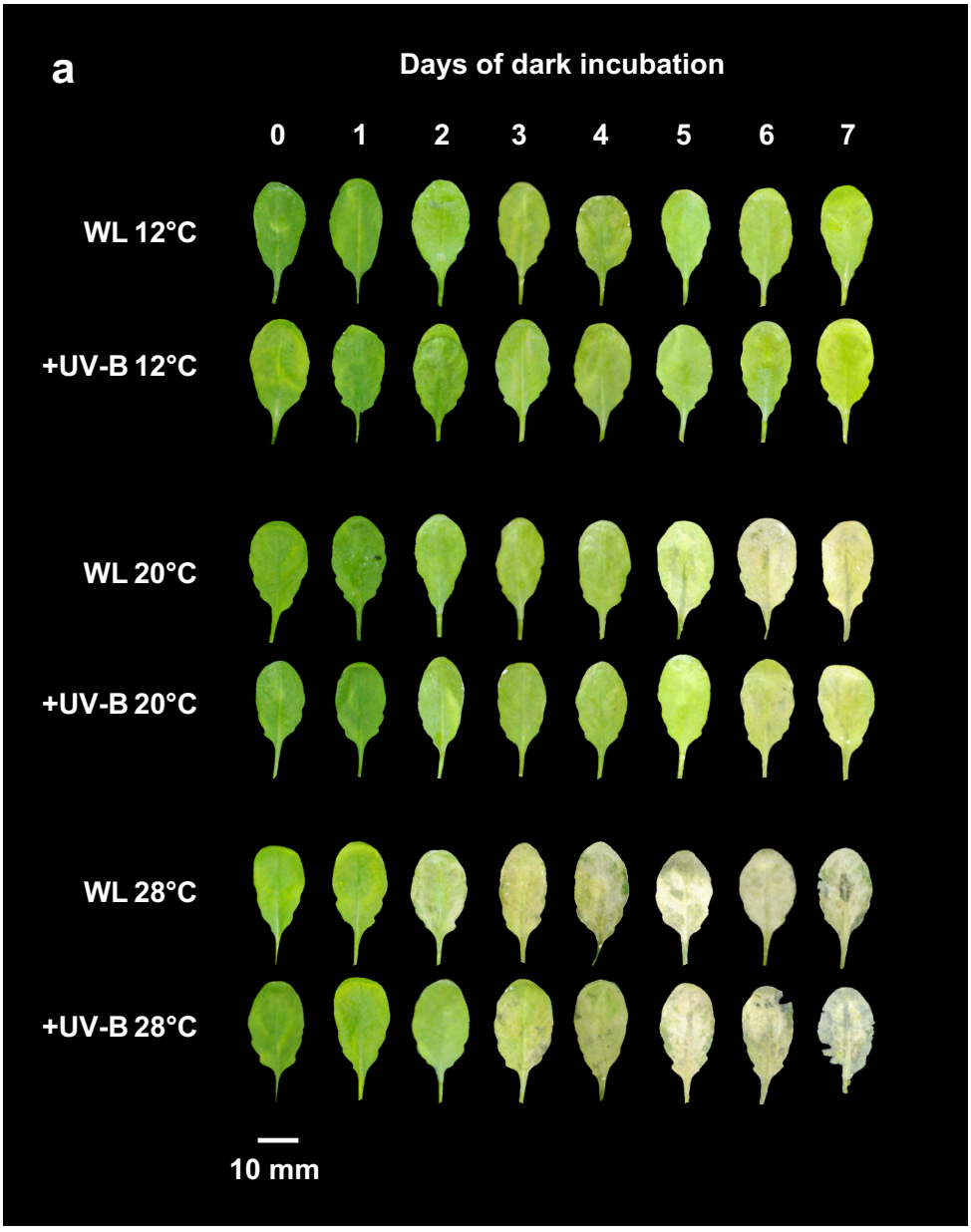
a
Days of dark incubation
0
1
2
3
4
5
6
7
WL 12°C
+UV-B 12°C
WL 20°C
+UV-B 20°C
WL 28°C
+UV-B 28°C
10 mm

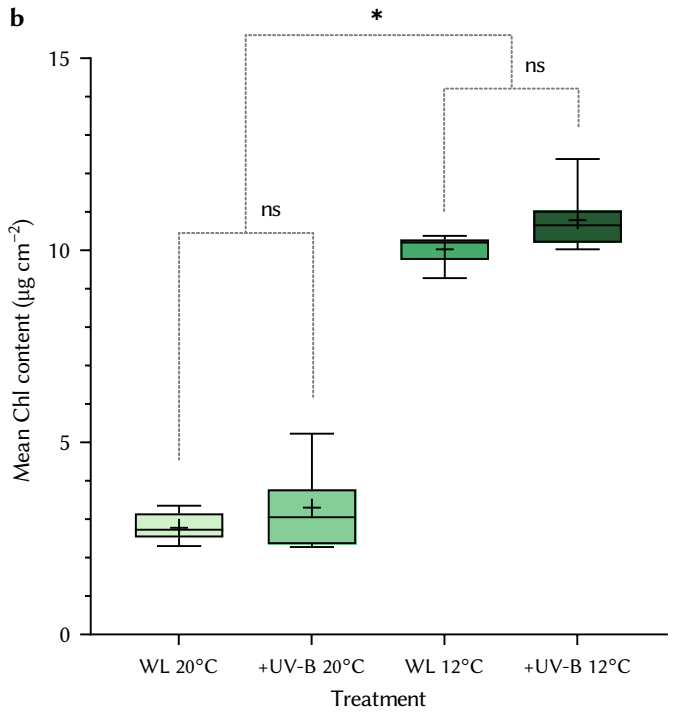

Figure 10. Preharvest treatment with low-dose UV-B enhances DIS suppression by low ambient temperature and suppresses DIS in leaves maintained at high ambient temperature. Four-week-old Arabidopsis plants were treated with either WL or WL supplemented with low-dose UV-B (1 µmol m^{-1} s^{-1}; +UV-B) for 4 h at dawn. Fourth and fifth rosette leaves were detached and dark-incubated for 0–7 d at 12°C, 20°C, or 28°C. **(a)** Visual comparison of WL- and +UV-B–treated leaves photographed on buffer following 0–7 DDI at 12°C, 20°C, or 28°C. **(b)** Mean Chl content (µg cm^{-2}) for WL- and +UV-B–treated leaves following 7 DDI at 12°C or 20°C. Mean Chl content was determined by performing Dualex measurements at four predetermined locations on the leaf surface. Samples incubated at 28°C were too highly degraded at 7 DDI for Dualex measurement and were excluded from statistical analyses. Centre lines of box plots represent medians, + represent means, boxes delimit 25th and 75th percentiles, whiskers represent minimum and maximum values. Asterisk indicates statistically significant at $p \leq .05$ (ns, non-significant; $n = 7$).

waste. LAT storage is commonly used to suppress DIS and extend crop shelf life. However, high operating costs and intolerance of certain species to LATs highlight the need for alternative solutions. We previously demonstrated that UV-B^{LD} treatments could suppress dark-induced Chl degradation in leaves maintained at 20°C. However, whether these treatments are effective for leaves stored at different ambient temperatures is unknown. By probing this interaction, we hope to provide insight into the relative and combined value of UV-B^{LD} and LAT storage. This could facilitate efforts to develop optimised strategies for DIS suppression.

In these experiments, we compared the effects of UV-B^{LD} on DIS in Arabidopsis leaves incubated at 12°C (LAT treatment), 20°C, or 28°C (HAT treatment). By combining Dualex- and photography-based assays, we showed that rates of dark-induced Chl degradation increased with ambient temperature. This result supports a previous study in Arabidopsis, which reported that DIS progressed more rapidly in

leaves incubated at 28°C than 20°C (Kim *et al.*, 2020). Research has shown that PIF4 protein accumulates at HATs (Kim *et al.*, 2020), resulting in transcriptional reprogramming towards DIS (Sakuraba *et al.*, 2014; Song *et al.*, 2014; Kim *et al.*, 2020). Therefore, it is likely that DIS acceleration at HAT results from elevated PIF4 activity.

These experiments have also demonstrated that preharvest UV-B^{LD} additively enhances DIS suppression by LAT. This finding supports an application for UV-B^{LD} as a means of potentiating DIS suppression by LAT storage. The additive effects of UV-B^{LD} and LAT may be attributable to their independent modes of action. It is speculated that UV-B^{LD} suppresses DIS partly via UVR8-dependent PIF4/5 inhibition (see section 1.4.1.2.3.2). Conversely, LATs suppress DIS via two or more UVR8-independent mechanisms: (1) LATs suppress the thermal inactivation of phyB, resulting in DIS suppression via phyB-mediated PIF4/5 inhibition (Kim *et al.*, 2020); (2) LATs limit respiration rate, which positively correlates with that of DIS (Jayas & Jeyamkondan, 2002; Devanesan *et al.*, 2011). LATs may also suppress DIS by disrupting the activity of the DIS-promoting phytohormone ethylene. Research in *Brassica* sp. has shown that leaves dark-incubated at 4°C exhibited lower expression of ethylene biosynthetic and signalling genes than at 25°C (Ahlawat & Liu, 2021). Future work could combine laser-based photoacoustic spectroscopy analysis and qPCR to determine whether the abundance of ethylene and its target gene transcripts are downregulated at LATs in Arabidopsis (van de Poel & van der Straeten, 2017). It would also be of interest to test whether additional postharvest UV-B^{LD} treatments could further enhance the effect of LAT. However, this was not tested due to time constraints.

In addition to its effect at LAT, our photographic data indicated that UV-B^{LD} treatment suppressed DIS in leaves incubated at 28°C. In warmer climates and seasons, storage temperatures can rise in the absence of temperature control measures. It is possible that UV-B^{LD} treatment could be used to partially mitigate temperature-mediated DIS acceleration under such conditions. Although UV-B^{LD}–induced DIS suppression was apparent in leaves maintained at 28°C at 2 and 3 DDI, high levels of structural degradation precluded the use of the Dualex sensor at 7 DDI. Future work could perform Dualex measurement at earlier time points or employ biochemical Chl extraction and spectrophotometry to quantify our results.

We also found that a preharvest UV-B^{LD} treatment was less effective than LAT for suppressing DIS. This result indicates that preharvest UV-B^{LD} treatment is not sufficiently effective to substitute LAT storage. We previously reported that the suppressive effect of preharvest UV-B^{LD} on DIS at 20°C was significantly enhanced by a second postharvest UV-B^{LD} treatment administered at 2 DDI. We also predicted further enhancement by a third treatment administered at 4 DDI (Fig. 9). Postharvest UV-B^{LD} treatments could augment the effects of UV-B^{LD} to a level comparable to LAT. However, this could not be tested due to time constraints. Our photography-based assays also indicated that the suppressive effect of UV-B^{LD} was most apparent at 5 DDI in leaves incubated at 20°C. It is possible that Dualex-based measurement performed at 5 DDI could have identified a significant effect for UV-B^{LD} at this temperature.

In these experiments, we have shown that rate of DIS positively correlates with ambient temperature in Arabidopsis leaves. Our findings could inform translational studies, assessing the duration that crops

can remain in transport and storage at different ambient temperatures. We have also demonstrated that preharvest UV-B^{LD} treatment slightly enhances DIS suppression at 12°C and with a more significant visual effect observed at 20°C. Furthermore, we found that UV-B^{LD} treatment suppressed DIS in leaves maintained at 28°C. Finally, we have shown that UV-B^{LD} treatment is less effective than LAT for DIS suppression. These results support applications for UV-B^{LD} treatment as a means of enhancing the effects of LAT storage and preventing temperature-associated DIS acceleration. UV-B^{LD} could also potentially be used to enhance DIS suppression by more energy-efficient, slightly raised LATs.

CHAPTER 5

Overall Discussion

The growing global population is driving an increased demand for food. Simultaneously, the intensification and expansion of agriculture threaten to cause irreversible damage to our ecosystems and climate. Thus, to safeguard future food security, it is crucial to identify and address sources of postharvest waste in the food supply chain. In crops, one such source is premature leaf yellowing caused by DIS. This form of cosmetic depreciation results from the active breakdown of Chl during transport and storage in the dark. Although LAT storage is widely used to suppress DIS, this approach is costly and harmful to chilling-sensitive species, necessitating the development of alternatives.

UV-B treatments supplied by cost-effective LED lighting systems have been identified as a potential means of suppressing DIS. Studies have shown that high-intensity UV-B treatments can suppress DIS in agriculturally relevant species, an effect that is speculated to result from enhanced production of antioxidant compounds (Aiamla-or *et al.*, 2010; Srilaong *et al.*, 2011; Sztatelman *et al.*, 2015). However, these treatments also promote cell death, thus limiting their commercial value (Sztatelman *et al.*, 2015). More recently, well-tolerated UV-B^{LD} treatments were shown to induce the UVR8-dependant degradation of the central DIS promoters, PIF4/5 (Hayes *et al.*, 2014, 2017; Sharma *et al.*, 2019; Tavridou *et al.*, 2020). Independent preliminary data also suggests that preharvest UV-B^{LD} suppresses DIS in a UVR8-dependent manner (Sweetman, unpublished, MSc thesis, University of Bristol). UV-B^{LD} treatment therefore warrants investigation as a DIS suppression technology.

Here, we have shown that UV-B^{LD} modulates DIS in Arabidopsis leaves independently of ambient temperature (Figs 5, 7, 8, & 10). Treatment with UV-B^{LD} for 4 h preharvest caused suppression of Chl degradation in leaves dark-incubated at 20°C (Figs 5, 10). We found that this effect was at least partly attributable to UV-B^{LD}–induced repression of *ORE1* transcription (Fig. 6). An additional postharvest UV-B^{LD} treatment administered at 1, 2, 3, 4, or 5 DDI enhanced DIS suppression in leaves maintained at 20°C with the most significant effect produced by retreatment at 2 DDI (Figs 7, 8). To explore suitable

applications for UV-B^{LD}, we also examined its efficacy in leaves maintained at LAT (12°C) and HAT (28°C). We found that preharvest UV-B^{LD} treatment additively enhanced DIS suppression by LAT (Fig. 9). Preharvest UV-B^{LD} treatment also suppressed DIS in leaves maintained at HAT. Based on these findings and preceding research, we can infer a general framework of the effects of UV-B^{LD} on DIS in Arabidopsis. Specifically, as UV-B^{LD} promotes PIF4/5 degradation, these treatments likely promote DIS suppression by disrupting PIF4/5-induced *ORE1* expression.

In addition to senescence suppression, evidence in Arabidopsis indicates that UV-B^{LD} treatments (0.66 kJ m^{-2} d^{-1} for 7 d) can significantly enhance concentrations of health-associated antioxidant compounds (Csepregi *et al.*, 2017). This effect has also been reported in a variety of horticulturally relevant species. For example, preharvest UV-B treatment (20 or 40 kJ m^{-2}) was shown to enhance total phenolic and flavonoid contents in tomato, resulting in increased antioxidant capacity (Liu *et al.*, 2011). Independent research also demonstrated that daily UV-B^{LD} supplementation (6.08 kJ m^{-2} d^{-1} for 10–22 d) increased antioxidant content in tomato flesh and peel, specifically carotenoids and ascorbate (Castagna *et al.*, 2013). Pro-antioxidant effects following UV-B^{LD} treatment have also been recorded in sweet basil, broccoli, radish (*Raphanus sativus*), and coriander (*Coriandrum sativum*; Sakalauskaitė *et al.*, 2013; Fraser *et al.*, 2017; Martínez-Zamora *et al.*, 2021). A recent study also examined the effect of UV-B^{LD} on concentrations of cancer-fighting compounds in *Brassicaceae* sprouts. This experiments showed that UV-B treatments (15 kJ m^{-2} d^{-1} for 2 d) enhanced sulforaphene and glucosinolate contents by 37.5% and ~30%, respectively, in broccoli sprouts and 72% and ~30% in radish sprouts (Martínez-Zamora *et al.*, 2021). These findings suggest that UV-B treatments could have significant commercial value as a means of enhancing the nutraceutical properties of horticultural crops. Several further benefits of UV-B treatments have also been documented. For example, UV-B treatments maintained firmness and delayed colour development in tomato, resulting in enhanced sensory qualities (Liu *et al.*, 2011). UV-B^{LD} treatments also increased dry biomass and leaf area in sweet basil and reduced postharvest weight loss in broccoli (Sakalauskaitė *et al.*, 2013; Darré *et al.*, 2017). In coriander, UV-B^{LD} treatment suppressed stem elongation in dense stands, leading to a compact phenotype with enhanced aesthetic properties (Fraser *et al.*, 2017).

Several studies suggest that UV-B^{LD} treatment can also confer increased resistance to pests and pathogens. For example, UV-B^{LD} treatment (2.5 or 5.0 kJ m^{-2} for 7 h) enhanced the resistance of field-grown rice (*Oryza sativa* 'Baijiaolaojing') to fungal infection by *Magnaporthe oryzae* (Li *et al.*, 2018). Similarly, a UV-B^{LD} treatment (1–2 kJ m^{-2} for 6 h) suppressed powdery mildew (*Podosphaera pannosa*) in greenhouse-grown roses (*Rose x hybrid* 'Valerie' and 'Rote Rose'; Kobayashi *et al.*, 2014). In Arabidopsis, UV-B^{LD} treatments have been used to induce resistance to caterpillars (*S. litura*; 1 kJ m^{-2} for 5 d; Qi *et al.*, 2018) and the fungus *B. cinerea* (5.5 kJ m^{-2} for 4 h; Demkura & Ballaré, 2012). Our findings inform potential applications for UV-B^{LD} treatments. Specifically, they suggest that their commercial value may be greatest when applied in combination with LAT storage. Our results also suggest that UV-B^{LD} treatments could have significant value for crops maintained at elevated ambient temperatures.

5.1. Conclusions and future directions

This work has demonstrated that UV-B^{LD} treatments can be used to suppress DIS in Arabidopsis leaves maintained at 20°C and that this effect results partly from UV-B^{LD}–induced downregulation of *ORE1* expression. It has also shown that preharvest UV-B^{LD} treatment remains effective in leaves maintained at HAT and additively enhances DIS suppression by LAT. This investigation contributes to a growing body of research indicating that UV-B^{LD} treatments may have beneficial applications for crop production (Demkura & Ballaré, 2012; Castagna *et al.*, 2013; Sakalauskaitė *et al.*, 2013; Kobayashi *et al.*, 2014; Darré *et al.*, 2017; Fraser *et al.*, 2017; Qi *et al.*, 2018; Li *et al.*, 2018). It is important to reiterate that in these experiments dark-incubated leaves were suspended on a liquid buffer, in accordance with published DIS protocols (Sakuraba *et al.*, 2014; Kim *et al.*, 2018). Storage in this manner could cause DIS to progress differently relative to leaves kept in commercial packaging. To support agricultural applications for UV-B^{LD}, future studies could repeat these experiments under commercially relevant conditions. It will also be also crucial to ascertain whether our results are replicable in agricultural species.

Significant questions remain regarding the optimum duration and dosage of UV-B treatments to achieve maximum DIS suppression whilst ensuring minimum tissue damage. Here, we report that a 4-h UV-B^{LD} treatment was sufficient to elicit DIS suppression. However, discrepancies in the existing literature suggest that the effect of UV-B^{LD} varies significantly depending on the duration of exposure. For example, a recent qPCR analysis reported that *PIF4/5* expression was unaffected by a 6-h UV-B^{LD} treatment, suggesting that UV-B^{LD}–mediated inhibition of PIF4/5 occurs exclusively post-translationally (Tavridou *et al.*, 2020a). By contrast, a subsequent study found that a 3-h UV-B^{LD} treatment suppressed *PIF4/5* expression, indicating that UV-B^{LD} disrupts *PIF4/5* transcription by an unknown mechanism (Tavridou *et al.*, 2020b). These results suggest that prolonged UV-B^{LD} exposure might prevent beneficial transcriptional effects. To determine an optimum dosage, future studies could employ Chl assays and Trypan Blue staining to monitor DIS suppression and cellular damage following UV-B^{LD} treatments of different durations. PAM fluorometry could also enable the efficient detection of UV-B^{LD}–induced photosynthetic damage.

Data presented here support a model in which UV-B^{LD} antagonises DIS by suppressing PIF4/5 transcript and protein abundance, resulting in repression of *ORE1* transcription. To test this, future studies could employ ChIP-qPCR to confirm whether PIF4/5 binding to the *ORE1* promoter is impaired following UV-B^{LD} treatment. This work also suggests that UV-B^{LD} is most effective when administered both preharvest and postharvest. Moving forward, an important avenue for research will be to determine the number of UV-B^{LD} treatments required to achieve optimal DIS suppression. This could be combined with RNA-Seq analysis to characterise changes in the expression of additional SAGs following UV-B^{LD} treatment.

Bibliography

Abdallah, M., Dubousset, L., Meuriot, F., Etienne, P., Avice, J. C. and Ourry, A. [2010], 'Effect of mineral sulphur availability on nitrogen and sulphur uptake and remobilization during the vegetative growth of *Brassica napus* L.', *Journal of Experimental Botany* **61**, 2635–2646.

Abeles, F. B., Dunn, L. J., Morgens, P., Callahan, A., Dinterman, R. E. and Schmidt, J. [1988], 'Induction of 33-kD and 60-kD peroxidases during ethylene-induced senescence of cucumber cotyledons', *Plant Physiology* **87**, 609–615.

Ahlawat, Y. and Liu, T. [2021], 'Varied expression of senescence-associated and ethylene-related genes during postharvest storage of brassica vegetables', *International Journal of Molecular Sciences* **22**, 1–14.

Aiamla-or, S., Kaewsuksaeng, S., Shigyo, M. and Yamauchi, N. [2010], 'Impact of UV-B irradiation on chlorophyll degradation and chlorophyll-degrading enzyme activities in stored broccoli (*Brassica oleracea* L. Italica Group) florets', *Food Chemistry* **120**, 645–651.

Ali, A., Gao, X. and Guo, Y. [2018], Initiation, progression, and genetic manipulation of leaf senescence, *in* Y. Guo, ed., 'Plant senescence: methods and protocols', Springer, New York, chapter 2, pp. 9–31.

Allu, A. D., Soja, A. M., Wu, A., Szymanski, J. and Balazadeh, S. [2014], 'Salt stress and senescence: identification of cross-talk regulatory components', *Journal of Experimental Botany* **65**, 3993–4008.

Aphalo, P. J. [2017], Quantification of UV radiation, *in* B. R. Jordan, ed., 'UV-B radiation and plant life: molecular biology to ecology', CABI, Egham, chapter 2, pp. 10–22.

Balazadeh, S., Riaño-Pachón, D. M. and Mueller-Roeber, B. [2008], 'Transcription factors regulating leaf senescence in *Arabidopsis thaliana*', *Plant Biology* **10**, 63–75.

Balevi, A., Üstüner, P., Kakşi, S. A. and Özdemir, M. [2018], 'Narrow-band UV-B phototherapy: an effective and reliable treatment alternative for extensive and recurrent pityriasis versicolor', *Journal of Dermatological Treatment* **29**, 252–255.

Binkert, M., Kozma-Bognár, L., Terecskei, K., De Veylder, L., Nagy, F. and Ulm, R. [2014], 'UV-B-responsive association of the *Arabidopsis* bZIP transcription factor ELONGATED HYPOCOTYL5 with target genes, including its own promoter', *Plant Cell* **26**, 4200–4213.

Bischof, S. [2020], 'Chimeric activators and repressors define HY5 activity', *Plant Cell* **32**, 793–794.

Biswal, U. C., Kasemir, H. and Mohr, H. [1982], 'Phytochrome control of degreening of attached cotyledons and primary leaves of mustard (*Sinapis Alba* L.) seedlings', *Photochemistry and Photobiology* **35**, 237–241.

Björn, L. O. [2015], 'Ultraviolet-A, B, and C', *UV4Plants Bulletin* **2015**, 17–18.

Bleecker, A. B. and Kende, H. [2000], 'Ethylene: a gaseous signal molecule in plants', *Annual Review of Cell and Developmental Biology* **16**, 1–18.

Bridge, L. J., Franklin, K. A. and Homer, M. E. [2013], 'Impact of plant shoot architecture on leaf cooling: a coupled heat and mass transfer model', *Journal of the Royal Society Interface* **10**, 20130326.

Briggs, W. R. and Christie, J. M. [2002], 'Phototropins 1 and 2: versatile plant blue-light receptors', *Trends in Plant Science* **7**, 204–210.

Brown, B. A. and Jenkins, G. I. [2008], 'UV-B signaling pathways with different fluence-rate response profiles are distinguished in mature *Arabidopsis* leaf tissue by requirement for UVR8, HY5, and HYH', *Plant Physiology* **146**, 576.

Buchanan-Wollaston, V., Page, T., Harrison, E., Breeze, E., Lim, P. O., Nam, H. G., Lin, J. F., Wu, S. H., Swidzinski, J., Ishizaki, K. and Leaver, C. J. [2005], 'Comparative transcriptome analysis reveals significant differences in gene expression and signalling pathways between developmental and dark/starvation-induced senescence in Arabidopsis', *The Plant Journal* **42**, 567–585.

Burgie, E. S. and Vierstra, R. D. [2014], 'Phytochromes: an atomic perspective on photoactivation and signaling', *Plant Cell* **26**, 568–4583.

Casal, J. J. [2013], 'Photoreceptor signaling networks in plant responses to shade', *Annual Review of Plant Biology* **64**, 403–427.

Casal, J. J. and Balasubramanian, S. [2019], 'Thermomorphogenesis', *Annual Review of Plant Biology* **70**, 321–346.

Castagna, A., Chiavaro, E., Dall'Asta, C., Rinaldi, M., Galaverna, G. and Ranieri, A. [2013], 'Effect of postharvest UV-B irradiation on nutraceutical quality and physical properties of tomato fruits', *Food Chemistry* **137**, 151–158.

Christie, J. M., Arvai, A. S., Baxter, K. J., Heilmann, M., Pratt, A. J., O'Hara, A., Kelly, S. M., Hothorn, M., Smith, B. O., Hitomi, K., Jenkins, G. I. and Getzoff, E. D. [2012], 'Plant UVR8 photoreceptor senses UV-B by tryptophan-mediated disruption of cross-dimer salt bridges', *Science* **335**, 1492–1496.

Chrobok, D., Law, S. R., Brouwer, B., Lindén, P., Ziolkowska, A., Liebsch, D., Narsai, R., Szal, B., Moritz, T., Rouhier, N., Whelan, J., Gardeström, P. and Keech, O. [2016], 'Dissecting the metabolic role of mitochondria during developmental leaf senescence', *Plant Physiology* **172**, 2132–2153.

Cloix, C., Kaiserli, E., Heilmann, M., Baxter, K. J., Brown, B. A., O'Hara, A., Smith, B. O., Christie, J. M. and Jenkins, G. I. [2012], 'C-terminal region of the UV-B photoreceptor UVR8 initiates signaling through interaction with the COP1 protein', *Proceedings of the National Academy of Sciences* **109**, 16366–16370.

Crawford, A. J., McLachlan, D. H., Hetherington, A. M. and Franklin, K. A. [2012], 'High temperature exposure increases plant cooling capacity', *Current Biology* **22**, R396–R397.

Csepregi, K., Coffey, A., Cunningham, N., Prinsen, E., Hideg, É. and Jansen, M. A. K. [2017], 'Developmental age and UV-B exposure co-determine antioxidant capacity and flavonol accumulation in Arabidopsis leaves', *Environmental and Experimental Botany* **140**, 19–25.

Darré, M., Valerga, L., Ortiz Araque, L. C., Lemoine, M. L., Demkura, P. V., Vicente, A. R. and Concellón, A. [2017], 'Role of UV-B irradiation dose and intensity on color retention and antioxidant elicitation in broccoli florets (*Brassica oleracea* var. *Italica*)', *Postharvest Biology and Technology* **128**, 76–82.

de Lucas, M., Davière, J. M., Rodríguez-Falcón, M., Pontin, M., Iglesias-Pedraz, J. M., Lorrain, S., Fankhauser, C., Blázquez, M. A., Titarenko, E. and Prat, S. [2008], 'A molecular framework for light and gibberellin control of cell elongation', *Nature* **451**, 480–484.

Demarsy, E. and Fankhauser, C. [2009], 'Higher plants use LOV to perceive blue light', *Current Opinion in Plant Biology* **12**, 69–74.

Demkura, P. V. and Ballaré, C. L. [2012], 'UVR8 mediates UV-B-induced *Arabidopsis* defense responses against *Botrytis cinerea* by controlling sinapate accumulation', *Molecular Plant* **5**, 642–652.

Depenbusch, L. and Klasen, S. [2019], 'The effect of bigger human bodies on the future global calorie requirements', *PLoS ONE* **14**, 1–15.

Devanesan, J. N., Karuppiah, A. and Kavitha Abirami, C. V. [2011], 'Effect of storage temperatures, O_2 concentrations and variety on respiration of mangoes', *Journal of Agrobiology* **28**, 119–128.

Di, D. W., Wu, L., Zhang, L., An, C. W., Zhang, T. Z., Luo, P., Gao, H. H., Kriechbaumer, V. and Guo, G. Q. [2016], 'Functional roles of Arabidopsis *CKRC2/YUCCA8* gene and the involvement of PIF4 in the regulation of auxin biosynthesis by cytokinin', *Scientific Reports* **6**, 1–9.

Dodge, J. D. [1970], 'Changes in chloroplast fine structure during the autumnal senescence of *Betula* leaves', *Annals of Botany* **34**, 817–824.

Ezer, D., Jung, J. H., Lan, H., Biswas, S., Gregoire, L., Box, M. S., Charoensawan, V., Cortijo, S., Lai, X., Stöckle, D., Zubieta, C., Jaeger, K. E. and Wigge, P. A. [2017], 'The evening complex coordinates environmental and endogenous signals in *Arabidopsis*', *Nature Plants* **3**, 1–12.

FAOSTAT [2019], 'FAOSTAT: statistical database', https://www.fao.org/faostat/en/#home. Accessed: 2020-11-16.

Favero, D. S. [2020], 'Mechanisms regulating PIF transcription factor activity at the protein level', *Physiologia Plantarum* **169**, 325–335.

Favory, J. J., Stec, A., Gruber, H., Rizzini, L., Oravecz, A., Funk, M., Albert, A., Cloix, C., Jenkins, G. I., Oakeley, E. J., Seidlitz, H. K., Nagy, F. and Ulm, R. [2009], 'Interaction of COP1 and UVR8 regulates UV-B-induced photomorphogenesis and stress acclimation in *Arabidopsis*', *EMBO Journal* **28**, 591–601.

Fernández-Milmanda, G. L. and Ballaré, C. L. [2021], 'Shade avoidance: expanding the color and hormone palette', *Trends in Plant Science* **26**, 509–523.

Findlay, K. M. W. and Jenkins, G. I. [2016], 'Regulation of UVR8 photoreceptor dimer/monomer photoequilibrium in Arabidopsis plants grown under photoperiodic conditions', *Plant Cell and Environment* **39**, 1706–1714.

Fiorucci, A. S., Galvão, V. C., Ince, Y. Ç., Boccaccini, A., Goyal, A., Petrolati, L. A., Trevisan, M. and Fankhauser, C. [2020], 'PHYTOCHROME INTERACTING FACTOR 7 is important for early responses to elevated temperature in Arabidopsis seedlings', *New Phytologist* **226**, 50–58.

Franklin, K. A. [2008], 'Shade avoidance', *New Phytologist* **179**, 930–944.

Franklin, K. A., Lee, S. H., Patel, D., Kumar, S. V., Spartz, A. K., Gu, C., Ye, S., Yu, P., Breen, G., Cohen, J. D., Wigge, P. A. and Gray, W. M. [2011], 'PHYTOCHROME-INTERACTING FACTOR 4 (PIF4) regulates auxin biosynthesis at high temperature', *Proceedings of the National Academy of Sciences* **108**, 20231–20235.

Franklin, K. A. and Quail, P. H. [2010], 'Phytochrome functions in *Arabidopsis* development', *Journal of Experimental Botany* **61**, 11–24.

Fraser, D. P., Sharma, A., Fletcher, T., Budge, S., Moncrieff, C., Dodd, A. N. and Franklin, K. A. [2017], 'UV-B antagonises shade avoidance and increases levels of the flavonoid quercetin in coriander (*Coriandrum sativum*)', *Scientific Reports* **7**, 17758.

Fujiki, Y., Yoshikawa, Y., Sato, T., Inada, N., Ito, M., Nishida, I. and Watanabe, A. [2001], 'Dark-inducible genes from *Arabidopsis thaliana* are associated with leaf senescence and repressed by sugars', *Physiologia Plantarum* **111**, 345–352.

Gan, S. [2018], Concepts and types of senescence in plants, *in* Y. Guo, ed., 'Plant senescence: methods and protocols', Springer, New York, pp. 3–8.

Gao, S., Gao, J., Zhu, X., Song, Y., Li, Z., Ren, G., Zhou, X. and Kuai, B. [2016], 'ABF2, ABF3, and ABF4 promote ABA-mediated chlorophyll degradation and leaf senescence by transcriptional activation of chlorophyll catabolic genes and senescence-associated genes in *Arabidopsis*', *Molecular Plant* **9**, 1272–1285.

Girondé, A., Etienne, P., Trouverie, J., Bouchereau, A., Le Cahérec, F., Leport, L., Orsel, M., Niogret, M. F., Nesi, N., Carole, D., Soulay, F., Masclaux-Daubresse, C. and Avice, J. C. [2015], 'The contrasting N management of two oilseed rape genotypes reveals the mechanisms of proteolysis associated with leaf N remobilization and the respective contributions of leaves and stems to N storage and remobilization during seed filling', *BMC Plant Biology* **15**, 1–22.

Goulas, Y., Cerovic, Z. G., Cartelat, A. and Moya, I. [2004], 'Dualex: a new instrument for field measurements of epidermal ultraviolet absorbance by chlorophyll fluorescence', *Applied Optics* **43**, 4488–4496.

Gray, W. M., Östin, A., Sandberg, G., Romano, C. P. and Estelle, M. [1998], 'High temperature promotes auxin-mediated hypocotyl elongation in *Arabidopsis*', *Proceedings of the National Academy of Sciences* **95**, 7197–7202.

Gruber, H., Heijde, M., Heller, W., Albert, A., Seidlitz, H. K. and Ulm, R. [2010], 'Negative feedback regulation of UV-B-induced photomorphogenesis and stress acclimation in *Arabidopsis*', *Proceedings of the National Academy of Sciences* **107**, 20132–20137.

Guo, Y. and Gan, S. [2012], 'Convergence and divergence in gene expression profiles induced by leaf senescence and 27 senescence-promoting hormonal, pathological and environmental stress treatments', *Plant, Cell & Environment* **35**, 644–655.

Guo, Y., Ren, G., Zhang, K., Li, Z., Miao, Y. and Guo, H. [2021], 'Leaf senescence: progression, regulation, and application', *Molecular Horticulture* **1**, 5.

Gustavsson, J., Cederberg, C., Sonesson, U., Van Otterdijk, R. and Meybeck, A. [2011], Global food losses and food Waste: extent, causes and prevention, Technical report, FAO.

Hayes, S., Sharma, A., Fraser, D. P., Trevisan, M., Cragg-Barber, C. K., Tavridou, E., Fankhauser, C., Jenkins, G. I. and Franklin, K. A. [2017], 'UV-B perceived by the UVR8 photoreceptor inhibits plant thermomorphogenesis', *Current Biology* **27**, 120–127.

Hayes, S., Velanis, C. N., Jenkins, G. I. and Franklin, K. A. [2014], 'UV-B detected by the UVR8 photoreceptor antagonizes auxin signaling and plant shade avoidance', *Proceedings of the National Academy of Sciences* **111**, 11894–11899.

Heijde, M. and Ulm, R. [2013], 'Reversion of the *Arabidopsis* UV-B photoreceptor UVR8 to the homodimeric ground state', *Proceedings of the National Academy of Sciences* **110**, 1113–1118.

Heilmann, M., Christie, J. M., Kennis, J. T. M., Jenkins, G. I. and Mathes, T. [2015], 'Photoinduced transformation of UVR8 monitored by vibrational and fluorescence spectroscopy', *Photochemical and Photobiological Sciences* **14**, 252–257.

Heilmann, M., Velanis, C. N., Cloix, C., Smith, B. O., Christie, J. M. and Jenkins, G. I. [2016], 'Dimer/monomer status and *in vivo* function of salt-bridge mutants of the plant UV-B photoreceptor UVR8', *The Plant Journal* **88**, 71–81.

Hoecker, U. [2017], 'The activities of the E3 ubiquitin ligase COP1/SPA, a key repressor in light signaling', *Current Opinion in Plant Biology* **37**, 63–69.

Hoecker, U. and Quail, P. H. [2001], 'The phytochrome A-specific signaling intermediate SPA1 interacts directly with COP1, a constitutive repressor of light signaling in *Arabidopsis*', *Journal of Biological Chemistry* **276**, 38173–38178.

Hollósy, F. [2002], 'Effects of ultraviolet radiation on plant cells', *Micron* **33**, 179–197.

Holm, M., Ma, L. G., Qu, L. J. and Deng, X. W. [2002], 'Two interacting bZIP proteins are direct targets of COP1-mediated control of light-dependent gene expression in *Arabidopsis*', *Genes & Development* **16**, 1247–1259.

Horie, Y., Ito, H., Kusaba, M., Tanaka, R. and Tanaka, A. [2009], 'Participation of chlorophyll *b* reductase in the initial step of the degradation of light-harvesting chlorophyll *a*/*b*-protein complexes in *Arabidopsis*', *Journal of Biological Chemistry* **284**, 17449–17456.

Hornitschek, P., Lorrain, S., Zoete, V., Michielin, O. and Fankhauser, C. [2009], 'Inhibition of the shade avoidance response by formation of non-DNA binding bHLH heterodimers', *EMBO Journal* **28**, 3893–3902.

Hörtensteiner, S. and Lee, D. [2007], Chlorophyll catabolism and leaf coloration, *in* S. Gan, ed., 'Annual reviews of senescence processes in plants', Vol. 26, Blackwell, chapter 2, pp. 12–38.

Huber, M., Nieuwendijk, N. M., Pantazopoulou, C. K. and Pierik, R. [2021], 'Light signalling shapes plant–plant interactions in dense canopies', *Plant, Cell & Environment* **44**, 1014–1029.

Jayas, D. S. and Jeyamkondan, S. [2002], 'PH–postharvest technology: modified atmosphere storage of grains meats fruits and vegetables', *Biosystems Engineering* **82**, 235–251.

Jung, J. H., Domijan, M., Klose, C., Biswas, S., Ezer, D., Gao, M., Khattak, A. K., Box, M. S., Charoensawan, V., Cortijo, S., Kumar, M., Grant, A., Locke, J. C. W., Schäfer, E., Jaeger, K. E. and Wigge, P. A. [2016], 'Phytochromes function as thermosensors in *Arabidopsis*', *Science* **354**, 886–889.

Kaiserli, E. and Jenkins, G. I. [2007], 'UV-B promotes rapid nuclear translocation of the *Arabidopsis* UV-B-specific signaling component UVR8 and activates its function in the nucleus', *Plant Cell* **19**, 2662–2673.

Keech, O., Pesquet, E., Ahad, A., Askne, A., Nordvall, D. A. G., Vodnala, S. M., Tuominen, H., Hurry, V., Dizengremel, P. and Garedestöm, P. E. R. [2007], 'The different fates of mitochondria and chloroplasts during dark-induced senescence in *Arabidopsis* leaves', *Plant, Cell & Environment* **30**, 1523–1534.

Kim, C., Kim, S. J., Jeong, J., Park, E., Oh, E., Park, Y. I., Lim, P. O. and Choi, G. [2020], 'High ambient temperature accelerates leaf senescence via PHYTOCHROME-INTERACTING FACTOR 4 and 5 in *Arabidopsis*', *Molecules and Cells* **43**, 645–661.

Kim, H. J., Hong, S. H., Kim, Y. W., Lee, I. H., Jun, J. H., Phee, B. K., Rupak, T., Jeong, H., Lee, Y., Hong, B. S., Nam, H. G., Woo, H. R. and Lim, P. O. [2014], 'Gene regulatory cascade of senescence-associated NAC transcription factors activated by ETHYLENE-INSENSITIVE2-mediated leaf senescence signalling in *Arabidopsis*', *Journal of Experimental Botany* **65**, 4023–4036.

Kim, J. H., Woo, H. R., Kim, J., Lim, P. O., Lee, I. C., Choi, S. H., Hwang, D. and Nam, H. G. [2009], 'Trifurcate feed-forward regulation of age-dependent cell death involving *miR164* in *Arabidopsis*', *Science* **323**, 1053–1057.

Kim, J., Kim, J. H., Lyu, J. I., Woo, H. R. and Lim, P. O. [2018a], 'New insights into the regulation of leaf senescence in *Arabidopsis*', *Journal of Experimental Botany* **69**, 787–799.

Kim, J., Park, S. J., Lee, I. H., Chu, H., Penfold, C. A., Kim, J. H., Buchanan-Wollaston, V., Nam, H. G., Woo, H. R. and Lim, P. O. [2018b], 'Comparative transcriptome analysis in Arabidopsis *ein2*/*ore3* and *ahk3*/*ore12* mutants during dark-induced leaf senescence', *Journal of Experimental Botany* **69**, 3023–3036.

Kliebenstein, D. J., Lim, J. E., Landry, L. G. and Last, R. L. [2002], 'Arabidopsis UVR8 regulates ultraviolet-B signal transduction and tolerance and contains sequence similarity to human *regulator of chromatin condensation 1*', *Plant Physiology* **130**, 234–243.

Klose, C., Nagy, F. and Schäfer, E. [2020], 'Thermal reversion of plant phytochromes', *Molecular Plant* **13**, 386–397.

Klose, C., Venezia, F., Hussong, A., Kircher, S., Schäfer, E. and Fleck, C. [2015], 'Systematic analysis of how phytochrome B dimerization determines its specificity', *Nature Plants* **1**, 1–9.

Kobayashi, M., Kanto, T., Fujikawa, T., Yamada, M., Ishiwata, M., Satou, M. and Hisamatsu, T. [2014], 'Supplemental UV radiation controls rose powdery mildew disease under the greenhouse conditions', *Environmental Control in Biology* **51**, 157–163.

Koini, M. A., Alvey, L., Allen, T., Tilley, C. A., Harberd, N. P., Whitelam, G. C. and Franklin, K. A. [2009], 'High temperature-mediated adaptations in plant architecture require the bHLH transcription factor PIF4', *Current Biology* **19**, 408–413.

Kuai, B., Chen, J. and Hörtensteiner, S. [2018], 'The biochemistry and molecular biology of chlorophyll breakdown', *Journal of Experimental Botany* **69**, 751–767.

Kusaba, M., Ito, H., Morita, R., Iida, S., Sato, Y., Fujimoto, M., Kawasaki, S., Tanaka, R., Hirochika, H., Nishimura, M. and Tanaka, A. [2007], 'Rice NON-YELLOW COLORING1 is involved in light-harvesting complex II and grana degradation during leaf senescence', *Plant cell* **19**, 1362–1375.

Lagarias, J. C. and Rapoport, H. [1980], 'Chromopeptides from phytochrome. The structure and linkage of the PR form of the phytochrome chromophore', *Journal of the American Chemical Society* **102**, 4821–4828.

Lange, D. D. and Cameron, A. C. [1994], 'Postharvest shelf life of sweet basil (*Ocimum basilicum*)', *HortScience* **29**, 102–103.

Lau, K., Podolec, R., Chappuis, R., Ulm, R. and Hothorn, M. [2019], 'Plant photoreceptors and their signaling components compete for COP1 binding via VP peptide motifs', *EMBO Journal* **38**, e102140.

Lee, I. C., Hong, S. W., Whang, S. S., Lim, P. O., Nam, H. G. and Koo, J. C. [2011], 'Age-dependent action of an ABA-inducible receptor kinase, RPK1, as a positive regulator of senescence in *Arabidopsis* leaves', *Plant and Cell Physiology* **52**, 651–662.

Legris, M., Klose, C., Burgie, E. S., Rojas, C. C., Neme, M., Hiltbrunner, A., Wigge, P. A., Schäfer, E., Vierstra, R. D. and Casal, J. J. [2016], 'Phytochrome B integrates light and temperature signals in *Arabidopsis*', *Science* **354**, 897–900.

Li, K., Yu, R., Fan, L. M., Wei, N., Chen, H. and Deng, X. W. [2016], 'DELLA-mediated PIF degradation contributes to coordination of light and gibberellin signalling in *Arabidopsis*', *Nature Communications* **7**, 1–11.

Li, X., He, Y., Xie, C., Zu, Y., Zhan, F., Mei, X., Xia, Y. and Li, Y. [2018], 'Effects of UV-B radiation on the infectivity of *Magnaporthe oryzae* and rice disease-resistant physiology in Yuanyang terraces', *Photochemical and Photobiological Sciences* **17**, 8–17.

Li, X., Liu, Z., Ren, H., Kundu, M., Wang, L., Gao, J. and Zhong, D. [2020a], 'Dynamics and mechanism of light harvesting in UV photoreceptor UVR8', *Chemical Science* **11**, 12553–12569.

Li, Z., Peng, J., Wen, X. and Guo, H. [2013], '*ETHYLENE-INSENSITIVE3* is a senescence-associated gene that accelerates age-dependent leaf senescence by directly repressing *miR164* transcription in *Arabidopsis*', *Plant Cell* **25**, 3311–3328.

Li, Z., Zhang, Y., Zou, D., Zhao, Y., Wang, H. L., Zhang, Y., Xia, X., Luo, J., Guo, H. and Zhang, Z. [2020b], 'LSD 3.0: a comprehensive resource for the leaf senescence research community', *Nucleic Acids Research* **48**, D1069–D1075.

Lin, C. [2002], 'Blue light receptors and signal transduction', *Plant Cell* **14**, S207–S225.

Liu, C., Han, X., Cai, L., Lu, X., Ying, T. and Jiang, Z. [2011], 'Postharvest UV-B irradiation maintains sensory qualities and enhances antioxidant capacity in tomato fruit during storage', *Postharvest Biology and Technology* **59**, 232–237.

Liu, X., Li, Z., Jiang, Z., Zhao, Y., Peng, J., Jin, J., Guo, H. and Luo, J. [2011], 'LSD: a leaf senescence database', *Nucleic Acids Research* **39**, D1103–D1107.

Lorrain, S., Allen, T., Duek, P. D., Whitelam, G. C. and Fankhauser, C. [2008], 'Phytochrome-mediated inhibition of shade avoidance involves degradation of growth-promoting bHLH transcription factors', *The Plant Journal* **53**, 312–323.

Lutts, S., Kinet, J. M. and Bouharmon, J. [1996], 'NaCl-induced senescence in leaves of rice (*Oryza sativa* L.) cultivars differing in salinity resistance', *Annals of Botany* **78**, 389–398.

Ma, D., Li, X., Guo, Y., Chu, J., Fang, S., Yan, C., Noel, J. P. and Liu, H. [2016], 'Cryptochrome 1 interacts with PIF4 to regulate high temperature-mediated hypocotyl elongation in response to blue light', *Proceedings of the National Academy of Sciences* **113**, 224–229.

Makino, A., Sakuma, H., Sudo, E. and Mae, T. [2003], 'Differences between maize and rice in N-use efficiency for photosynthesis and protein allocation', *Plant and Cell Physiology* **44**, 952–956.

Martínez-Zamora, L., Castillejo, N. and Artés-Hernández, F. [2021], 'Postharvest UV-B and UV-C radiation enhanced the biosynthesis of glucosinolates and isothiocyanates in *Brassicaceae* sprouts', *Postharvest Biology and Technology* **181**, 111650.

Mathes, T., Heilmann, M., Pandit, A., Zhu, J., Ravensbergen, J., Kloz, M., Fu, Y., Smith, B. O., Christie, J. M., Jenkins, G. I. and Kennis, J. T. M. [2015], 'Proton-coupled electron transfer constitutes the photoactivation mechanism of the plant photoreceptor UVR8', *Journal of the American Chemical Society* **137**, 8113–8120.

McCree, K. J. [1971], 'The action spectrum, absorptance and quantum yield of photosynthesis in crop plants', *Agricultural Meteorology* **9**, 191–216.

Meguro, M., Ito, H., Takabayashi, A., Tanaka, R. and Tanaka, A. [2011], 'Identification of the 7-hydroxymethyl chlorophyll *a* reductase of the chlorophyll cycle in *Arabidopsis*', *Plant Cell* **23**, 3442–3453.

Miersch, I., Heise, J., Zelmer, I. and Humbeck, K. [2000], 'Differential degradation of the photosynthetic apparatus during leaf senescence in barley (*Hordeum vulgare* L.)', *Plant Biology* **2**, 618–623.

Müller, T., Ulrich, M., Ongania, K.-H. and Kräutler, B. [2007], 'Colorless tetrapyrrolic chlorophyll catabolites found in ripening fruit are effective antioxidants', *Angewandte Chemie International Edition* **46**, 8699–8702.

Nozue, K., Covington, M. F., Duek, P. D., Lorrain, S., Fankhauser, C., Harmer, S. L. and Maloof, J. N. [2007], 'Rhythmic growth explained by coincidence between internal and external cues', *Nature* **448**, 358–361.

Nusinow, D. A., Helfer, A., Hamilton, E. E., King, J. J., Imaizumi, T., Schultz, T. F., Farré, E. M. and Kay, S. A. [2011], 'The ELF4-ELF3-LUX complex links the circadian clock to diurnal control of hypocotyl growth', *Nature* **475**, 398–404.

Oberhuber, M., Berghold, J. and Kräutler, B. [2008], 'Chlorophyll breakdown by a biomimetic route', *Angewandte Chemie International Edition* **47**, 3057–3061.

Oh, S. A., Park, J., Lee, G. I., Paek, K. H., Park, S. K. and Nam, H. G. [1997], 'Identification of three genetic loci controlling leaf senescence in *Arabidopsis thaliana*', *The Plant Journal* **12**, 527–535.

O'Hara, A. and Jenkins, G. I. [2012], 'In vivo function of tryptophans in the *Arabidopsis* UV-B photoreceptor UVR8', *Plant Cell* **24**, 3755–3766.

Osterlund, M. T., Hardtke, C. S., Wei, N. and Deng, X. W. [2000], 'Targeted destabilization of HY5 during light-regulated development of *Arabidopsis*', *Nature* **405**, 462–466.

Park, E., Kim, J., Lee, Y., Shin, J., Oh, E., Chung, W. I., Jang, R. L. and Choi, G. [2004], 'Degradation of phytochrome interacting factor 3 in phytochrome-mediated light signaling', *Plant and Cell Physiology* **45**, 968–975.

Park, E., Kim, Y. and Choi, G. [2018], 'Phytochrome B requires PIF degradation and sequestration to induce light responses across a wide range of light conditions', *Plant Cell* **30**, 1277–1292.

Park, E., Park, J., Kim, J., Nagatani, A., Lagarias, J. C. and Choi, G. [2012], 'Phytochrome B inhibits binding of phytochrome-interacting factors to their target promoters', *The Plant Journal* **72**, 537–546.

Paul, N. D. and Gwynn-Jones, D. [2003], 'Ecological roles of solar UV radiation: towards an integrated approach', *Trends in Ecology and Evolution* **18**, 48–55.

Pfeiffer, H. and Kleudgen, H. K. [1980], 'Investigations on the phytochrome control of senescence in the photosynthetic apparatus of *Hordeum vulgare* L.', *Zeitschrift für Pflanzenphysiologie* **100**, 437–445.

Pham, V. N., Kathare, P. K. and Huq, E. [2018a], 'Phytochromes and phytochrome interacting factors', *Plant Physiology* **176**, 1025–1038.

Pham, V. N., Kathare, P. K. and Huq, E. [2018b], 'Dynamic regulation of PIF5 by COP1–SPA complex to optimize photomorphogenesis in Arabidopsis', *The Plant Journal* **96**, 260–273.

Pham, V. N., Xu, X. and Huq, E. [2018c], 'Molecular bases for the constitutive photomorphogenic phenotypes in *Arabidopsis*', *Development* **145**, dev169870.

Podolec, R., Demarsy, E. and Ulm, R. [2021], 'Perception and signaling of ultraviolet-B radiation in plants', *Annual Review of Plant Biology* **72**, 793–822.

Pružinská, A., Anders, I., Aubry, S., Schenk, N., Tapernoux-Lüthi, E., Müller, T., Kräutler, B. and Hörtensteiner, S. [2007], 'In vivo participation of red chlorophyll catabolite reductase in chlorophyll breakdown', *Plant Cell* **19**, 369–387.

Pružinská, A., Tanner, G., Anders, I., Roca, M. and Hörtensteiner, S. [2003], 'Chlorophyll breakdown: pheophorbide *a* oxygenase is a rieske-type iron–sulfur protein, encoded by the *accelerated cell death 1* gene', *Proceedings of the National Academy of Sciences* **100**, 15259–15264.

Pyung, O. L., Hyo, J. K. and Hong, G. N. [2007], 'Leaf senescence', *Annual Review of Plant Biology* **58**, 115–136.

Qi, J., Zhang, M., Lu, C., Hettenhausen, C., Tan, Q., Cao, G., Zhu, X., Wu, G. and Wu, J. [2018], 'Ultraviolet-B enhances the resistance of multiple plant species to lepidopteran insect herbivory through the jasmonic acid pathway', *Scientific Reports* **8**, 277.

Qiu, K., Li, Z., Yang, Z., Chen, J., Wu, S., Zhu, X., Gao, S., Gao, J., Ren, G., Kuai, B. and Zhou, X. [2015], 'EIN3 and ORE1 accelerate degreening during ethylene-mediated leaf senescence by directly activating chlorophyll catabolic genes in *Arabidopsis*', *PLoS Genetics* **11**, 1–20.

Quint, M., Delker, C., Franklin, K. A., Wigge, P. A., Halliday, K. J. and Van Zanten, M. [2016], 'Molecular and genetic control of plant thermomorphogenesis', *Nature Plants* **2**, 1–9.

Ramankutty, N., Evan, A. T., Monfreda, C. and Foley, J. A. [2008], 'Farming the planet: 1. geographic distribution of global agricultural lands in the year 2000', *Global Biogeochemical Cycles* **22**, GB1003.

Ramankutty, N., Mehrabi, Z., Waha, K., Jarvis, L., Kremen, C., Herrero, M. and Rieseberg, L. H. [2018], 'Trends in global agricultural land use: implications for environmental health and food security', *Annual Review of Plant Biology* **69**, 789–815.

Rauf, M., Arif, M., Dortay, H., Matallana-Ramírez, L. P., Waters, M. T., Gil Nam, H., Lim, P. O., Mueller-Roeber, B. and Balazadeh, S. [2013], 'ORE1 balances leaf senescence against maintenance by antagonizing G2-like-mediated transcription', *EMBO Reports* **14**, 382–388.

Rizzini, L., Favory, J. J., Cloix, C., Faggionato, D., O'Hara, A., Kaiserli, E., Baumeister, R., Schäfer, E., Nagy, F., Jenkins, G. I. and Ulm, R. [2011], 'Perception of UV-B by the *Arabidopsis* UVR8 protein', *Science* **332**, 103–106.

Romero-Montepaone, S., Sellaro, R., Esteban Hernando, C., Costigliolo-Rojas, C., Bianchimano, L., Ploschuk, E. L., Yanovsky, M. J. and Casal, J. J. [2021], 'Functional convergence of growth responses to shade and warmth in *Arabidopsis*', *New Phytologist* **231**, 1890–1905.

Rosenthal, S. I. and Camm, E. L. [1996], 'Effects of air temperature, photoperiod and leaf age on foliar senescence of western larch (*Larix occidentalis* Nutt.) in environmentally controlled chambers', *Plant, Cell & Environment* **19**, 1057–1065.

Sakalauskaitė, J., Viskelis, P., Dambrauskienė, E., Sakalauskienė, S., Samuolienė, G., Brazaitytė, A., Duchovskis, P. and Urbonavičienė, D. [2013], 'The effects of different UV-B radiation intensities on morphological and biochemical characteristics in *Ocimum basilicum* L.', *Journal of the Science of Food and Agriculture* **93**, 1266–1271.

Sakuraba, Y. [2021], 'Light-mediated regulation of leaf senescence', *International Journal of Molecular Sciences* **22**, 3291.

Sakuraba, Y., Jeong, J., Kang, M. Y., Kim, J., Paek, N. C. and Choi, G. [2014a], 'Phytochrome-interacting transcription factors PIF4 and PIF5 induce leaf senescence in *Arabidopsis*', *Nature Communications* **5**, 1–13.

Sakuraba, Y., Park, S. Y., Kim, Y. S., Wang, S. H., Yoo, S. C., Hörtensteiner, S. and Paek, N. C. [2014b], '*Arabidopsis* STAY-GREEN2 is a negative regulator of chlorophyll degradation during leaf senescence', *Molecular Plant* **7**, 1288–1302.

Salomé, P. A., Xie, Q. and McClung, C. R. [2008], 'Circadian timekeeping during early Arabidopsis development', *Plant Physiology* **147**, 1110–1125.

Sato, Y., Morita, R., Katsuma, S., Nishimura, M., Tanaka, A. and Kusaba, M. [2009], 'Two short-chain dehydrogenase/reductases, NON-YELLOW COLORING 1 and NYC1-LIKE, are required for chlorophyll *b* and light-harvesting complex II degradation during senescence in rice', *The Plant Journal* **57**, 120–131.

Schelbert, S., Aubry, S., Burla, B., Agne, B., Kessler, F., Krupinska, K. and Hörtensteiner, S. [2009], 'Pheophytin pheophorbide hydrolase (pheophytinase) is involved in chlorophyll breakdown during leaf senescence in *Arabidopsis*', *Plant Cell* **21**, 767–785.

Schippers, J. H. M., Schmidt, R., Wagstaff, C. and Jing, H. C. [2015], 'Living to die and dying to live: the survival strategy behind leaf senescence', *Plant Physiology* **169**, 914–930.

Sharma, A. [2012], 'An ultraviolet-sterilization protocol for microtitre plates', *Journal of Experimental Microbiology and Immunology* **16**, 144–147.

Sharma, A., Sharma, B., Hayes, S., Kerner, K., Hoecker, U., Jenkins, G. I. and Franklin, K. A. [2019], 'UVR8 disrupts stabilisation of PIF5 by COP1 to inhibit plant stem elongation in sunlight', *Nature Communications* **10**, 4417.

Shen, H., Zhu, L., Castillon, A., Majee, M., Downie, B. and Huq, E. [2008], 'Light-induced phosphorylation and degradation of the negative regulator PHYTOCHROME-INTERACTING FACTOR1 from *Arabidopsis* depend upon its direct physical interactions with photoactivated phytochromes', *Plant Cell* **20**, 1586–1602.

Shen, Y., Khanna, R., Carle, C. M. and Quail, P. H. [2007], 'Phytochrome induces rapid PIF5 phosphorylation and degradation in response to red-light activation', *Plant Physiology* **145**, 1043–1051.

Shimoda, Y., Ito, H. and Tanaka, A. [2016], 'Arabidopsis *STAY-GREEN*, Mendel's green cotyledon gene, encodes magnesium-dechelatase', *Plant Cell* **28**, 2147–2160.

Silva, C. S., Nayak, A., Lai, X., Hutin, S., Hugouvieux, V., Jung, J. H., López-Vidriero, I., Franco-Zorrilla, J. M., Panigrahi, K. C. S., Nanao, M. H., Wigge, P. A. and Zubieta, C. [2020], 'Molecular mechanisms of Evening Complex activity in *Arabidopsis*', *Proceedings of the National Academy of Sciences* **117**, 6901–6909.

Smart, C. M. [1994], 'Gene expression during leaf senescence', *New Phytologist* **126**, 419–448.

Smith, H. [1982], 'Light quality, photoperception, and plant strategy', *Annual Review of Plant Physiology* **33**, 481–518.

Smith, H. [2000], 'Phytochromes and light signal perception by plants—an emerging synthesis', *Nature* **407**, 585–591.

Song, Y., Yang, C., Gao, S., Zhang, W., Li, L. and Kuai, B. [2014], 'Age-triggered and dark-induced leaf senescence require the bHLH transcription factors PIF3, 4, and 5', *Molecular Plant* **7**, 1776–1787.

Srilaong, V., Aiamla-or, S., Soontornwat, A., Shigyo, M. and Yamauchi, N. [2011], 'UV-B irradiation retards chlorophyll degradation in lime (*Citrus latifolia* Tan.) fruit', *Postharvest Biology and Technology* **59**, 110–112.

Stavang, J. A., Gallego-Bartolomé, J., Gómez, M. D., Yoshida, S., Asami, T., Olsen, J. E., García-Martínez, J. L., Alabadí, D. and Blázquez, M. A. [2009], 'Hormonal regulation of temperature-induced growth in Arabidopsis', *The Plant Journal* **60**, 589–601.

Steensland, A. and Thompson, T. [2020], 2020 global agricultural productivity report: productivity in a time of pandemics, Technical report, Virginia Tech College of Agriculture and Life Sciences, Blacksburg, VA, USA.

Sun, J., Qi, L., Li, Y., Chu, J. and Li, C. [2012], 'PIF4–mediated activation of *YUCCA8* expression integrates temperature into the auxin pathway in regulating *Arabidopsis* hypocotyl growth', *PLoS Genetics* **8**, e1002594.

Sweetman, J. M. [2020], The effects of ultraviolet B radiation on dark-induced foliar senescence in *Arabidopsis thaliana*, Master's thesis, School of Biological Sciences, University of Bristol.

Sztatelman, O., Grzyb, J., Gabryś, H. and Banaś, A. K. [2015], 'The effect of UV-B on Arabidopsis leaves depends on light conditions after treatment', *BMC Plant Biology* **15**, 1–16.

Tavridou, E., Pireyre, M. and Ulm, R. [2020a], 'Degradation of the transcription factors PIF4 and PIF5 under UV-B promotes UVR8-mediated inhibition of hypocotyl growth in Arabidopsis', *The Plant Journal* **101**, 507–517.

Tavridou, E., Schmid-Siegert, E., Fankhauser, C. and Ulm, R. [2020b], 'UVR8-mediated inhibition of shade avoidance involves HFR1 stabilization in Arabidopsis', *PLoS Genetics* **16**, e1008797.

Tucker, D. J. [1981], 'Phytochrome regulation of leaf senescence in cucumber and tomato', *Plant Science Letters* **23**, 103–108.

Ueda, H., Ito, T., Inoue, R., Masuda, Y., Nagashima, Y., Kozuka, T. and Kusaba, M. [2020], 'Genetic interaction among phytochrome, ethylene and abscisic acid signaling during dark-induced senescence in *Arabidopsis thaliana*', *Frontiers in Plant Science* **11**, 1–11.

UN DESA [2019], World population prospects 2019: highlights (ST/ESA/SER. A/423), Technical report, UN DESA, New York (US).

van de Poel, B. and van der Straeten, D. [2017], 'Plant ethylene detection using laser-based photoacoustic spectroscopy', *Methods in Molecular Biology* **1573**, 11–26.

van der Graaff, E., Schwacke, R., Schneider, A., Desimone, M., Flügge, U. I., Kunze, R., Flügge, U.-I. and Kunze, R. [2006], 'Transcription analysis of Arabidopsis membrane transporters and hormone pathways during developmental and induced leaf senescence', *Plant Physiology* **141**, 776–792.

Vu, L. D., Xu, X., Gevaert, K. and De Smet, I. [2019], 'Developmental plasticity at high temperature', *Plant Physiology* **181**, 399–411.

Wang, N. N., Yang, S. F. and Charng, Y. [2001], 'Differential expression of 1-aminocyclopropane-1-carboxylate synthase genes during orchid flower senescence induced by the protein phosphatase inhibitor okadaic acid', *Plant Physiology* **126**, 253–260.

Wang, Y., Liu, C., Li, K., Sun, F., Hu, H., Li, X., Zhao, Y., Han, C., Zhang, W., Duan, Y., Liu, M. and Li, X. [2007], '*Arabidopsis EIN2* modulates stress response through abscisic acid response pathway', *Plant Molecular Biology* **64**, 633–644.

Wargent, J. J. [2016], 'UV LEDs in horticulture: from biology to application', *Acta Horticulturae* **1134**, 25–32.

Weaver, L. M. and Amasino, R. M. [2001], 'Senescence is induced in individually darkened Arabidopsis leaves, but inhibited in whole darkened plants', *Plant Physiology* **127**, 876–886.

Williams, A. G. and Whitham, T. G. [1986], 'Premature leaf abscission: an induced plant defense against gall aphids', *Ecology* **67**, 1619–1627.

Witham, F. H., Blaydes, D. F. and Devlin, R. M. [1971], *Experiments in plant physiology*, Van Nostrand Reinhold, New York.

Woo, H. R., Goh, C. H., Park, J. H., de la Serve, B. T., Kim, J. H., Park, Y. I. and Nam, H. G. [2002], 'Extended leaf longevity in the *ore4-1* mutant of *Arabidopsis* with a reduced expression of a plastid ribosomal protein gene', *The Plant Journal* **31**, 331–340.

Woo, H. R., Kim, H. J., Lim, P. O. and Nam, H. G. [2019], 'Leaf senescence: systems and dynamics aspects', *Annual Review of Plant Biology* **70**, 347–376.

Wu, D., Hu, Q., Yan, Z., Chen, W., Yan, C., Huang, X., Zhang, J., Yang, P., Deng, H., Wang, J., Deng, X. and Shi, Y. [2012], 'Structural basis of ultraviolet-B perception by UVR8', *Nature* **484**, 214–219.

Wu, M., Eriksson, L. A. and Strid, Å. [2013], 'Theoretical prediction of the protein–protein interaction between *Arabidopsis thaliana* COP1 and UVR8', *Theoretical Chemistry Accounts* **132**, 1371.

Wu, S., Li, Z., Yang, L., Xie, Z., Chen, J., Zhang, W., Liu, T., Gao, S., Gao, J., Zhu, Y., Xin, J., Ren, G. and Kuai, B. [2016], 'NON-YELLOWING2 (NYE2), a close paralog of NYE1, plays a positive role in chlorophyll degradation in *Arabidopsis*', *Molecular Plant* **9**, 624–627.

Xu, X., Kathare, P. K., Pham, V. N., Bu, Q., Nguyen, A. and Huq, E. [2017], 'Reciprocal proteasome-mediated degradation of PIFs and HFR1 underlies photomorphogenic development in *Arabidopsis*', *Development* **144**, 1831–1840.

Yamaguchi, R., Nakamura, M., Mochizuki, N., Kay, S. A. and Nagatani, A. [1999], 'Light-dependent translocation of a phytochrome B-GFP fusion protein to the nucleus in transgenic *Arabidopsis*', *Journal of Cell Biology* **145**, 437–445.

Yang, J., Worley, E. and Udvardi, M. [2014], 'A NAP-AAO3 regulatory module promotes chlorophyll degradation via ABA biosynthesis in *Arabidopsis* leaves', *Plant Cell* **26**, 4862–4874.

Yang, Y., Liang, T., Zhang, L., Shao, K., Gu, X., Shang, R., Shi, N., Li, X., Zhang, P. and Liu, H. [2018], 'UVR8 interacts with WRKY36 to regulate *HY5* transcription and hypocotyl elongation in *Arabidopsis*', *Nature Plants* **4**, 98–107.

Yin, R., Arongaus, A. B., Binkert, M. and Ulm, R. [2015], 'Two distinct domains of the UVR8 photoreceptor interact with COP1 to initiate UV-B signaling in Arabidopsis', *Plant Cell* **27**, 202–213.

Yin, R., Skvortsova, M. Y., Loubéry, S. and Ulm, R. [2016], 'COP1 is required for UV-B-induced nuclear accumulation of the UVR8 photoreceptor', *Proceedings of the National Academy of Sciences* **113**, E4415–E4422.

Zeng, X., Ren, Z., Wu, Q., Fan, J., Peng, P. P., Tang, K., Zhang, R., Zhao, K. H. and Yang, X. [2015], 'Dynamic crystallography reveals early signalling events in ultraviolet photoreceptor UVR8', *Nature Plants* **1**, 1–6.

Zhang, K., Xia, X., Zhang, Y. and Gan, S. [2012], 'An ABA-regulated and Golgi-localized protein phosphatase controls water loss during leaf senescence in Arabidopsis', *The Plant Journal* **69**, 667–678.

Zhang, Y., Liu, Z., Chen, Y., He, J. X. and Bi, Y. [2015], 'PHYTOCHROME-INTERACTING FACTOR 5 (PIF5) positively regulates dark-induced senescence and chlorophyll degradation in *Arabidopsis*', *Plant Science* **237**, 57–68.

Zhao, L., Xia, Y., Wu, X.-Y., Schippers, J. H. M. and Jing, H.-C. [2018], Phenotypic analysis and molecular markers of leaf senescence, *in* Y. Guo, ed., 'Plant senescence: methods and protocols', Springer, New York, pp. 35–48.

Zhao, Y., Chan, Z., Gao, J., Xing, L., Cao, M., Yu, C., Hu, Y., You, J., Shi, H., Zhu, Y., Gong, Y., Mu, Z., Wang, H., Deng, X., Wang, P., Bressan, R. A. and Zhu, J. K. [2016], 'ABA receptor PYL9 promotes drought resistance and leaf senescence', *Proceedings of the National Academy of Sciences* **113**, 1949–1954.

Zhao, Y., Gao, J., Im Kim, J., Chen, K., Bressan, R. A. and Zhu, J.-K. [2017], 'Control of plant water use by ABA induction of senescence and dormancy: an overlooked lesson from evolution', *Plant and Cell Physiology* **58**, 1319–1327.

Zhu, D., Maier, A., Lee, J.-H., Laubinger, S., Saijo, Y., Wang, H., Qu, L.-J., Hoecker, U. and Deng, X. W. [2008], 'Biochemical characterization of *Arabidopsis* complexes containing CONSTITUTIVELY PHOTOMORPHOGENIC1 and SUPPRESSOR OF PHYA proteins in light control of plant development', *Plant Cell* **20**, 2307–2323.

Appendix

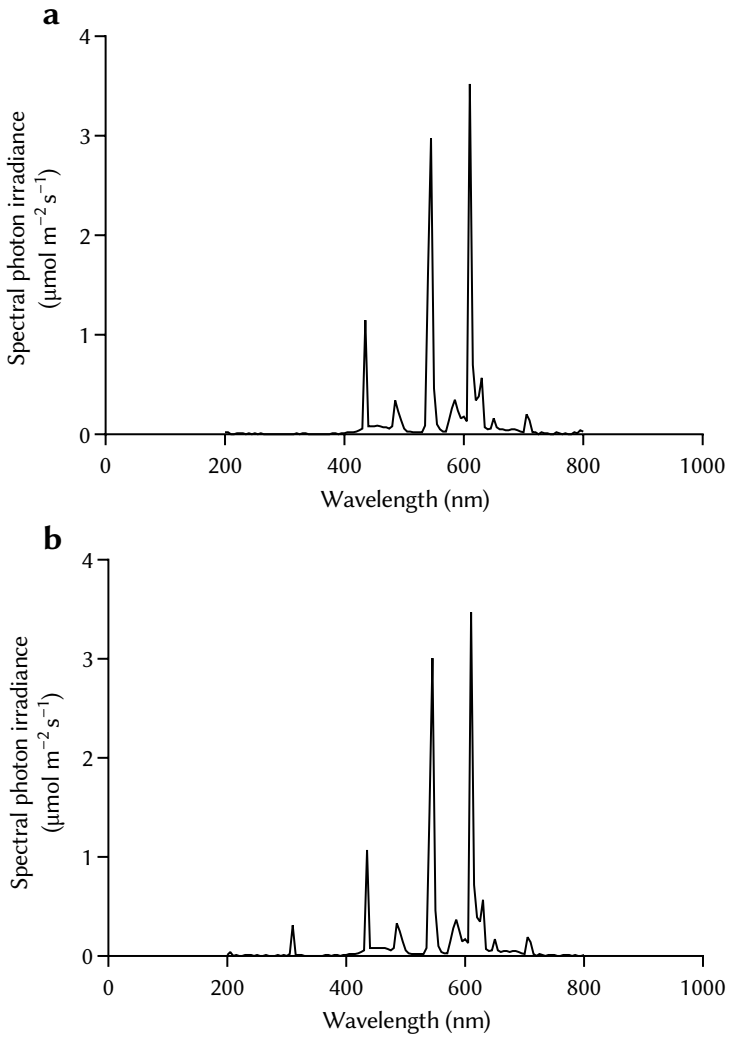

Figure S1. Emission spectra of **(a)** WL and **(b)** WL with UV-B light sources.

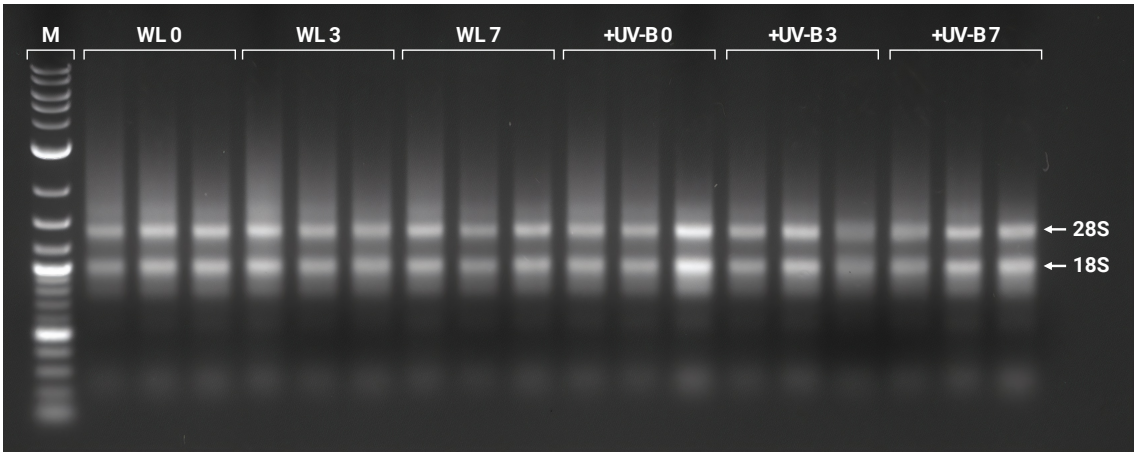

Figure S2. Assessment of RNA integrity using 1% agarose electrophoresis. Electrophoretic profiles of total RNA from WL- and +UV-B–treated Arabidopsis leaves at 0, 3, and 7 DDI (lanes 2–19). Three biological replicates were used for each treatment and at each time point. Lane M contains 1 kb DNA ladder. Arrows indicate 18S and 28S ribosomal RNA bands.

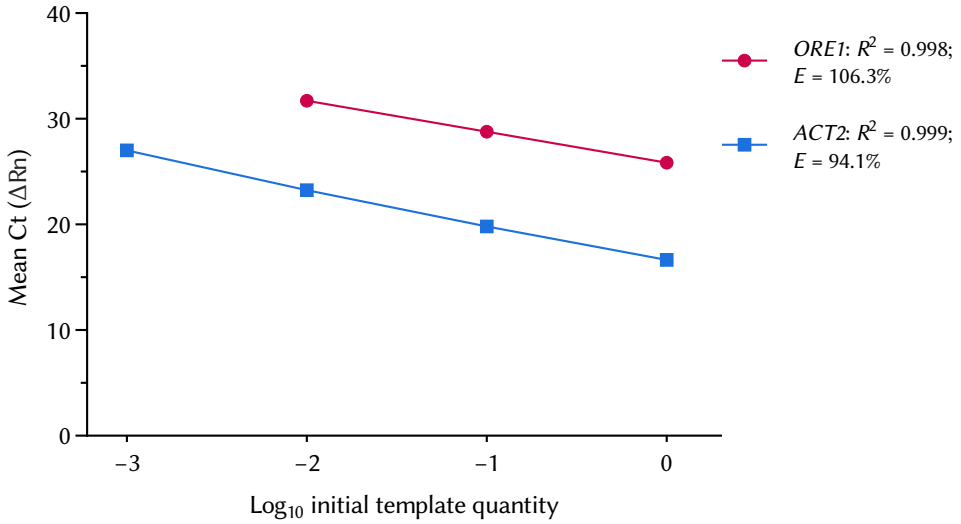

Figure S3. Standard curve assessment of PCR primer efficiency. Standard curves for *ORE1* and *ACT2* primers were generated by performing qPCR on serial 10-fold diluted cDNA samples. Amplification efficiencies (E) were calculated from resultant slopes according to the following equation: $E\,(\%) = (10^{-1/\text{slope}}) \times 100$. Mean correlation coefficient (R^2) and E values are shown.

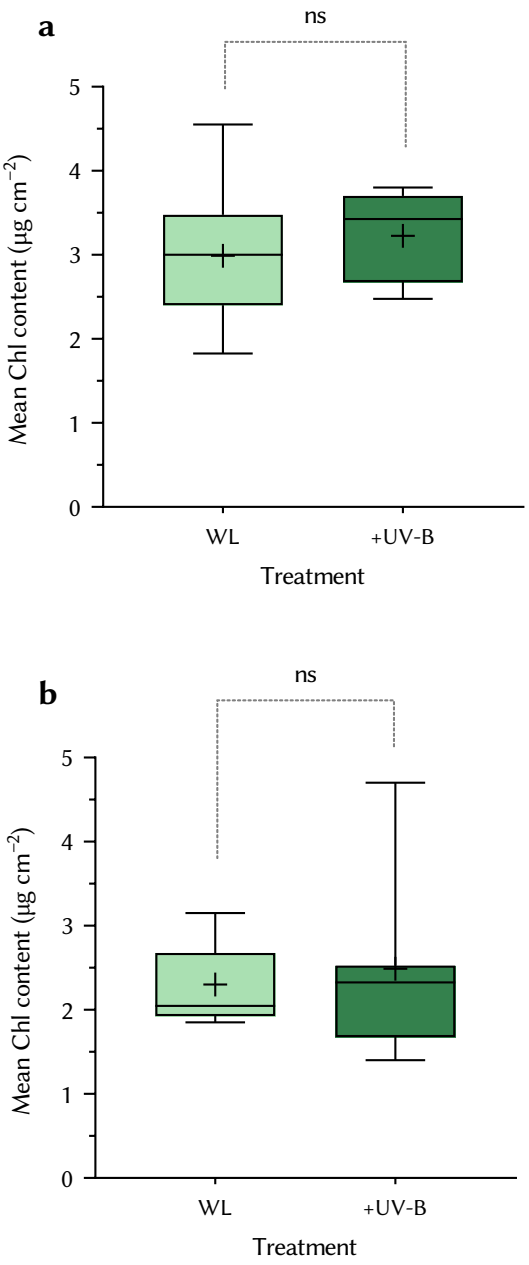

Figure S4. Experimental replicates of Fig. 5 using independently grown plants. Four-week-old Arabidopsis plants were treated with either WL or WL supplemented with low-dose UV-B (+UV-B; 1 µmol m^{-1} s^{-1}) for 4 h at dawn. Fourth and fifth rosette leaves were detached and dark-incubated for 7 d at 20°C. Mean Chl content (µg cm^{-2}) was determined by performing Dualex measurement at four predetermined locations on the adaxial leaf surface. Centre lines of box plots represent medians, + represent means, boxes delimit 25th and 75th percentiles, whiskers represent minimum and maximum values. ns indicates no statistically significant difference at $p \leq .05$ ($n = 7$).

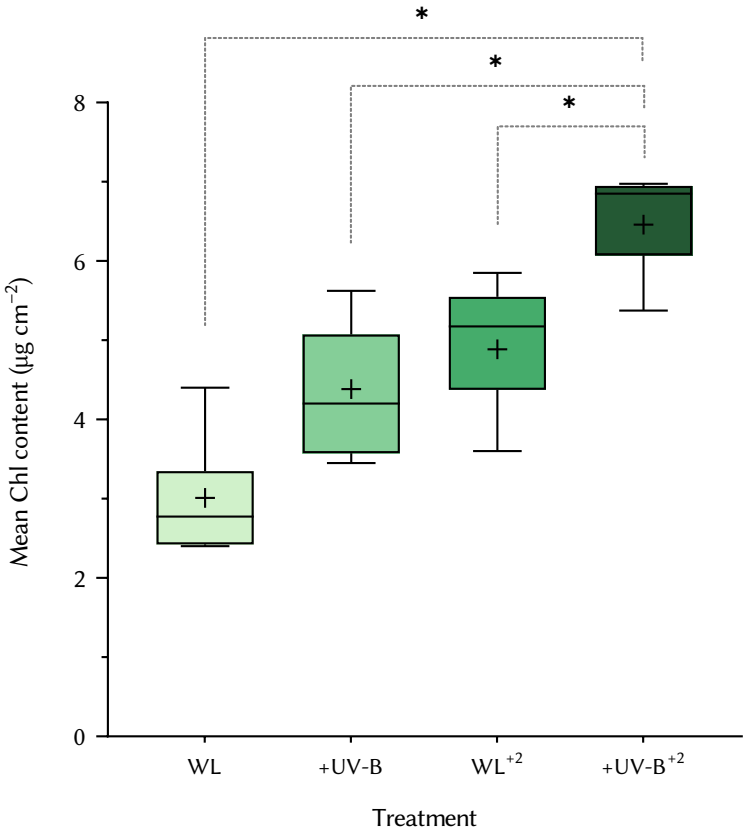

Figure S5. Experimental replicate of Fig. 8 using independently grown plants. Four-week-old Arabidopsis plants were treated with either WL or WL supplemented with low-dose UV-B (1 µmol m^{-1} s^{-1}; +UV-B) for 4 h at dawn. Fourth and fifth rosette leaves were detached and either dark-incubated for 7 d at 20°C or retreated at 2 DDI for 2 h with WL or +UV-B (WL+2 or +UV-B+2). Mean Chl content (µg cm^{-2}) was determined by performing Dualex measurement at four predetermined locations on the adaxial leaf surface. Centre lines of box plots represent medians, + represent means, boxes delimit 25th and 75th percentiles, whiskers represent minimum and maximum values. Asterisks indicate statistically significant differences at $p \leq .05$ ($n = 7$).

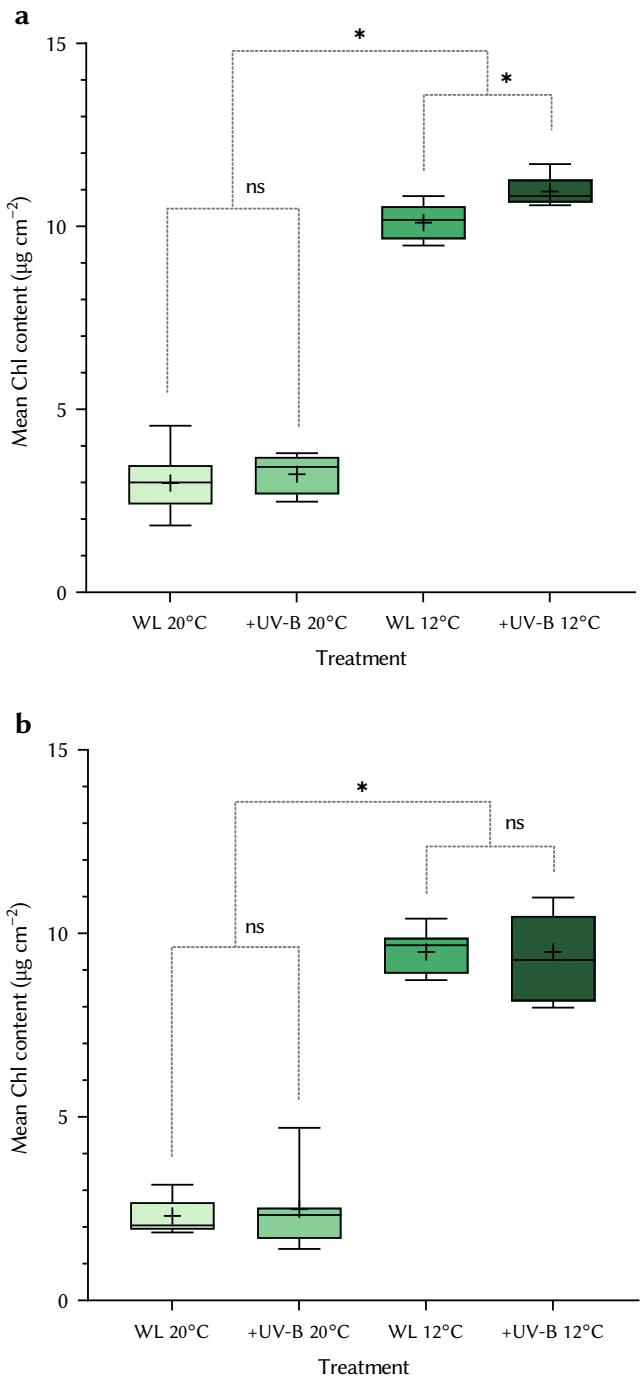

Figure S6. Experimental replicates of Fig. 10b using independently grown plants. Four-week-old Arabidopsis plants were treated with either WL or WL supplemented with low-dose UV-B (1 µmol m^{-1} s^{-1}; +UV-B) for 4 h at dawn. Fourth and fifth rosette leaves were detached and dark-incubated for 0–7 d at 12°C or 20°C. Mean Chl content was determined by performing Dualex measurement at four predetermined locations on the leaf surface. Centre lines of box plots represent medians, + represent means, boxes delimit 25th and 75th percentiles, whiskers represent minimum and maximum values. Asterisks indicate statistically significant differences at $p \leq .05$ (ns, non-significant; $n = 7$).